International Journal of Mining and Mineral Engineering

ISSN: 1754-8918
2015-Volume 6 Number 2

A linkage of truck-and-shovel operations to short-term mine plans using discrete-event simulation

Elmira Torkamani and Hooman Askari-Nasab*

Mining Optimization Laboratory (MOL),
School of Mining and Petroleum Engineering,
Department of Civil & Environmental Engineering,
University of Alberta,
3-133 Markin/CNRL Natural Resources Engineering Facility,
Edmonton, Alberta, T6G 2W2, Canada
Fax: (780) 492-0249
Email: torkaman@ualberta.ca
Email: hooman@ualberta.ca
*Corresponding author

Abstract: The economics of today's mining industry requires more efficient usage of truck-shovel systems. In this paper, a discrete-event simulation model is developed, implemented, and verified to analyse the behaviour of a stochastic truck-shovel materials-handling and haulage system in open-pit mining. A mixed integer linear programming model (MILP) is also developed to deal with the allocation problem in which trucks and shovels are assigned to mining faces. The simulation model is linked to the optimal short-term mine production schedule generated by mathematical programming using exact solution methodology. The simulation model imitates the complex truck-shovel system, and considers the uncertainties associated with the operations of trucks and shovels. The simulation model provides a tool to improve the system's efficiency, and guarantees that the operational plans will honour the optimum net present value obtained in the production-scheduling phase.

Keywords: truck-shovel system; short-term mine planning; stochastic discrete-event simulation; MILP.

Reference to this paper should be made as follows: Torkamani, E. and Askari-Nasab, H. (2015) 'A linkage of truck-and-shovel operations to short-term mine plans using discrete-event simulation', *Int. J. Mining and Mineral Engineering*, Vol. 6, No. 2, pp.97–118.

Biographical notes: Elmira Torkamani is a Research Assistant at the Mining Optimization Laboratory (MOL) at the University of Alberta. She holds a Bachelor's and Master's degree in Industrial Engineering from Amir Kabir University of Technology, Iran and a Master's in Mining Engineering from University of Alberta, Canada. Her research interests are in the area of applications of operations research specifically discrete event simulation of mining systems.

Hooman Askari-Nasab is an Associate Professor of Mining Engineering at the University of Alberta, Canada. He holds a MSc from Tehran Polytechnic University and PhD from the University of Alberta. He teaches and conducts research into applications of operations research in mine planning and design.

He is the director of industrial research consortium, 'Mining Optimization Laboratory' (MOL) at the University of Alberta. He is a Professional Engineer registered with APEGA in Alberta. He offers consulting services to mining industry through OptiTek Mining Consulting Ltd. in the area of open pit mine planning and design and simulation of mining systems.

This paper is a revised and expanded version of a paper entitled 'Truck-shovel operational planning using discrete event simulation' presented at *Applications of Computers and Operations Research in Mineral Industry – 36th APCOM*, Porto Alegre, Brazil, 4–8 November, 2013

1 Introduction

The fundamental objective of any mining project is to maximise mine profit by extracting ore at the lowest possible cost over the mine life. Especially in open-pit mines, acquiring the optimal production at minimum cost is an essential issue, because open-pit mine operations are highly capital intensive. Operating costs are one of the major expenditures in open-pit mines. A significant portion of operating costs is related to operations of equipment involved in materials-handling and haulage systems. Trucks and shovels constitute 50–60% of an open-pit mine's overall operating costs (Ercelebi and Bascetin, 2009). An efficient truck-shovel system creates savings by reducing hauling, operating, and maintenance costs. Nowadays, with increasing equipment capacity and haul distances, deepening pits, and a more competitive mineral market, the problem of improving the utilisation of available fleet becomes even more important and challenging. The problem is challenging because truck-shovel systems are complicated due to the uncertainties associated with their operations and the vast number of parameters and resulting interactions involved in the problem.

Resource allocation problems are central to many real-world planning problems, including load distribution, production planning, computer scheduling, portfolio selection, etc. In this paper, resource allocation refers to the allocation of trucks and shovels to mining faces. The scope of this research is concerned with improving truck-shovel systems' efficiency using simulation and mathematical programming. The objective is to build a linkage between the optimal short-term mine schedule and the truck-shovel material-handling-and-haulage system considering the uncertainties associated with the operations in order to improve the utilisation of these resources while meeting optimal short-term production targets.

We present two main modelling components as the means to achieve the research objective:

- a MILP model to allocate trucks and shovels to mining faces over a shift-by-shift basis so that the operating costs are minimised and resource utilisations are maximised through the planning horizon
- a discrete-event simulation model to analyse the behaviour of a truck-shovel haulage system considering the associated uncertainties within mining operations.

Ultimately, the goal is to develop an integrated model of the truck-shovel allocation MILP and the discrete-event simulation, where the two components interact with each

other. The current paper includes the MILP model formulation and the complete verified simulation model which is linked to the optimal short-term mine production schedule.

The main contribution of this research so far, is the development, implementation, and verification of a simulation model with a link to optimal short-term mine schedule and extraction sequence of mining faces, which assists in achieving high-level of mine plan compliance across short-term planning and operational planning time horizons. The generated production schedule by the simulation model is derived from the overall mine plan requirements according to the economic and operational objectives, not only the shovels' requirements, which is the common approach in the literature and industry.

The tasks that were completed to achieve the objective are as follows:

- carry out a thorough literature survey on modelling truck-shovel systems
- develop MILP model to deal with allocation problem
- analyse a real world truck-shovel system to obtain insight into the activities and prevalent factors involved in truck-shovel systems
- conceptualise the simulation model
- perform data analysis on historical dispatching data to fit suitable probability density functions
- develop the actual model using Arena simulation software
- verify the model
- test the model on a real world open-pit mine
- run multiple scenarios and document results.

The output of the optimal short-term mine production schedule generated by Eivazy and Askari-Nasab (2012a, 2012b) using MILP is the input into the simulation model in this study. The simulation model imitates the complex truck-shovel system, and considers the uncertainties associated with the operations of trucks and shovels. This approach guarantees that the operational plans will honour the objectives of the production scheduling phases. Two main sub-problems are considered in this research. First is the equipment selection problem, in which the number of trucks and shovels are determined. The second is the behaviour of the designed system with the selected number of equipment. Using defined key performance indicators (KPIs), the efficiency of the system is measured under different operational scenarios.

Different methods for modelling truck-shovel systems are reported in the literature. These methods can be classified into three main categories:

- mathematical programming
- simulation
- other stochastic methods such as queuing theory.

Among current methods, simulation is widely accepted as a way to assess the performance of mining operations, because it makes it possible to incorporate the system's inherent variability and complexity. The other commonly used approaches like mathematical programming and stochastic methods require significant computational

effort. Due to complexity and high uncertainty of the truck-shovel operations, none of these methods can comprehensively capture all aspects of truck-shovel systems. Most approaches usually ignore the stochastic nature of the truck-shovel operations and use deterministic solutions.

Although mathematical programming-based models have been developed for truck-shovel systems, most have shortcomings. These models do not take into account the stochastic nature of the truck-shovel systems, the economic parameters, and the multi-time-period nature of the mining operations (Gurgur et al., 2011), so they are usually combined with simulation models or other stochastic approaches, as seen in studies by Temeng et al. (1997), Fioroni et al. (2008), and Yuriy and Vayenas (2008). Some other studies have developed models based on mathematical programming approaches to optimise production scheduling and truck dispatching problems in the same framework, such as works by Yan and Lai (2007), Yan et al. (2008), and Gurgur et al. (2011).

Simulation studies about truck-shovel systems are mostly implemented for specific cases. Each of these studies tries to apply the simulation modelling for a real mine such as models developed by Sturgul and Eharrison (1987) for a surface mine in Australia, Peng et al. (1988) for an iron ore mine in northeast China, Forsman et al. (1993) for a copper ore mine in northern Sweden, and Awuah-Offei et al. (2003) for a typical hard rock auriferous mine in Ghana. The majority of these simulation studies, such as those by Wang et al. (2006), and Burt and Caccetta (2007), are only evaluating truck dispatching rules, while others, such as Karami et al. (1996) and Awuah-Offei et al. (2003), try to also consider the operations involved in the truck-shovel systems.

Some studies have applied the queuing theory to analyse truck-shovel haulage systems in open-pit mining. The first application of queuing theory in mining context was done by Koenigsberg (1958). His work was followed by Carmichael (1987, 1986), Kappas and Yegulalp (1991), Muduli and Yegulalp (1996), Czaplicki (1999), Trivedi et al. (1999), Alkass et al. (2003), Krause and Musingwini (2007), Ercelebi and Bascetin (2009), and Ta et al. (2010). There is limited literature on stochastic programming applied in the field of mining. It seems that only Ta et al. (2005) have used the stochastic programming directly in evaluating a truck-shovel system. The major limitations in the current research on truck-shovel systems in open-pit mining are:

1 The stochastic nature of the truck-shovel systems is usually treated as deterministic. This drawback is mostly seen in mathematical programming techniques.

2 The system is modelled based on the shovel production requirement, which is stated as the shovel's hourly production rate. With this approach, the shovels are assumed to work continuously and the focus is on the operations of trucks only.

3 The source of material is defined as a mining-zone or a mining face. This approach treats each zone as a single complete unit that has single grade and tonnage characteristics. This imposes the assumption that all blocks in a mining-zone are identical. However, in the real world, trucks and shovels extract mining faces which comprising of blocks, which have distinct ore and waste percentages and grades.

4 A considerable amount of research focuses on the truck-shovel system as a closed system, the interactions with other systems in the mine such as the processing systems is ignored.

The simulation model developed in this study addresses the four problems mentioned above. The next section of the paper covers the MILP formulation for truck-shovel allocation to mining faces. Sections 3 and 4 present problem definition and simulation model development, while Section 5 presents an application of the simulation model to an iron-ore open pit mine. Finally, the last section presents the conclusions and future work.

2 MILP formulation

This section presents the MILP formulation for truck-and-shovel allocation to the mining faces. It should be noted that the implementation, verification, and integration with the discrete-event simulation model is part of the future work and is not presented in this paper.

The following assumptions are the basis of the mathematical programming model developed for the truck-shovel allocation problem. An open-pit mine consisting of different mining faces is taken into account. These mining faces are located on several benches. There are two fixed destinations for the trucks: a crusher and a waste dump. It is assumed that shovels and trucks of different types with different sizes are available. Due to failures and scheduled maintenance, the number of available trucks of each type and available shovels may vary from one period to another. At the beginning of each period, a decision is made about assigning trucks and shovels to the mining faces, which are ready to be extracted. The model considers grades of materials in the mining faces. Shovels and trucks are allocated to the mining faces to meet the blending constraints at the crusher. Any deviation from the target production at the crusher results in a penalty, which translates to extra costs. In addition, there are costs associated with the trips that trucks take from a mining face to different destinations. The cost of a shovel travelling from its location to a new mining face location is also considered. Other assumptions considered in building the MILP model are:

- Each mining face is available to be extracted at specific periods
- There is a maximum and minimum limit on the crusher's production capacity
- Specific types of trucks can work with specific types of shovels
- The number of available trucks of each type is known at the beginning of the period
- The number of available shovels is known at the beginning of the period
- Maximum and minimum production capacity of shovels and load capacity of trucks are known
- A truck's capacity, in terms of tonnes, depends on the type of material it is hauling
- Only one shovel operates at each mining face at a time
- Each shovel can operate at only one mining face at a time.

Sets

$I = \{1,\ldots,I\}$: Set of mining faces

$J = \{1,\ldots,J\}$: Set of shovels

$K = \{1,\ldots,K\}$: Set of types of trucks.

Indices

$i \in I$: Index for mining faces

$j \in J$: Index for shovels

$k \in K$: Index for types of trucks.

Parameters

$MAT_i \in \{0,1\}$: Current material type of mining face i. It is equal to 1 if current material type of mining face i is ore; otherwise it is equal 0

ORE_i : Remaining ore tonnage at mining face i (tonnes)

$WASTE_i$: Remaining waste tonnage at mining face i (tonnes)

$AVL_i^{face} \in \{0,1\}$: Availability of mining face i. It is equal to 1 if mining face i is available; otherwise it is equal to 0

$AVL_j^{shovel} \in \{0,1\}$: Availability of shovel j. It is equal to 1 if shovel j is available; otherwise it is equal to 0.

$SHCAP_j^{\max}$: Maximum production capacity of shovel j (tonnes per hour)

$SHCAP_j^{\min}$: Minimum production capacity of shovel j (tonnes per hour)

NUM_k : Number of available trucks of type k

$COMP_{jk} \in \{0,1\}$: Compatibility of truck k with shovel j. It is equal to 1 if truck k is compatible with shovel j; otherwise it is equal to 0

CT_{ik}^{ore} : Cycle time of truck type k transferring ore from mining face i to the crusher (seconds)

CT_{ik}^{waste} : Cycle time of truck type k transferring waste from mining face i to the waste dump (seconds)

CAP_k^{ore} : Capacity of truck type k when transferring ore (tonnes)

CAP_k^{waste} : Capacity of truck type k when transferring waste (tonnes)

GR_{il} : Grade of element l at mining face i (%)

UB_l : Upper bound of grade blending for element l

LB_l : Lower bound of grade blending for element l

$PMAX$: Maximum processing capacity of the crusher (tonnes)

$PMIN$: Minimum processing capacity of the crusher (tonnes)

MC_{ij} : Trip cost of shovel j travelling from its current location to mining face i ($)

TRC_{ik}^{ore} : Trip cost of truck type k travelling from mining face i to the crusher ($)

TRC_{ik}^{waste} : Trip cost of truck type k travelling from mining face i to the waste dump ($)

DC : Cost of deviation from target production ($ per ton)

T : Planning time duration (hours).

Decision variables

$a_{ij} \in \{0,1\}$: Binary integer decision variable representing assigning of shovel *j* to mining face *i*. It is equal to 1 if shovel *j* is assigned to mining face *i*; otherwise it is equal to 0

n_{ik}^{ore}: Continuous decision variable representing number of trips of truck type *k* from mining face *i* to the crusher

n_{ik}^{waste}: Continuous decision variable representing number of trips of truck type *k* from mining face *i* to the waste dump

x_i: Extracted material tonnage from mining face *i* (tonnes).

Objective function

$$\text{Minimize } Z = \sum_{i\in I}\sum_{j\in J} MC_{ij}\cdot a_{ij} + \sum_{i\in I}\sum_{k\in K}(TRC_{ik}^{ore}\cdot n_{ik}^{ore} + TRC_{ik}^{waste}\cdot n_{ik}^{waste}) + DC\cdot(PMAX - \sum_{i\in I} MAT_i\cdot x_i) \quad (1)$$

Subject to

$$\sum_{j\in J} a_{ij} \le AVL_i^{face} \quad \forall i \in I \quad (2)$$

$$\sum_{i\in I} a_{ij} \le AVL_j^{shovel} \quad \forall j \in J \quad (3)$$

$$CT_{ik}^{ore}\cdot n_{ik}^{ore} \le 3600\cdot T\cdot NUM_k\cdot MAT_i \quad \forall i \in I, k \in K \quad (4)$$

$$CT_{ik}^{waste}\cdot n_{ik}^{waste} \le 3600\cdot T\cdot NUM_k\cdot (1-MAT_i) \quad \forall i \in I, k \in K \quad (5)$$

$$n_{ik}^{ore} \le \sum_{j\in J} a_{ij}\cdot COMP_{jk} \quad \forall i \in I, k \in K \quad (6)$$

$$n_{ik}^{waste} \le \sum_{j\in J} a_{ij}\cdot COMP_{jk} \quad \forall i \in I, k \in K \quad (7)$$

$$\sum_{i\in I} n_{ik}^{ore}\cdot CT_{ik}^{ore} + \sum_{i\in I} n_{ik}^{waste}\cdot CT_{ik}^{waste} \le 3600\cdot T\cdot NUM_k \quad \forall k \in K \quad (8)$$

$$x_i \le \sum_{j\in J} T\cdot SHCAP_j^{\max}.a_{ij} \quad \forall i \in I \quad (9)$$

$$x_i \ge \sum_{j\in J} T\cdot SHCAP_j^{\min}.a_{ij} \quad \forall i \in I \quad (10)$$

$$\sum_{i\in i} x_i\cdot MAT_i \le PMAX \quad (11)$$

$$\sum_{i\in i} x_i\cdot MAT_i \ge PMIN \quad (12)$$

$$x_i \cdot MAT_i \le ORE_i \quad \forall i \in I \tag{13}$$

$$x_i \cdot (1 - MAT_i) \le WASTE_i \quad \forall i \in I \tag{14}$$

$$x_i = \sum_{k \in K} CAP_{ik}^{ore} \cdot n_{ik}^{ore} + \sum_{k \in K} CAP_{ik}^{waste} \cdot n_{ik}^{waste} \quad \forall i \in I \tag{15}$$

$$\sum_{i \in I} GR_{il} \cdot x_i \le \sum_{i \in I} UB_l \cdot x_i \quad \forall l \in L \tag{16}$$

$$\sum_{i \in I} GR_{il} \cdot x_i \ge \sum_{i \in I} LB_l \cdot x_i \quad \forall l \in L \tag{17}$$

$$a_{ij} \in \{0,1\} \quad \forall i \in I, j \in J \tag{18}$$

$$n_{ik}^{ore}, n_{ik}^{waste} \in Z \quad \forall i \in I, k \in K \tag{19}$$

$$x_i \ge 0 \quad \forall i \in I \tag{20}$$

In the developed MILP formulation, the objective function tries to minimise the costs associated with truck-shovel operations. The first term in equation (1) is the total cost of shovels travelling to new mining faces. The second term is the total transportation cost of trucks travelling to the waste dump or to the crusher. The last term in equation (1) is the cost of negative deviation from the production target at the crusher.

Equation (2) indicates that at each available mining face only one shovel can operate, and if a mining face is not available, no shovel should be assigned to that mining face. Equation (3) assures that each available shovel can operate at only one mining face. Equation (4) limits the number of trips for a fleet of trucks travelling from each mining face to the crusher. Equation (5) restricts the number of trips for a fleet of trucks travelling from each mining face to the waste dump. Equations (6) and (7) guarantee that a truck could travel to a mining face only if a shovel is assigned to that mining face and the shovel is compatible with that type of truck. Equation (8) denotes that the total number of trips that each truck type makes to the crusher or to the waste dump is less than the maximum possible trips of that truck type. Equations (9) and (10) ensure that the production of each mining face is between the minimum and maximum possible production of the shovel assigned to that mining face. Equations (11) and (12) aim to meet the crusher's limits of processing capacity. Equations (13) and (14) force each mining face to produce less than the maximum amount of available material. Equation (15) defines the production of each mining face based on the number of trips made by each fleet of trucks. Equations (16) and (17) ensure that the grade blending at the crusher is between specified upper and lower limits. Equations (18)–(20) define types of different decision variables. Solving the MILP model with an optimisation tool and integrating it with a simulation model is recommended for future research.

3 Truck-shovel system description

The iron ore open-pit mine studied in this paper consists of a pit-exit point and three possible destinations for the mined material:

- waste dumps
- stockpiles
- processing plants (crushers).

A reclamation strategy from stockpiles to appropriate crushers based on the short-term plan is not available. The main element of interest in the deposit is iron, phosphor and sulphur are considered as contaminants.

The employed truck-shovel system operates with a link to the optimal short-term production schedule. Short-term production schedule and mining-cut extraction sequences provided by Eivazy and Askari-Nasab (2012a, 2012b) are the inputs into the simulation. The short-term production schedule provides information about the number and IDs of mining-cuts that should be extracted in each month. Also, the following information is available in the short-term production schedule for each mining-cut:

- mining-cuts that should be extracted prior to mining any particular mining-cut
- coordinates of the mining-cuts' location
- material content of the mining-cut which is defined as ore tonnage and waste tonnage
- grades of different elements, which include phosphor, sulphur, and magnetic iron ore
- periods during which the mining-cut is supposed to be extracted
- destinations where the mining-cut's material should be delivered to
- the portion of the mining-cut that should be extracted in each period and delivered to a specific destination
- the number and length of the ramp through which the material is hauled to the pit-exit point.

In this paper, a typical truck-shovel system is studied, Classification of material as ore, stockpile, and waste material, as well as the material's respective destination, is based on the optimal short-term schedule, which is an input into the simulation model. At each of the destinations, there is limited space available for trucks to dump. No more than a specific number of trucks can dump simultaneously at a destination. Regarding the rehandling process, a loader and a truck are used to reclaim material from stockpiles.

The proposed model includes the uncertainties associated with the operations of trucks and shovels. The stochastic variables are represented by probability density functions, which are estimated, based on the historical data and goodness of fit tests. The uncertainty is captured by using the following random variables in the discrete-event-simulation model:

- the tonnage that a shovel can extract at each load-pass
- the time that it takes to complete one load-pass
- the time that it takes to dump a load at a destination
- moving velocity of a shovel, which account for the time that it takes the shovel to travel from one mining face to another based on their distance

- velocity of a truck when it is loaded and when it is unloaded during day and night shifts
- mean time between failures (MTBF) and mean time to repair (MTTR) for shovels
- MTBF and MTTR for truck minor and major failures
- MTBF and MTTR for crushers.

4 Model development

Due to the complexity of truck-shovel systems, simulation is used to study the system. In the model, trucks, shovels, waste dumps, stockpiles, and crushers are modelled as resources of the truck-shovel operations. The flowchart of the model's logic is represented in Figure 1. The modelling and analysing the truck-shovel system in an open-pit mine is divided into two sub-problems.

In the first sub-problem, the equipment selection problem is considered. In this study, it is assumed that all trucks and shovels are identical. To determine the required number of resources, different scenarios with different number of trucks and shovels are generated. For this purpose, Arena Process Analyser (Arena Simulation Software, Ver. 13.9, 2010) is used. The dominant criterion used to evaluate each scenario is the production target of ore and waste, which is determined by the optimal short-term production schedule. With this approach, scenarios in which the production target is met are considered feasible. To choose the best scenario among feasible ones, other criteria that include average shovel utilisation and average truck utilisation are used.

The chosen number of trucks and shovels are used as a resource in the simulation model, and further analysis on the system's KPIs is done in the second sub-problem. Most of the KPIs are evaluated for a time span of a month or a shift. As the outcome, a 95% confidence level at 50 replications is used to generate tight half-widths around the mean of the major KPIs. This study considers the following KPIs: total delivered material tonnage; average truck utilisation and average shovel utilisation; average grades of elements such as phosphor, sulphur, and magnetic iron; average truck waiting time; average truck queue lengths; and average truck cycle time.

Among these KPIs, this study aims to reduce the truck waiting time, where possible. Any improvement in truck waiting time would affect the truck queue length and truck cycle time and, thus, improve the system's total efficiency. A truck waits for a resource because the resource is either busy or has failed. The largest contributor to the truck waiting time is the crusher failures. It is recommended that if a crusher has failed, the optimal short-term production schedule would not be followed and instead, trucks be redirected to the stockpiles. Following the new strategy, the content of stockpile at each period is sourced from two different flows of material. One is a planned flow of material that is based on the short-term production schedule and the other is the material flow, which was supposed to go to the processing plant, but is delivered to the stockpile, because of the crusher's failure. The latter material flow is referred as unplanned flow of material. The proposed simulation model is developed and tested in Arena simulation environment (Arena Simulation Software, Ver. 13.9, 2010).

Figure 1 Flow chart of the main simulation model

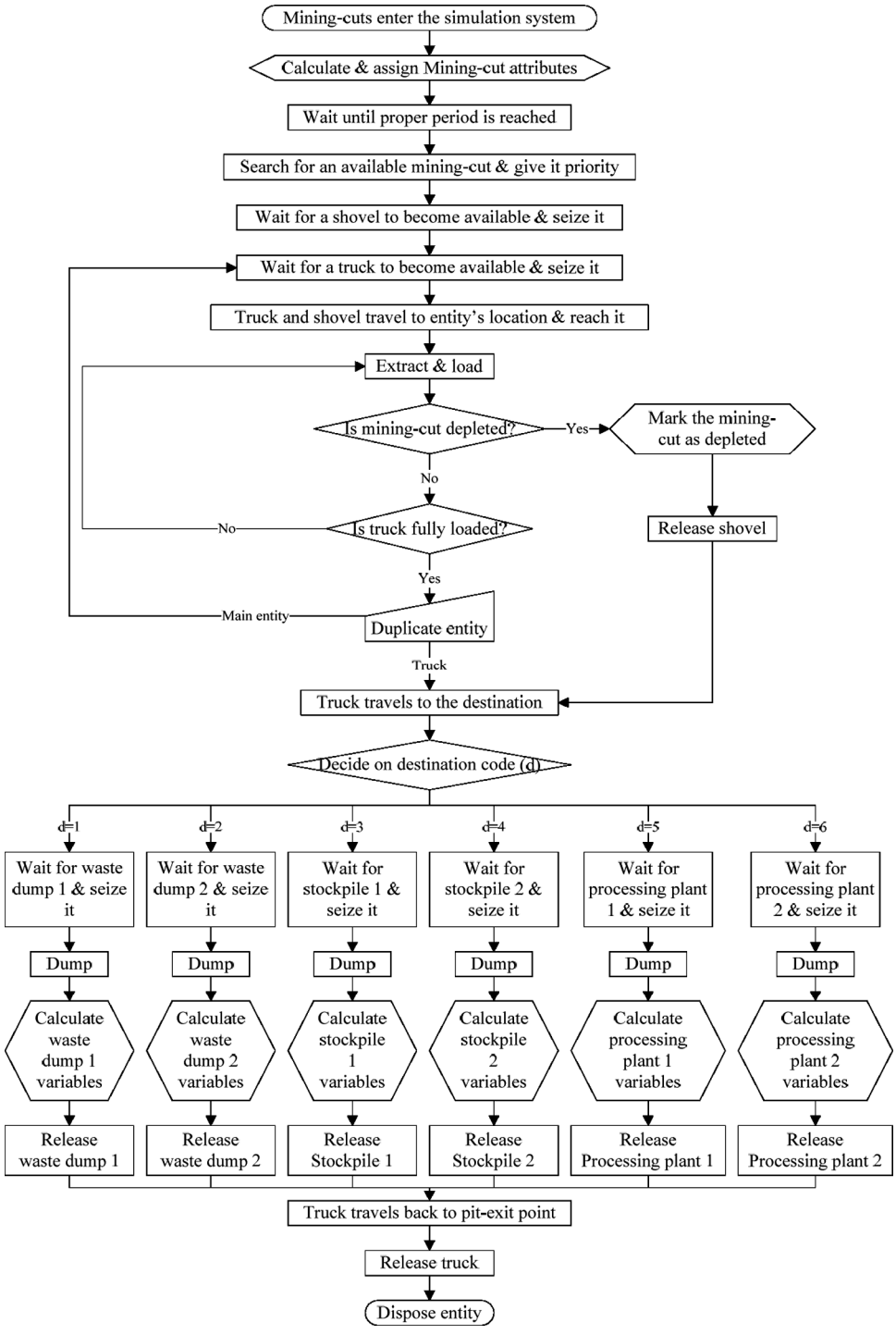

5 Case study

The proposed simulation model is applied to the data of an open-pit mine, Gol-E-Gohar, in the south of Iran. There are six different destinations in the mine: two waste dumps, two stockpiles, and two processing plants. It is assumed that stockpile one feeds only crusher one and stockpile two only feeds crusher two. The information about the tonnage and grade of material reclaimed from each stockpile in each period is determined by the optimal short-term production schedule with the objective of cost minimisation. The optimal short-term production plan for this mine is developed by Eivazy and Askari-Nasab (2012a, 2012b) for a time horizon of one year, with a monthly resolution. The mine production bar-chart in terms of tonnage of material sent to the processing plants, stockpiles, and waste dumps is shown in Figure 2. Figure 3 shows the schematic view of the mine and the distances between the pit-exit point and different destinations, as well as the distances between the processing plants and the corresponding stockpiles.

Figure 2 Optimal short-term schedule developed by Eivazy and Askari-Nasab (2012a, 2012b) (see online version for colours)

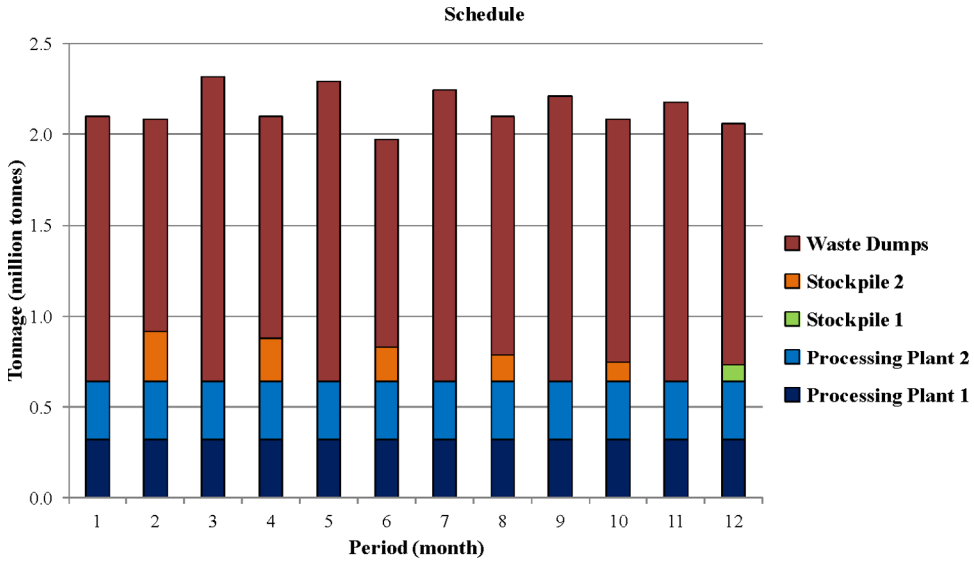

The total number of mining-cuts that should be extracted during the year is 330. Total rock tonnage and ore tonnage of these mining-cuts are 25 and 8 million tonnes, respectively. The mine employs CAT 785D mining trucks and CAT 7295 HD electric rope shovels. The truck's nominal payload capacity is 120 tonnes and the shovel's nominal dipper payload capacity is 40 tonnes. A truck is fully loaded by three load-passes. The equipment works 24 hours a day: one day shift and one night shift. It is assumed that only one truck can dump at each of the processing plants or each of the stockpiles at the same time. There is room for three trucks at each of the waste dumps. Each stochastic variable of the truck-shovel system is represented with a probability density function, which are presented in Table 1.

Figure 3 Schematic view of the mine (see online version for colours)

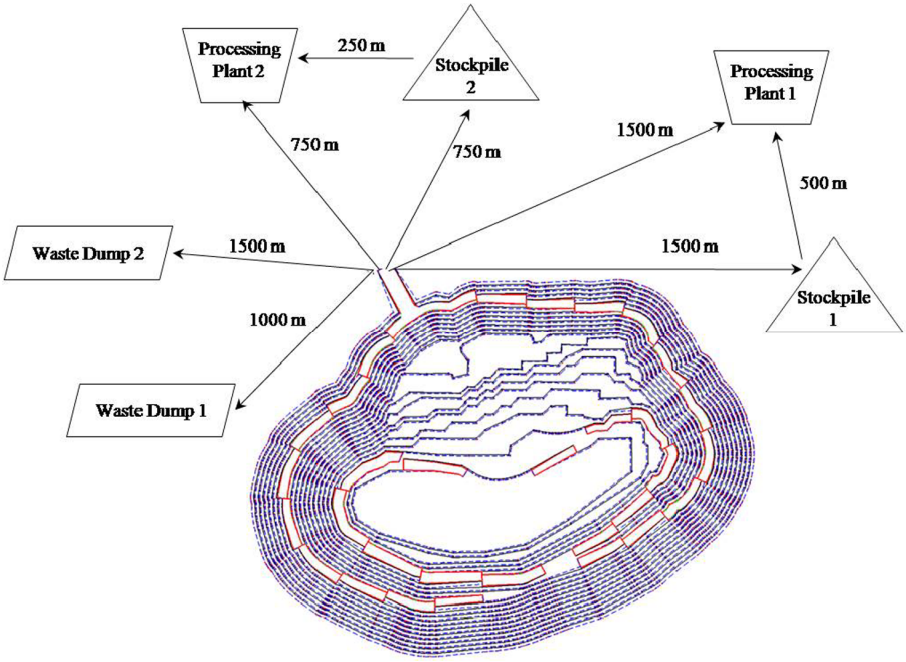

The proposed simulation model is developed using Arena simulation software (Arena Simulation Software, Ver. 13.9, 2010). The model reads all input data from an Excel.csv format file for easier input data entry and modifications. The model also exports all statistics to an Excel.csv format file. The simulation model is verified by:

- running the simulation model with no failures and also all random variables are replaced with their mean values; the results of the model are compared against manual calculation for 20 sample mining-cuts in terms of the cycle times of the trucks and tonnage of delivered material
- comparison of the mine production chart and weighted average head-grade output resulted from the simulation to the input production chart resulted from the MILP production scheduling model (Eivazy and Askari-Nasab, 2012a; 2012b).

5.1 Determination of number of trucks and shovels

To determine the required number of trucks and shovels, different scenarios are examined. The optimum scenario is the one that meets the production target in terms of ore and waste movement and has the highest truck and shovel utilisations. As shown in Figure 4, in scenario 18, with 3 shovels and 11 trucks, the production target is met. The average shovel utilisation is about 93% and the average truck utilisation is about 67% in this scenario. Accordingly, this scenario is chosen as the best scenario. Further increasing the number of shovels or trucks produces more feasible scenarios but decreases the utilisations.

The average truck and shovel utilisations during each month are monitored. As presented in Figure 5, the average utilisations in the odd months (1, 3, 5, 7, 9 and 11)

are less than those in the even months (2, 4, 6, 8, 10 and 12). The monthly difference in utilisation is due to the stockpiling and reclaiming strategy developed in the optimal short-term schedule. During the odd months less material has been delivered directly from the mine to the processing plants. Instead, some material is reclaimed from stockpiles during these months (see Figure 2).

Table 1 Stochastic variables and their representative probability density functions

Stochastic variable	*Probability density function*
Loaded truck velocity during day shift (km/h)	Normal (18, 3)
Loaded truck velocity during night shift (km/h)	Triangular (15, 15, 18)
Empty truck velocity during day shift (km/h)	Normal (36, 3)
Empty Truck Velocity During Night Shift (km/h)	Triangular (30, 30, 33)
Shovel velocity during day shift (km/h)	Normal (6, 0.6)
Shovel velocity during night shift (km/h)	Triangular (5.1, 5.1, 5.7)
Load time (s)	Triangular (12, 15, 18)
Dump time (s)	Triangular (10.2, 12, 15)
Load-pass tonnage (tonnes)	Triangular (30, 35, 40)
MTBF for truck minor failure (h)	Weibull (27, 200)
MTTR for truck minor failure (h)	Gamma (1.4, 1.5)
MTBF for Truck Major Failure (h)	Weibull (65, 200)
MTTR for truck major failure (h)	Gamma (0.25, 24)
MTBF for shovel failure (h)	Weibull (32, 216)
MTTR for shovel failure (h)	Gamma (1.4, 1.5)
MTBF for crusher failure (h)	Weibull (90, 200)
MTTR for crusher failure (h)	Gamma (0.25, 24)

Figure 4 Delivered material tonnage in a year and resource utilisations (see online version for colours)

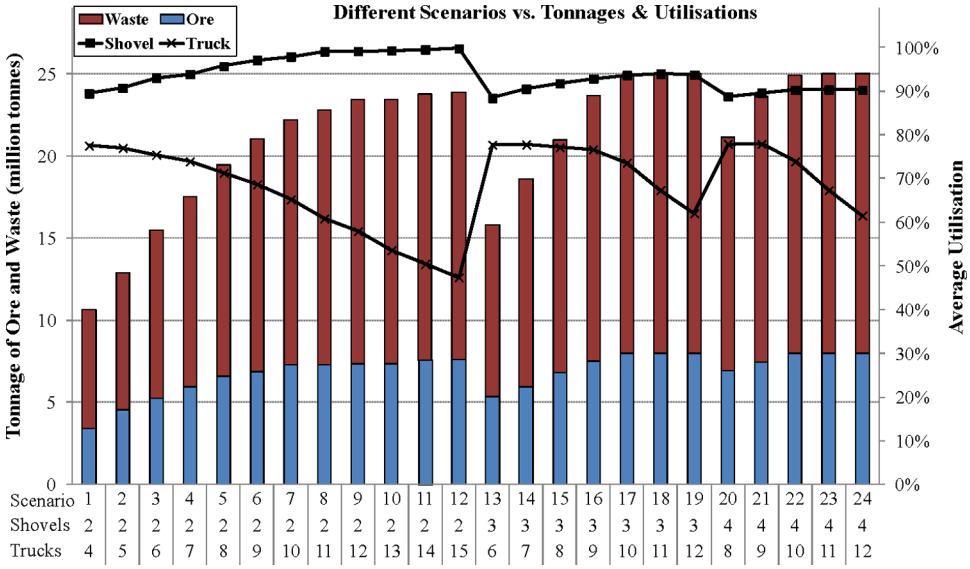

Figure 5 Average utilisation of resources with 3 shovels and 11 trucks (see online version for colours)

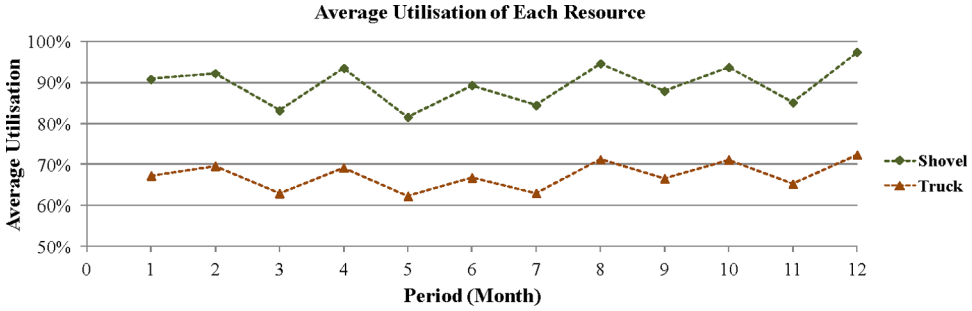

In order to make sure that the equipment on-site is used efficiently during odd months, the mine may run with less number of trucks during those months. To study the feasibility of such an alternative, another scenario analysis is implemented with the focus on odd months. Scheduled maintenance is introduced for trucks during the odd months. As shown in Figure 6, scenario 15, with 3 shovels and 10 trucks, is the best scenario that meets the 25 million tonne production target and generates the highest utilisations. The resulting average truck and shovel utilisations are shown in Figure 7. Compared to the previous scenario, which uses fixed number of trucks and shovels throughout the year, the new scenario results in steadier equipment utilisation and increases the average shovel utilisation to 94%, and increases the average truck utilisation to 71%.

Figure 6 Delivered material tonnage in a year and resource utilisations reassessing scenarios (see online version for colours)

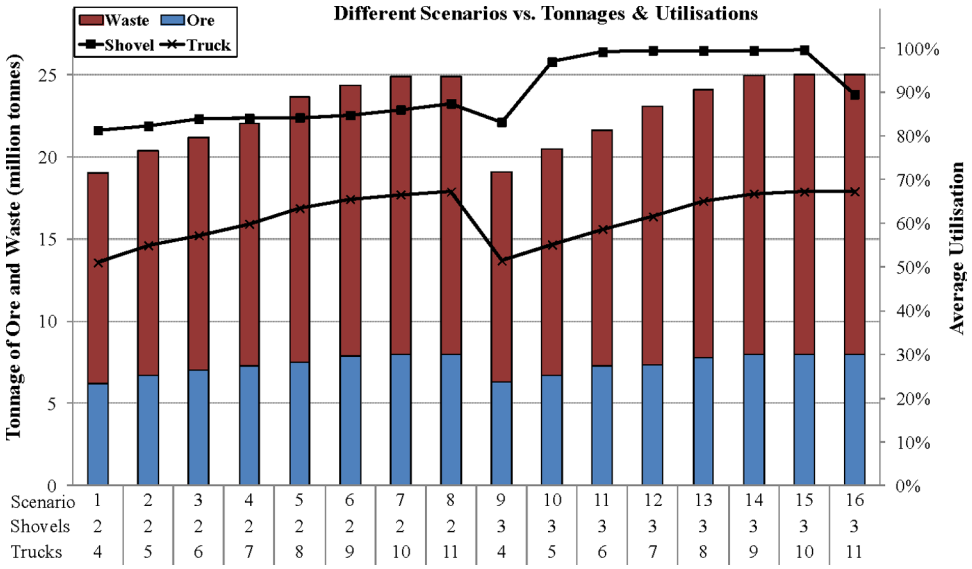

Figure 7 Average utilisations of resources considering maintenance schedule (see online version for colours)

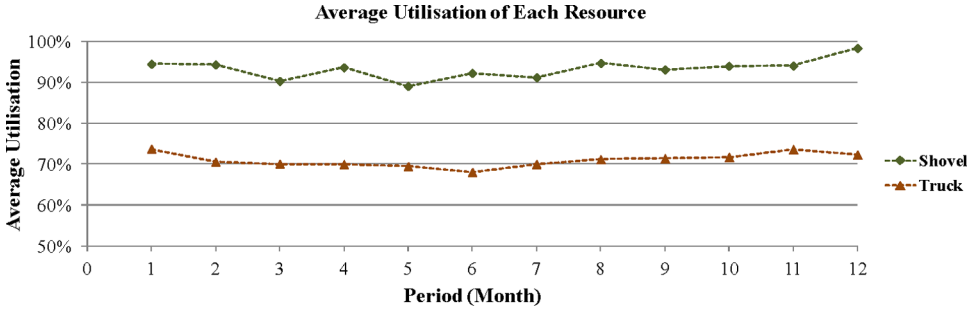

5.2 KPI evaluation

Using 3 shovels and 10 trucks in odd months, and 3 shovels and 11 trucks in even months, the simulation model is run for 50 replications to generate tight half-widths on the major KPIs. To show the results clearly, box plots are used in this study. Each box plot is a short graphical representation of a set of data resulting from a set of replications. The box plots of the average utilisation of shovels and trucks are shown in Figures 8 and 9, respectively.

Figure 10 illustrates the production bar-chart as the simulation output. The simulation output regenerates the input production schedule presented in Figure 2. Although there are stochastic variables associated with truck-shovel operations, the total delivered material tonnage to the destinations is consistent in different replications, because the number of trucks and shovels has been determined in such a way as to meet the production target set by the deterministic production schedule. As the main element of interest, the weighted average grade of magnetic iron (MWT) is shown in Figure 11. Following the short-term production schedule the same material is mined in every replication, therefore the head-grade does not vary in different replications.

Figure 8 Box plot of average monthly shovel utilisation

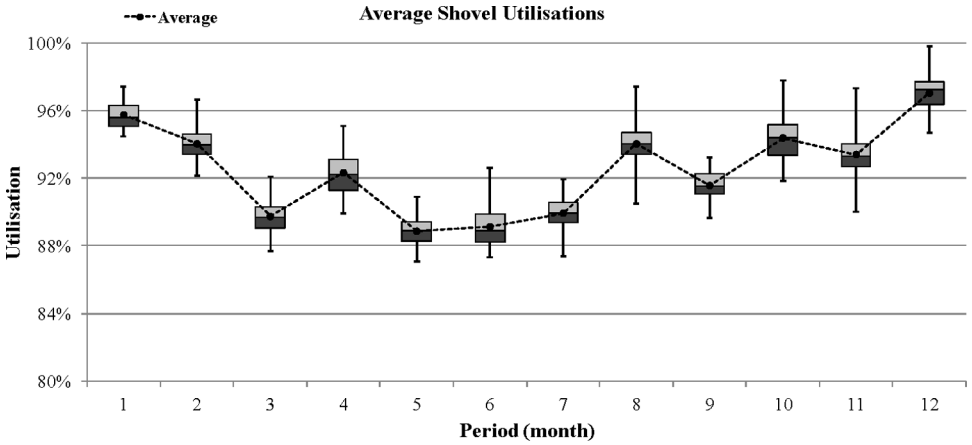

The waiting time at different destinations is one of the main KPIs that shows how effectively the trucks are used. The destination facility may be unavailable due to two reasons:

- other trucks are dumping at the destination and there is no room for the truck
- the destination facility has failed.

As shown in Figure 12, most of the truck waiting times occur at processing plants (around 2.25 minutes). Trucks do not wait at the other destinations, because there are no failures at waste dumps and stockpiles.

Figure 9 Box plot of average monthly truck utilisation

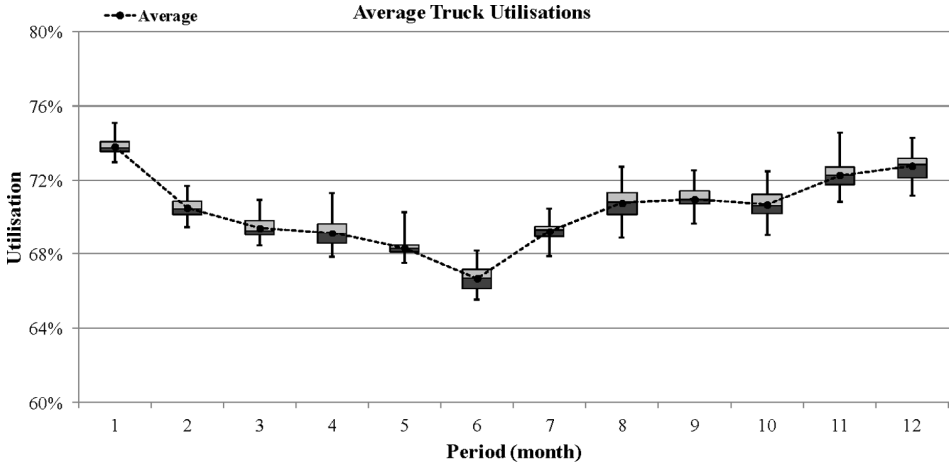

Figure 10 Material tonnage delivered to different destinations (see online version for colours)

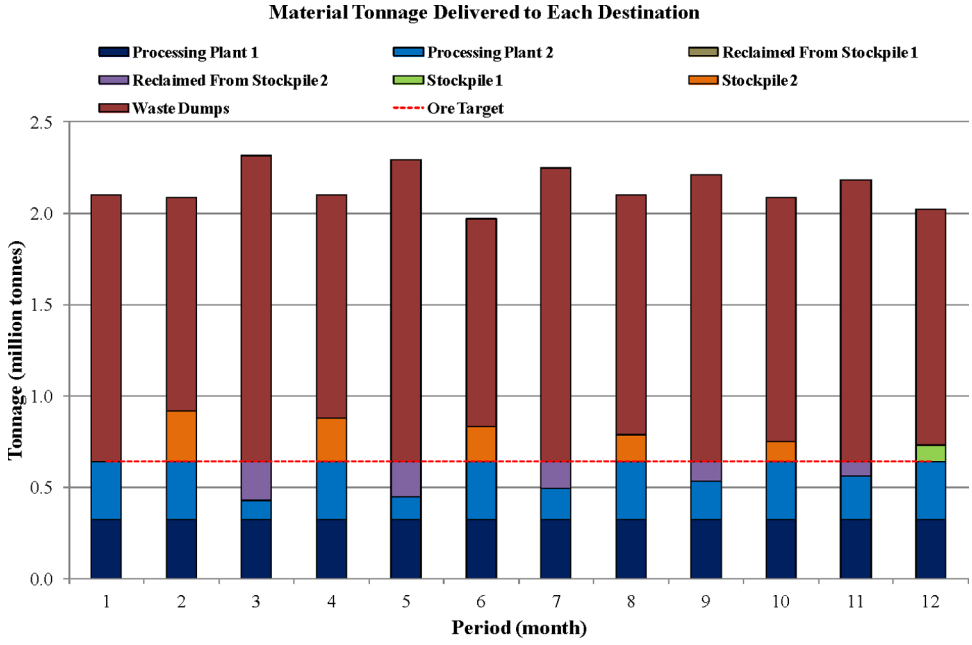

Figure 11 Average MWT grade of material delivered to processing plants 1 (PR1) and 2 (PR2) with corresponding upper bounds (UB) and lower bounds (LB) (see online version for colours)

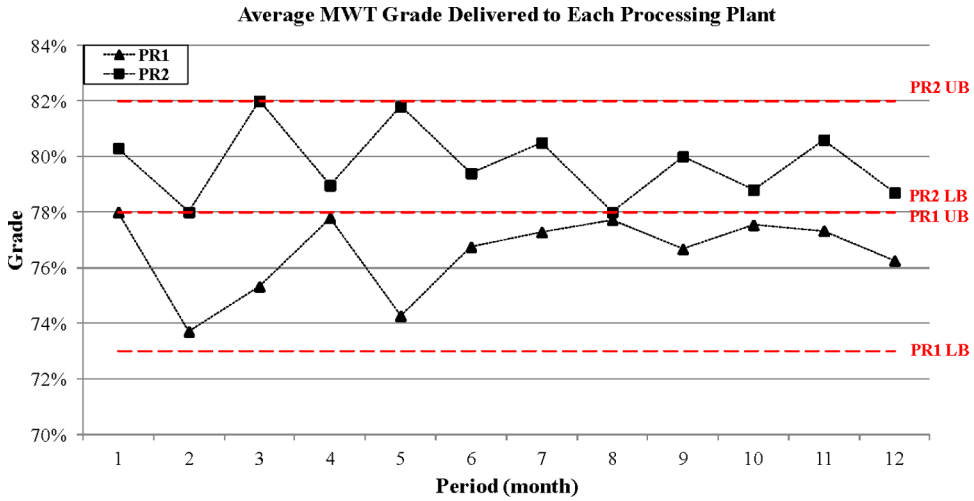

Figure 12 Average truck waiting time at each destination

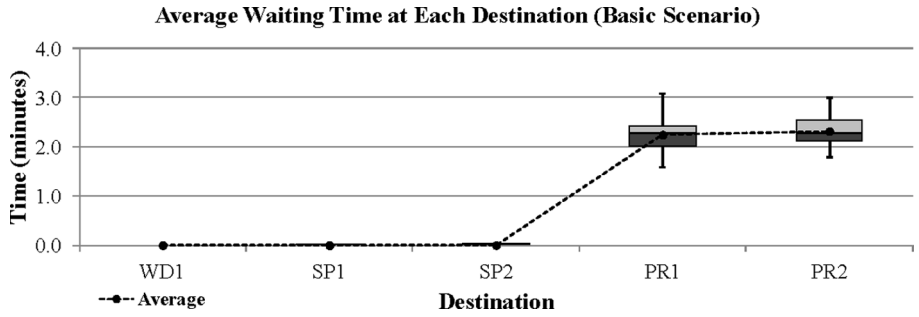

Truck cycle time is another critical KPI that is addressed in this research. The main stochastic variable that affects the truck cycle time is the velocity of trucks. Because the velocity of trucks differs during day and night shifts, the average truck cycle times during day and night shifts are assessed in detail. Truck cycle time during day shifts is less than that during night shifts because trucks travel faster during day shifts (see Figure 13).

Figure 13 Average truck cycle time during each shift

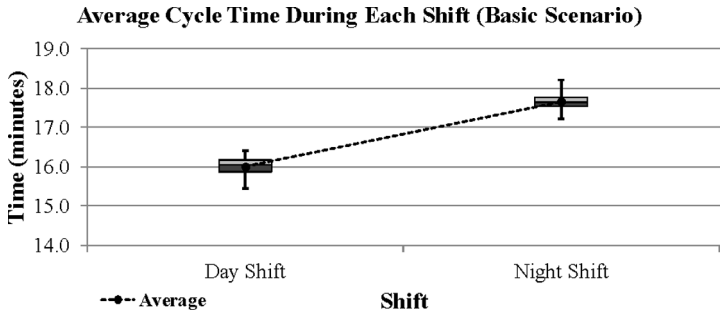

5.3 Improving the system efficiency

The largest contributor to truck waiting time is crusher failures. To improve the current truck-shovel system by reducing the truck waiting times at the processing plants, it is recommended that if a crusher has failed, we will deviate from the optimal production schedule and redirect truck to the stockpiles. In the new scenario, because the truck waiting time is decreased, the expectation is that there will be lower truck cycle times. The resulting average waiting times and cycle times are presented in Figures 14 and 15, respectively. Comparing these with those in the previous scenario, the average waiting times and cycle times at processing plants 1 and 2 are reduced significantly (see Tables 2 and 3).

Figure 14 Average truck waiting time in new scenario

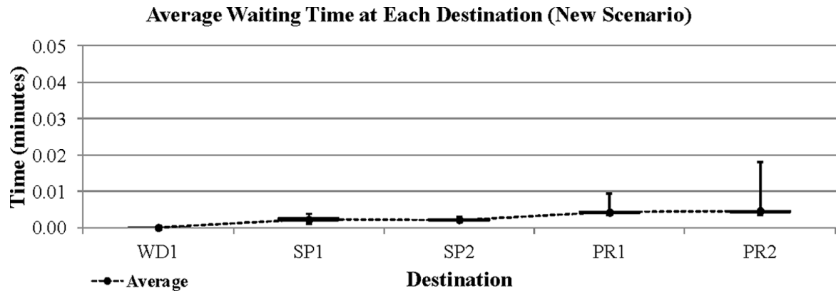

Figure 15 Average truck cycle time in new scenario

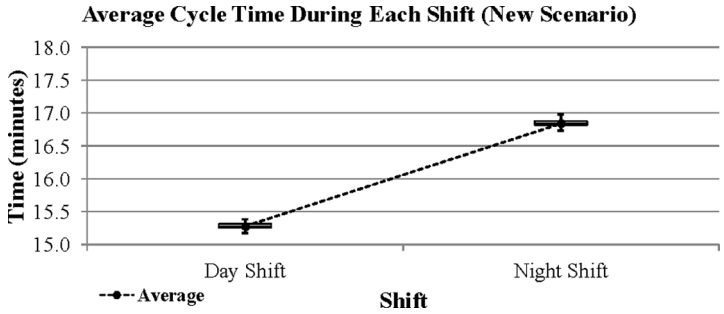

Table 2 Improvement percentages in waiting times at processing plants

	Average waiting time (min)		
Destination	*Base scenario*	*New scenario*	*Improvement* (%)
PR1	2.25	0.004	99.81
PR2	2.32	0.005	99.80

Table 3 Improvement percentages in cycle times at processing plants

	Average cycle time (min)		
Destination	*Base scenario*	*New scenario*	*Improvement* (%)
PR1	16.0	15.3	4.50
PR2	17.7	16.8	4.59

In the new scenario, the material that was scheduled for the processing plants is delivered to stockpiles because of the crusher failure. Because a crusher failure is a stochastic variable, the material delivered to the processing plants and stockpiles varies in different replications. To see these variations, monthly delivered material tonnages to each destination are studied in detail. The total ore tonnage delivered to processing plants, both directly delivered and reclaimed, deviates from the optimal target (from –8% to 6%). Figure 16 illustrates these deviations in terms of percentages of the optimal ore production target. These deviations occur because the deterministic optimal production schedule generated using mathematical programming assumes that the crusher is available all the time.

Figure 16 Box plot of the percentage of average delivered ore that has deviated from the ore production target

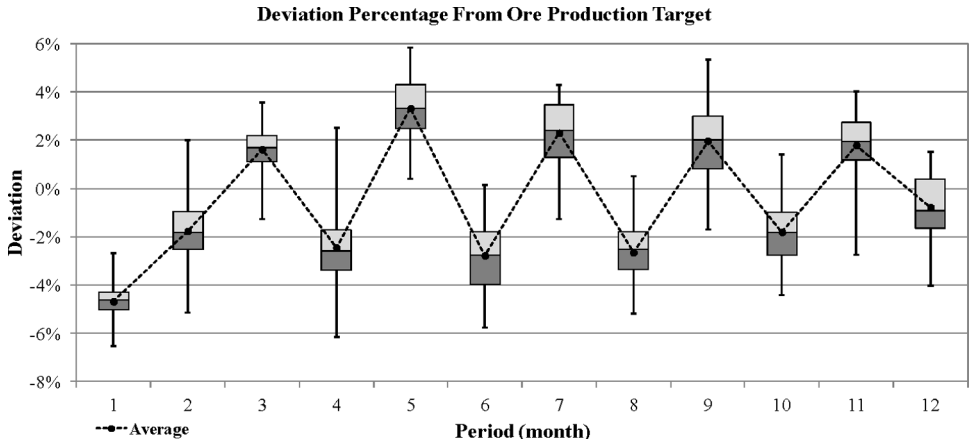

6 Conclusions

In this study, a stochastic discrete-event simulation model has been developed and verified to study truck-shovel systems in open-pit mining. The developed simulation model accurately monitors the system's KPIs that include average truck and shovel utilisations; delivered material tonnage to each destination; average grades of magnetic iron, phosphor, and sulphur; average truck waiting time and queue length at each destination; and average truck cycle time during day and night shifts. The simulation is run for 50 replications over a year to generate tight half-widths around the monthly and shift-based KPIs. When no failures were considered, the best scenario resulted in 81% average shovel utilisation and 84% average truck utilisation, with 2 shovels and 8 trucks. When considering failures, the best scenario has created 89% average shovel utilisation and 67% average truck utilisation, with 3 shovels and 11 trucks. Considering maintenance schedule, the final decision has been to employ 3 shovels, 10 trucks in odd months, and 11 trucks in even months. The average shovel and truck utilisations were 93% and 71% respectively.

The main contribution of this work is integration of the optimal short-term production mine schedule with simulation of truck-shovel operations. This integration allows selecting the required number of trucks and shovels based on the optimal short-term mine

plan, which is derived from the overall mine plan requirements according to the economic and operational objectives, rather than from the shovel's requirements, which is common in the literature and industry practice.

References

Alkass, S., El-Moslmani, K. and AlHussein, M. (2003) 'A computer model for selecting equipment for earthmoving operations using queuing theory', Paper presented at *CIB W78's 20th International Conference on Construction IT, Construction IT Bridging the Distance*, Waiheke Island, New Zealand, pp.133–140.

Arena Simulation Software, Ver. 13.9 (2010) Rockwell Automation Inc., Austin, USA.

Awuah-Offei, K., Temeng, V.A. and Al-Hassan, S. (2003) 'Predicting equipment requirements using SIMAN simulation a case study', *Institution of Mining and Metallurgy. Transactions. Section A: Mining Technology*, Vol. 112, No. 3, pp.A180–A184.

Burt, C.N. and Caccetta, L. (2007) 'Match factor for heterogeneous truck and loader fleets', *International Journal of Mining, Reclamation and Environment*, Vol. 21, No. 4, pp.262–270.

Carmichael, D.G. (1986) 'Shovel-truck queues: a reconciliation of theory and practice', *Construction Management and Economics*, Vol. 4, No. 2, pp.161–177.

Carmichael, D.G. (1987) 'Refined queueing model for earthmoving operations', *Civil Engineering Systems*, Vol. 4, No. 3, pp.153–159.

Czaplicki, J.M. (1999) 'A new method of truck number calculation for shovel-truck system', *Mineral Resources Engineering*, Vol. 8, No. 4, pp.391–404.

Eivazy, H. and Askari-Nasab, H. (2012a) 'A hierarchical open-pit mine production scheduling optimization model', *International Journal of Mining and Mineral Engineering*, Vol. 4, No. 2, pp.89–115.

Eivazy, H. and Askari-Nasab, H. (2012b) 'A mixed integer linear programming model for short-term open pit mine production scheduling', *Transactions of the Institutions of Mining and Metallurgy, Section A: Mining Technology*, Vol. 121, No. 2, pp.97–108.

Ercelebi, S.G. and Bascetin, A. (2009) 'Optimization of shovel-truck system for surface mining', *SIAMM - Journal of The South African Institute of Mining and Metallurgy*, Vol. 109, No. 7, pp.433–439.

Fioroni, M.M., Franzese, L.A.G., Bianchi, T.J., Ezawa, L., Pinto, L.R. and de Miranda, G. (2008) 'Concurrent simulation and optimization models for mining planning', Paper presented at *Simulation Conference, 2008. WSC 2008*, 7–10 December, 2008, Austin, USA, pp.759–767.

Forsman, B., Ronnkvist, E. and Vagenas, N. (1993) 'Truck dispatch computer simulation in Aitik open pit mine', *International Journal of Surface Mining & Reclamation*, Vol. 7, No. 3, pp.117–120.

Gurgur, C.Z., Dagdelen, K. and Artittong, S. (2011) 'Optimisation of a real-time multi-period truck dispatching system in mining operations', *International Journal of Applied Decision Sciences*, Vol. 4, No. 1, pp.57–79.

Kappas, G. and Yegulalp, T.M. (1991) 'Application of closed queueing networks theory in truck-shovel systems', *International journal of surface mining & reclamation*, Vol. 5, No. 1, pp.45–53.

Karami, A., Szymanski, J. and Planeta, S. (1996) 'A simulation analysis model of the ore truck haulage system in open pit mining', *Prace Naukowe Instytutu Gornictwa Politechniki Wroclawskiej*, No. 79, pp.164–171.

Koenigsberg, E. (1958) 'Cyclic queues', *Operational Research Quarterly*, Vol. 9, No. 1, March, pp.22–35.

Krause, A. and Musingwini, C. (2007) 'Modelling open pit shovel-truck systems using the machine repair model', *Journal of The South African Institute of Mining and Metallurgy*, Vol. 107, No. 8, pp.469–476.

Muduli, P.K. and Yegulalp, T.M. (1996) 'Modeling truck–shovel systems as closed queueing network with multiple job classes', *International Transactions in Operational Research*, Vol. 3, No. 1, pp.89–98.

Peng, S., Zhang, D. and Xi, Y. (1988) 'Computer simulation of a semi-continuous open-pit mine haulage system', *International Journal of Mining and Geological Engineering*, Vol. 6, No. 3, pp.267–271.

Sturgul, J.R. and Eharrison, J. (1987) 'Simulation models for surface mines', *International Journal of Surface Mining, Reclamation and Environment*, Vol. 1, No. 3, pp.187–189.

Ta, C.H., Ingolfsson, A. and Doucette, J. (2010) 'Haul truck allocation via queueing theory', *European Journal of Operational Research*, Vol. 231, No. 3, pp.770–778.

Ta, C.H., Kresta, J.V., Forbes, J.F. and Marquez, H.J. (2005) 'A stochastic optimization approach to mine truck allocation', *International Journal of Surface Mining, Reclamation and Environment*, Vol. 19, No. 3, pp.162–175.

Temeng, V.A., Otuonye, F.O. and Frendewey Jr., J.O. (1997) 'Real-time truck dispatching using a transportation algorithm', *International Journal of Surface Mining, Reclamation and Environment*, Vol. 11, No. 4, pp.203–207.

Trivedi, R., Rai, P. and Nath, R. (1999) 'Shovel-truck optimization study in an opencast mine – a queueing approach', *Indian Journal of Engineering and Materials Sciences*, Vol. 6, No. 3, pp.153–157.

Wang, Q., Zhang, Y., Chen, C. and Xu, W. (2006) 'Open-pit mine truck real-time dispatching principle under macroscopic control', Paper presented at *First International Conference on Innovative Computing, Information and Control*, 30 August–1 September, 2006, Beijing, China, pp.702–706.

Yan, S. and Lai, W. (2007) 'An optimal scheduling model for ready mixed concrete supply with overtime considerations', *Automation in Construction*, Vol. 16, No. 6, pp.734–744.

Yan, S., Lai, W. and Chen, M. (2008) 'Production scheduling and truck dispatching of ready mixed concrete', *Transportation Research Part E: Logistics and Transportation Review*, Vol. 44, No. 1, pp.164–179.

Yuriy, G. and Vayenas, N. (2008) 'Discrete-event simulation of mine equipment systems combined with a reliability assessment model based on genetic algorithms', *International Journal of Mining, Reclamation and Environment*, Vol. 22, No. 1, pp.70–83.

Experimental study on the influences of sodium sulphide on zinc tailings cement paste backfill in Huize Lead-Zinc Mine

Wei Sun, Aixiang Wu*, Hongjiang Wang, Tao Li and Sizhong Liu

Key Laboratory of the Ministry of Education of China for High-Efficient Mining and Safety of Metal Mines, University of Science and Technology Beijing, Beijing 100083, China

and

School of Civil and Environment Engineering, University of Science and Technology Beijing, Beijing 100083, China
Email: kmustsw@qq.com
Email: aolipu001@163.com
Email: wanghi1988@126.com
Email: litaoustbyy@163.com
Email: liusizhong11@126.com
*Corresponding author

Abstract: The universal existing features of long setting time and low early strength in zinc cement paste backfill (CPB) make the cycle of mining prolonged, the mining cost and safety risk increased. On the basis of the above work, sodium sulphide procoagulant experiments are carried out, which analyses the settingtime of fill paste, different ages of uniaxial compressive strength (UCS) and hydration products change law by adding different quantity of sodium sulphide. The test results show that zinc ions have obvious retarding function and sodium sulphide has great coagulant function for fill paste which is beneficial to improve the early strength of fill paste. Setting time decreased from 128 h to18 h and the 7d UCS of fill paste increased from 0.76 MPa to 1.87 MPa with the content of sodium sulphide changed from 0% to 0.2%.

Keywords: zinc tailings; setting time; early strength; sodium sulphide; CPB; cement paste backfill.

Reference to this paper should be made as follows: Sun, W., Wu, A., Wang, H., Li, T. and Liu, S. (2015) 'Experimental study on the influences of sodium sulphide on zinc tailings cement paste backfill in Huize Lead-Zinc Mine', *Int. J. Mining and Mineral Engineering*, Vol. 6, No. 2, pp.119–138.

Biographical notes: Wei Sun, 2006–2009, Postgraduate. He studied in Kunming University of Science & Technology, major in Mining Engineering, study on paste filling; 2009–2011, Engineer, Kunming prospecting design institute of China nonferrous metals industry; 2011- Present, PhD student. His research areas include paste filling, backfilling station design.

Aixiang Wu, 2008-present: Dean of School of Civil and Environment Engineering, University of Science and Technology Beijing; 2006-present: Professor, Yangtze River Scholar, University of Science and Technology Beijing; 2000–2005: Leader of Department of Science of Technology, Central South University (CSU); 1999–2000: Leader of Department of Foreign Affair, CSUT 1996–1999: Vice Director of College of Resource, Environment and Civil Engineering, CSUT; 1994–1996: Vice Director of Department of Resources and Exploitation Engineering, CSUT; 2001–2005: Professor, CSU; 1994–2001: Professor, CSUT; 1991–1993: Subdecanal of Institute of Mining, CSUT; 1987–1991: Associate Professor, CSUT.

Hongjiang Wang, 2002–2006, PhD, Central South University of Technology (CSUT); 2006–2012, Associate Professor, University of Science & Technology Beijing (USTB); 2012- Present, Professor, USTB.

Tao Li, 2011–2013, Postgraduate. He studied in University of Science & Technology Beijing, major in Mining Engineering, study on paste filling; 2013-Present, PhD student. His research areas include granular ore drawing migration law and fluid-solid coupling.

Sizhong Liu, 2011–2013, Postgraduate. He studied in University of Science & Technology Beijing, major in Mining Engineering, study on paste filling; 2013-Present, Engineer, JCHX mining management co., LTD.

1 Introduction

Cemented paste backfill (CPB) is one of the most used backfilling techniques in modern underground mines (Peyronnard and Benzaazoua, 2012). Fill paste is usually made of thickening tailings, gelling agent, coarse aggregate (gravel, slag, etc.), water and other additives. It makes working environment more secure as well as more ores are produced, eliminates environment pollution and hidden danger which initiated by tailings surface discharge and prevents the surface subsidence after fill paste filled into mine. The setting and strength properties of fill paste are significant if above-mentioned effects are expected to achieve. The setting and strength properties of fill paste are influenced by gelling agent adding quantity, mass concentration, tailings physical and chemical properties, etc. Different kinds of ore require different chemical additions during mineral process. Thus, it makes the amounts of the metal ions contained in tailings are different, which have a huge impact on properties of fill paste. Especially zinc tailings often make the fill paste's setting time extend, early strength decreased and have a serious impact on the normal mining production (Benkendorff, 2006).

The setting and strength properties of fill paste are significantly influenced by cementing materials and relevant scholars have studied the effects of zinc on the properties of ordinary Portland cement. Zinc can delay the hydration process of ordinary Portland cement and even can lead it to completely stopped (Arliguie and Grandet, 1985; Arliguie and Grandet, 1990a, 1990b). During the slag backfill which contains lead and zinc, with the increase of zinc content in tailings and slags, setting times and strength growth of fill paste will extend accordingly (Benkendorff, 2006). Zinc ions will reduce the early strength of ordinary Portland cement significantly when adding soluble heavy metal ions to its slurry (Gineys et al., 2010). ZnO can influence the setting time and early

strength of ordinary Portland cement but the influence on the later strength is very weak with the extension of time (Fernandez-Olmo et al., 2001).

Relevant researchers have put forward the corresponding theory to explain the phenomenon of zinc ions make ordinary portland cement's setting time extend and early strength decreased. The research suggests that Zn^{2+} consumes OH^- in C_3S-H_2O system during the process of cement hydration and forms amorphous zinc hydroxide, zincates and other substances which covered on the surface of C_3S after precipitation and this process makes the dissolution of Ca^{2+} and OH^- hard and it also inhabits the hydration of C_3S (Mellado et al., 2013; Thomas et al., 1981; Weeks et al., 2008; Peyronnard et al., 2009). Coating materials mainly are $CaZn_2$ $(OH)_6{\cdot}2H_2O$ (Mellado et al., 2013), $Ca_6Zn_3Al_4O_{15}$ (Gineys et al., 2011) and contain a spot of Zn $(OH)_2$, $Zn_5(CO_3)_2(OH)_6$ and $ZnCO_3$ (Mellado et al., 2013). According to the content of Zn^{2+}, these substances will break automatically in 1–5 days and C_3S continues to hydrate (Hamilton and Sammes, 1999). The content of C_3S in cement clinker reaches about 50% and even more than 60% sometimes. In the process of cement hydration, zinc mainly exists in C_3S and interstitial phase, namely C_3A and C_4AF, and zinc mainly acting on C_3S which makes cement's setting time extend and early strength decreased (Gineys et al., 2011). In addition, when zinc nitrate is added to the ordinary Portland cement, 60% of the water in the cement will lost directly which is found by observation. Water is not fully participated in the hydration of cement which leads to the decrease of hydration products and affects condensation and early strength properties (Ortego et al., 1991).

Many solid wastes contain higher content of harmful heavy metals and salts, such as Cd, Pb, Zn, and Cr, which are water leaching (Collivignarelli and Sorlini, 2002). Sulphide is often used to recycle or curing these harmful heavy metals (Kuchar et al., 2006; Fukuta et al., 2004). Sulphide has tiny influence on the properties of cement paste, but can passivate chemical activity of zinc ion in hardened cement paste effectively when it is mixed in cement paste which contains zinc ions (Shi and Shi, 2006). Sodium sulphide is a kind of commonly used reagents in mineral processing, it is widely used as depressant in flotation when processing non-ferrous metal minerals. Depressant is a kind of drug which can destroy or weaken the mineral adsorption of collector and increase mineral surface hydrophilic. The following methods can make the mineral depressed: eliminate activation ions in the solution (Chandra and Gerson, 2009), eliminate activation films on the surface of mineral and format hydrophilic films on the surface of mineral (Qiu et al., 2012).

Huize Lead-Zinc Mine is a large multi-plant enterprise whose business scope covers prospecting, mining, mineral processing and metallurgy fields. It is an important lead, zinc and germanium base of China, it is also the first metal mine (Figure 1) which uses paste filling technology successfully (After thickening by Deep Cone Thickener, the underflow concentration of tailing is greater than 70%, then mixed with cement and water quenching slag by mixer and pumped to underground filling) and the longest conveying distance of filling slurry has reached up to 5.2 km. Proved reserves of lead and zinc in Huize Lead-Zinc Mine is more than eight million tons, and the vertical buried depth of ore body is 700–1200 m (mining depth has got 1600 m now). Strike length of ore body is 150–300m, thickness is 5–40 m and the dip angle is 60–70°, average grade of lead and zinc is more than 37% and rich in rare metals such as silver, germanium and cadmium. The most obvious characteristic of deep ore body is ore rock fragmentation, strong in situ rock stress and rock burst possibility. Therefore, upward/downward drift stopping and cemented filling is applicative in deep mining.

Figure 1 The cemented paste backfill system of Huize Lead-Zinc Mine: (a) deep cone thickener and (b) CPB mixer (see online version for colours)

(a) (b)

In addition, the tailings pile amount of stock is up to 600,000 tons in Huize Lead-Zinc Mine, water quenching slag pile amount of stocks is up to one million tons and the discharge amount of them increases by 250,000–300,000 tons each year. At the same time, tailing dam and water quenching slag yard are closing to service life and they cannot be expended, being restricted by the mining area terrain. Mine areas belong to the water and soil conservation and environmental conservation of upper Yangtze River, and industrial waste and stockpiling are strictly restricted. As a result, the backfilling and water quenching slag become the preferred filling materials. In the actual production process, when unclassified tailings and water quenching slag are used as filling materials, it shows that coagulation time is abnormal and the earth strength is low. The experimental data shows that the initial setting time of filling paste is 120 h and the final setting time is 366 h when the concentration is 80% and the weight ratio of filling material is 1 : 1 : 7 (cement:water quenching slag:unclassified tailings). The setting time of filling paste will be longer and even no condensation if the concentration of filling paste or cement single consumption becomes lower. However, it requires 7 days to get to the next cycle of extraction in filling stope generally. So it cannot meet the requirements of mining technology obviously. Improving cement–sand ratio and the dosage of cement can solve this problem but this will increase the filling cost (20–25 USD/m^3) or increasing cycle period of mining stope and prolonging fill paste's maintenance time. However, this will reduce the stope production capacity. So it is necessary to find more suitable additive to shorten fill paste's setting time and improve its early strength and improve the performance of filling slurry by experiments. Reducing the filling cost and meeting the safety production are urgent problems for Huize Lead-Zinc Mine to solve.

This paper combines the key issues of fill paste's long setting time and low early strength in Huize Lead-Zinc Mine and analyses retarding mechanism by experiments. On the basis of above, research on sodium sulphide's procoagulant effects upon zinc tailings and a solution for fill paste's retarding and low early strength problem in Huize Lead-Zinc Mine will be put forward.

2 Material and methods

2.1 Material

2.1.1 Tailings characteristics

Tailings used in experiments are unclassified tailings which come from Huize Lead-Zinc Mine's ore dressing workshop after mineral floatation. Its density is 2.75 g/cm^3, bulk density is 1.75 g/cm^3 and porosity is 36.36% (Table 1). Average particle size is 75.59μm, the median particle size is 34.95 μm and the less than 20 μm particles content is 37.20% (particle size compositions as shown in Figure 2). The chemical composition and mineral composition are shown in Tables 2 and 3, respectively. The content of CaO is 31.23% and that of zinc is 2.46%. The main mineral components in tailings are calcite (52.47%) and dolomite (30.33%) and containing zinc mineral mainly are sphalerite (1.25%), cerusite (0.64%), galena (0.53%) and calamine (0.40%). So the main characteristics of tailings in Huize Lead-Zinc Mine are: grain sizes are fine and zinc content is high.

Table 1 Physical properties of the filling material

Item	*Special gravity*	*Bulk density* (g/cm^3)	*Porosity* (%)
Tailings	2.75	1.75	36.36
Slag	2.59	1.18	54.44
Cement	3.1	1.3	58.06

Figure 2 Particle size distribution of the tailings (see online version for colours)

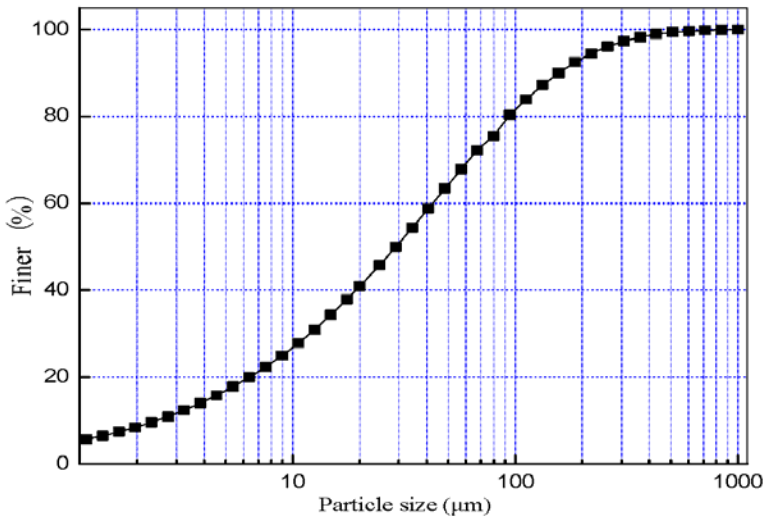

Table 2 Chemical composition of the tailings and slag

Compound	*Fe_2O_3*	*SiO_2*	*Al_2O_3*	*CaO*	*MgO*	*S*	*Pb*	*Zn*
Tailings/%	2.99	4.68	1.77	31.23	12.47	1.24	1.17	2.46
Slag/%	34.84	33.14	7.15	15.26	3.98	0.21	–	–

Table 3 Mineral composition of tailings %

Galena	*Sphalerite*	*Pyrite*	*Cerusite*	*Calamine*	*Limonite*	*Calcite*	*Dolomite*	*Quartz*
0.53	1.25	2.88	0.64	0.40	1.59	52.47	30.33	2.88

The high zinc content of tailings in Huize Lead-Zinc Mine mainly comes from the following two aspects:

- The raw ore belongs to mixed ore of oxygen and sulphur in which grade of zinc is 20.04%. The oxidation rate of zinc ore in raw ore is as high as 15.45%, belongs to mixed ore and is hard to separate. Zinc in ores mainly exists in the form of sulphide, zinc in sphalerite accounts for 83.39% of total zinc and zinc in smithsonite accounts for 13.41% of the total zinc, still there are 2.62% of zinc existed as the form of silicate minerals hemimorphite. Huize oxide lead-zinc ore mainly exists as the form of smithsonite ($ZnCO_3$) and hemimorphite ($Zn_4[Si_2O_7](OH)_2H_2O$) and it has been a problem for mineral processing industry in disposal and recycle this kind of ore. Therefore, a large amount of oxide lead-zinc ore which is hard to separate through flotation still exist in unclassified tailings and make the content of zinc on the high side.
- By adding the 1300–1500 g/t $ZnSO_4$ as inhibitors of sphalerite in the process of ore dressing, tailing slurry, whose concentration is 20–20% after dressing, pumped into Deep Cone Thickener to dewatering directly and manufactured into fill paste. So fill paste contains a small amount of zinc ions which come from flotation reagents.

2.1.2 Granulated slags

Coarse gravel sand filling mining method is always used in Huize Lead-Zinc Mine, and there have accumulated more than one billion tons of water quenching slag after 50 years of mining. The unclassified tailings backfilling system (Figure 1) was built in 2006, and fill paste which was prepared with tailings and water quenching slag (was) delivered into mine. The particle size distribution of the slag is shown in Table 4. It shows that the particle grade of water quenching slag is bolder than that of tailings. Combining both of them can improve the filling paste size fraction and make the size fraction tend to be more reasonable. The chemical composition of the slag is shown in Table 2 and the main chemical compositions of water quenching slag are Fe_2O_3 (34.84%), SiO_2 (33.14%) and CaO (15.26%). The unground slag samples blended in tailing/slag proportions is of 7/1 in the filling ratio.

Table 4 Particle size distribution of the slag

Particle size/mm	*0.071*	*0.087*	*0.11*	*0.15*	*0.2*	*0.3*	*0.45*	*1.25*	*2.5*	*3.5*
Cumulative passing/%	1	1.09	1.84	2.4	2.96	3.52	7.04	38.52	81.48	100

2.1.3 Cement

As upward/downward drift stoping and cemented filling is always used in Huize Lead-Zinc Mine, filling body must have a certain amount of strength to meet the mining operations of staff or trackless equipment on the upper/bottom of it. Thus, adding

P·O 32.5R grade cement as gelling agent is adopted. The density of the cement is 3.1g/cm^3. The bulk density of the cement is 1.3 g/cm^3. The main physical properties are shown in Table 1.

2.1.4 Water

Tap water was used to mix the cement and tailings. The amount of water was varied to obtain CPB mixtures with the desired consistency.

2.2 Retarding experiment of fill paste

In this paper, for the purpose of studying zinc ions impact on fill paste condensation, $Zn(NO_3)_2$ is used to change the content of zinc ion in filling paste, meanwhile study the change law of paste coagulability in different contents of zinc ions. Experiments are carried out in accordance with the existing paste filling ratio in Huize Lead-Zinc Mine, that is, paste concentration is 80% and the ratio of tailings:water quenching slag:cement is 7 : 1 : 1. Tailings used in experiments soaking in water for 48 h and flushing by water repeatedly as far as possible to remove the soluble zinc ions in it. $Zn(NO_3)_2$ is added according to the percentage of the total amount of tailings, and the adding quantity is 0%, 0.01%, 0.03%, 0.06%, 0.1% and 0.5%, respectively. Then take the fill paste setting time experiments in different contents of $Zn(NO_3)_2$.

2.3 Procoagulant experiment of fill paste

Taking the procoagulant experiment of fill paste based on the retarding experiment to reduce the fill paste setting time and improve the early strength.

Sulphide refers to a kind of compounds which is formed with metal or nonmetal that has a strong electricity and sulphur. According to the size of the metal sulphide solubility product, sulphide precipitated out abilities that range from easy to difficult are Hg^{2+}, Ag^{+}, As^{3+}, Bi^{3+}, Cu^{2+}, Pb^{2+}, Sn^{2+}, Zn^{2+}, Co^{2+}, Ni^{2+}, Fe^{2+} and Mn^{2+}. For the majority of inorganic sulphide, it is hard for the compounds to be dissolved as the sulphur ions are soft base and most of the metal ions except alkali metal are soft acid. And most of the alkali metal ions are hard acid, so the alkali metal sulphide is more easily dissolved. For example, Na_2S is commonly used in mineral processing. The solution shows alkali after hydrolysis. Na_2S is commonly used as base instead of NaOH in industry because of its low cost and the hydrolysis reaction is given as follows:

$$S^{2-} + H_2O \rightleftharpoons HS^{-} + OH^{-} \tag{1}$$

Industrial sodium sulphide (purity > 60%), which is commonly used in mineral processing, is applied as coagulant in experiments, and the ratio of tailings:water quenching slag:cement is 7:1:1 and the concentration of paste is 80%. Sodium sulphide is added according to the percentage of the total amount of tailings, and the adding quantity is 0%, 0.1%, 0.12%, 0.14%, 0.16%, 0.18% and 0.2%, respectively. To test the setting time of paste and 7d, 14d and 28d uniaxial compressive strength (UCS), respectively, analyse the hydration products by using differential scanning calorimetry (DSC).

2.4 Apparatus and testing procedures

2.4.1 Setting time test of CPBs

The same as the method used in the mortar, the mortar coagulating time tester SZ-100 is used to test the coagulation property of CPBs. And the penetration resistance is used to represent the coagulation rate and coagulation time.

Technical parameters of the mortar coagulating time Tester:

- *Range*: 0–100 N
- *Resolution*: 1%N
- *Maximum stroke*: 50 mm
- *Sectional area of the penetration needle*: 30 mm^2
- *Inner diameter and deep of the mould*: φ140 mm × 75 mm.

The testing procedure is carried out by the following steps:

- According to the proportion, mix the materials into paste, and place the paste into the moulds (Figure 3).

Figure 3 Setting time test of CPBs (see online version for colours)

- Measure the penetration resistance value. Adjust the penetration needle to just touch the upper surface of paste. Then control the needle to penetrate slowly and uniformly into the paste to 25 mm in 10 s, and the pressure is recorded from the scale. And make sure that the penetration needle be 12 mm away from the container's edge or the penetrated part.
- Under the condition that the temperature is (20 ± 2)°C, and after 2 h, start measuring the penetration resistances every half an hour. When the penetration resistance value is 0.3 MPa, measure the penetration resistance at 15-minute intervals, until the penetration resistance value is 0.7 MPa.

- The calculation of penetration resistance value is given as follows:

$$F = N \times g / A \tag{2}$$

where F is the penetration resistance value (MPa), N is the pressure gauge reading when the penetration depth reaches 25 mm (kg), g is the acceleration of gravity (m/s^2), and A represents the sectional area of the penetration needle, which is 30 mm^2.

- Determination of the coagulating time

The time and penetration resistance value are recorded, respectively. And the graph of relation between the time and penetration resistance value is drawn. Calculate the time needed, which is the coagulation time, when the penetration resistance value reaches 0.5 MPa from the graph.

The average coagulating time of two measurements at two samples of the same paste is calculated as the coagulating time of the paste. And the errors of two results should not be greater than 30 mins, otherwise it should be measured again.

2.4.2 Uniaxial compressive strength (UCS) test of the CPBs

The UCS of the CPBs is an important index for the organisation of the backfill procedure. On account of the coagulation experiment, the UCS test is to research the influence of Na2S on the CPBs' strength, especially the early stage influence.

The procedure of UCS test to place the paste, which is mixed under a certain proportion, into the 7.07 × 7.07 × 7.07 cm^3 three-in-one moulds is to maintain the CPBs in a standard curing room temperature: 20°C ± 1°C and humidity: more than 90%. The UCS test is carried out at a certain age, which is designed as 7d, 14d and 28d, and an electro hydraulic servo controlled rock pressure testing machine DYE-2000 is used in the lab. Its technical parameters are as follows:

- *Maximum force (KN)*: 2000
- *Resolution (%)*: ±1
- *Maximum distance between the two press plates (mm)*: 320
- *Size of press plate (mm)*: 250 × 25
- *Maximum stroke of the piston (mm)*: 50.

2.4.3 DSC of the hydration products

Thermal analysis is an important way to research the composition of the binder hydration products. The hydration products composition can be roughly known by the position of dehydration peak which is obtained through thermal analysis. The NETZSCH's DSC404C is used in the paper to research the influence of zinc ion and sodium sulphide on the hydration products according to the temperature when the endothermic peak appears.

3 Results and discussion

3.1 The influence of zinc ions content on fill paste setting time

Figure 4 shows the influence of different contents of zinc nitrate on the setting time of CPB. A conclusion got from Figure 4 is that zinc nitrate has obvious retarding effect on fill paste, and the retarding effect is most obvious when mixed with 0.06% of zinc nitrate, and the setting time will reach up to 127 h. With the increase of zinc nitrate, the setting time of fill paste decreases and the retarding effect of zinc nitrate reduces. Due to the addition of $ZnSO_4$ which is used as the inhibitor of sphalerite in mineral processing and residues containing zinc, it is inevitable to introduce zinc ions in tailings of Huize and make the setting time of fill paste extended.

Figure 4 Effect of zinc nitrate content on setting time of CPB

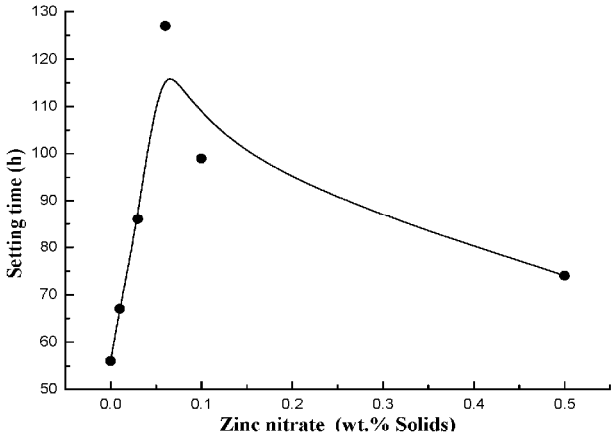

Fill paste shows the condensation characteristic as the addition of cement and zinc ions in tailings causes setting time extension as involved in the cement hydration. The content of tricalcium silicate (C_3S) in cement clinker is 50%, sometimes even more than 60%, so the gelling properties of fill paste depend on the hydration of C_3S, its product and the formed structure to a large extent. The hydration reaction of C_3S at room temperature is shown as follows:

$$3CaO \cdot SiO_2 + nH_2O = xCaO \cdot SiO_2 \cdot yH_2O + (3-x)Ca(OH)_2 \quad (3)$$

The above equation shows that the main hydration products of C_3S are C-S-H and C-H. The hydration rate of C_3S is quick and the hydration process can be divided into following five stages according to the hydration heat release rate-time curve (Figure 5):

1 *Preinduction period*: A sharp reaction appears immediately after adding water, but the time of this stage is very short, which could end in a few minutes.

2 *Induction period*: The reaction rate in this stage is very slow, it is almost stationary, and lasts 1–4 hours commonly, and this is because of that Portland cement could keep the plastic in a few hours. Initial setting time is basically equivalent to the end of the induction period.

3 *Acceleration period*: The reaction speeds up again, the reaction rate increases over time, the second exothermic peak appears and this stage ends up when the peak is reached (4–8 h). At this time, the final setting is over and begins to hardening.

4 *Deceleration period*: At this stage, the reaction rate falls over time, lasts approximately 12–24 h, hydration is affected by diffusion rate gradually.

5 *Stabilisation period*: The reaction almost stays in stable state, the reaction rate is very low and the hydration completely controlled by the diffusion rate.

Figure 5 Change curve of the hydration rate of C_3S and calcium concentration (see online version for colours)

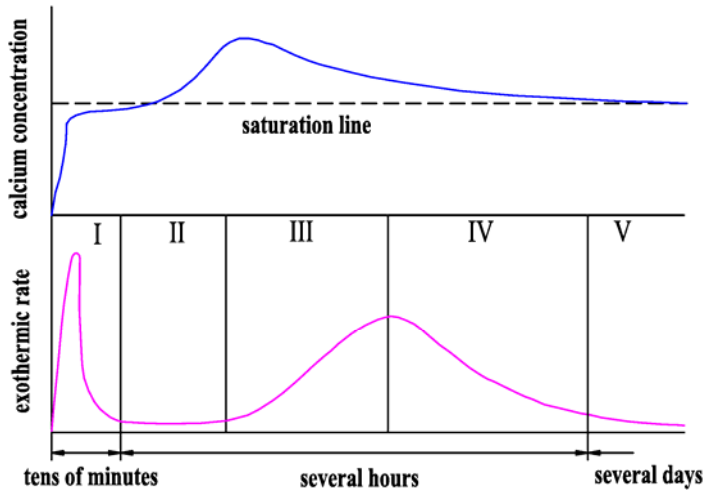

The hydrated process of calcium silicate shows that at the beginning of adding water, the reaction responses very quickly, but soon enters the induction period and the reaction rate becomes quite slow. With the ending of the induction period, the hydration accelerated again and generated more hydration products. The setting property of fill paste has a lot to do with the time of induction period to a large extent, and many scholars have done a lot of research about it and they have different ideas about the essence of the induction period.

- Protective coating theory (De and Stein, 1967). It insists that the induction period is due to the forming of protective film layer by the hydration products. The induction period ends with the damage of the protective film layer. Assuming C_3S is congruent dissolution in water, C_3SH_n, the originally generated first hydration products, formed a dense protective film layer around the C_3S, which hindered the further hydration of C_3S, make the heat release slowly and the dissolution rate of Ca^{2+} to the liquid phase correspondingly reduced, and lead the beginning of the induction period. When the first hydration products translated into the second hydration products which can more easily through the ions, hydration accelerated again, more Ca^{2+} and OH^- passed into the liquid phase and reached supersaturation, exothermic process accelerated and the induction period is over.

- Nucleation theory of delay. By this theory the induction period is due to the formation and growth of the calcium hydroxide or C-S-H or the crystal nucleus of them requires certain time which delayed the hydration. C_3S is incongruent dissolution initially and mainly Ca^{2+} and OH^- dissolved, the content of C/S is too high in liquid phase and makes the surface of C3S turned into calcium deficiency 'silica-rich layer' (Tadros and Kalyoncu, 1976). Then, Ca^{2+} adsorb onto the surface of the silica-rich layer, making itself bring positive charge and form the double electric layer. Thus, the velocity of Ca^{2+} dissolved from C_3S slowed down and led the beginning of the induction period. Only until the Ca^{2+} and OH^- increased slowly and achieved enough saturation, a stable nucleus of $Ca(OH)_2$ can formed. When the $Ca(OH)_2$ crystal grows to a certain size and quantity is big enough, the Ca^{2+} and OH^- can precipitate it quickly, impel C_3S dissolved and the hydration accelerated again.
- Summarising the above ideas (Jawed and Skalny, 1988). After contacting with water, the hydrolysis occurs at the site of lattice defects on the surface of C_3S, namely the activation site. The Ca^{2+} and OH^- enter into the solution and form a calcium deficiency 'silica-rich layer' at the surface of C_3S. Then Ca^{2+} adsorbed onto the surface of the silica-rich layer and formed the double electric layer, preventing the dissolve of C_3S and the induction period arose. On the other hand, the double electric layer induced ζ potential which made the particles in solution to keep in dispersion state and condensed until the potential declined close to zero. As the hydration of C_3S is still slow, the crystal of $Ca(OH)_2$ will be precipitated and lead the ending of the induction period when the concentration of $Ca(OH)_2$ in the solution reaches to a certain super saturation degree.

So the length of hydration induction period of the fill paste affects its coagulation characteristics directly. The research of effects of ZnO on hydration characteristics of ordinary Portland cement shows that the introduction of the zinc ions essentially affected the ongoing dynamic response of cement hydration (Gawlicki and Czamarska, 1992). The zinc ions in the fill paste exists in C_3S-H_2O system and forms amorphous zinc hydroxide, inhabiting the hydration of C_3S, and then further lead (leads) to the prolongation of C_3S hydration induction period. This is mainly due to the formation of zinc hydroxide or calcium zincate wrapped on the surface of C_3S and relative thickening of the 'protective film' or 'silica-rich layer' of C_3S and make the dissolution of Ca^{2+} and OH^- in C_3S difficult. On the other hand, zinc ions adsorbed on the incipient crystal of new phase during the process of hydration reduced the formation rate of incipient crystal in saturated solution and prevented the development of slurry initial structure. Due to the above-mentioned two aspects, zinc ions caused the prolongation of the induction period (Figure 6) and increased the setting time of fill paste. Thus, to eliminate the retarding effect of zinc ions on fill paste, the most important is to eliminate the formation of zinc hydroxide or zincate and shorten the induction period of hydration, so as to reduce the setting time of fill paste.

3.2 The influence of sodium sulphide content on fill paste setting time

Figure 7 shows the influence of different contents of sodium sulphide on the setting time of CPB. Figure 7 shows that the setting time of fill paste is 128 h without adding sodium sulphide. With the increase of sodium sulphide, the setting time of fill paste decreased

sharply and it is only 18 h when mixed with 0.2% of sodium sulphide which reduces 110 h than without adding sodium sulphide. Therefore, sodium sulphide has significant effect on fill paste procoagulant and can reduce the setting time greatly. It is not that the shorter the setting the better the actual filling of Huize Lead-Zinc Mine, but the setting time and mining production should coordinate with each other and generally the setting time is between 40 and 50 h according to the actual circumstance of mine. So it can meet the demand of mine on the setting time when the mass concentration of fill paste is 80%, the ratio of tailings:water quenching slag:cement is 7 : 1 : 1 and the addition amount of sodium sulphide is 0.12% of the tailings.

Figure 6 Diagram of CPB hydration reaction in different hydration periods (see online version for colours)

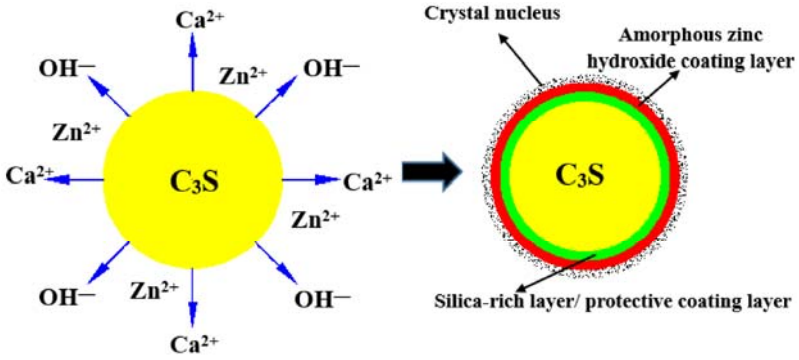

The industrial sodium sulphide ($Na_2S{\cdot}9H_2O$) chosen in experiments is purple flake solid, in which hydrolysis reaction can easily occur and make the solution strong alkaline. The reaction equations are given as follows:

$$Na_2S+H_2O \rightleftharpoons 2Na^+ + 2OH^- + H_2S \tag{4}$$

$$H_2S \rightleftharpoons H^+ + HS^- \tag{5}$$

$$HS^- \rightleftharpoons H^+ + S^{2-} \tag{6}$$

Figure 7 Effect of Na_2S content on setting time of CPB

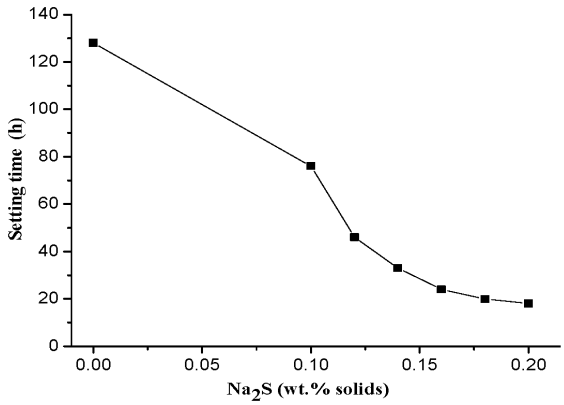

The above reaction equations show that the sodium sulphide solutions contain S^{2-}, HS^{-}, OH^{-}, Na^{+} and H_2S, they shorten the setting time of zinc contained fill paste. Its function is mainly reflected in the following two aspects:

- Ionised S^{2-} from sulphide solution can react with many metal ions, such as Cu^{2+}, Pb^{2+}, Zn^{2+}, Co^{2+}, Ni^{2+} and generate hard dissolve sulphide precipitate, just as reaction zinc ions in formula 7. Zinc ions in the tailings participate in hydration and the probability of affecting the induction period reduced greatly. Delfini et al. (2003) and others use this principle to remove the arsenic in the tailings by using sodium sulphide. The content of arsenic can be reduced from 2000 ppm to 500 ppm after adding sodium sulphide.

$$Zn^{2+} + S^{2-} = ZnS \downarrow \tag{7}$$

- It is inevitable to add some kinds of reagents in mineral process and a certain amount of mineral processing reagents are left in the tailings. When the tailings and cement mixed with water, these reagents adsorbed on the surface of the tailings and cement particles and formed hydrophobic membrane which hindered the hydration. As $HS^{-}$and S^{2-} have strong affinity with sulphide, they can desorb these reagents which are on the surface of the tailings by strong adsorption and form hydrophilic film on the surface of particles of the tailings and cement, and this can promote the hydration of fill paste.

3.3 The influence of Na_2S content on fill paste compressive strength

Figure 8 shows the influence of different contents of sodium sulphide on strength properties of CPB. Figure 8 shows that the 7d UCS of fill paste increases with the increase of the amount of sodium sulphide. When mixed with 0% sodium sulphide, the strength is only 0.76 MPa and it increased to 1.87 MPa when the content of sodium sulphide is 0.2%. The 14d and 28d UCS of fill paste all decreased with the increase of sodium sulphide content and different from the 7d UCS change trend. The 14d UCS decreased from 3.13 MPa to 2.40 MPa with the content of sodium sulphide changed from 0% to 0.2%, and the 28d UCS decreased from 3.93MPa to 3.35MPa with the content of sodium sulphide changed from 0% to 0.2%. Therefore, sodium sulphide can effectively improve the 7d UCS of fill paste and have a reducing effect on the 14d and 28d UCS. Based on the actual production situation in Huize Lead-Zinc Mine and considering the factors of trackless mining equipment and blasting vibration, the 7d UCS of fill paste greater than 1.2 MPa can meet the production requirements. So the addition of sodium sulphide improved the early strength of fill paste and correspondingly improved the mining efficiency in Huize Lead-Zinc Mine.

Generally, the strength of cement paste backfill (CPB) increases with the maintenance time prolongs. However, with the above experimental results, the addition of sodium sulphide improves the 7d UCS of fill paste and makes the 14d and 28d UCS decreased at the same time. Zinc ions have effects on the early strength of cement (Benkendorff, 2006; Gineys et al., 2010; Fernandez-Olmo et al., 2001) but have no significant effects on the strength with the maintenance time prolongs. So the addition of sodium sulphide relatively delays the effects of zinc ions on the strength of fill paste and makes the 14d and 28d UCS decreased. The sulphide in tailings can improve the early strength of fill paste but have adversely effects on the later strength (Zhang et al., 2004). Li et al. (2004)

and others chose zinc as the research object to study the effect of sodium sulphide on fill paste strength. The test results shows the strength of zinc tailings begin to decrease after 28d and this has important relationship with that the tailings contain a large number of sodium sulphide. By oxidation, the sodium sulphide in fill paste can generates sulphate which will react with cement hydration products in fill paste and generate $CaSO_4 \cdot 2H_2O$ and $3CaO \cdot Al_2O_3 \cdot 3CaSO_4 \cdot 32H_2O$. The products can lead to expansion cracks of fill paste and adverse to the enhancement of strength.

Figure 8 The effect of Na_2S content on the mechanical performance of CPB samples (see online version for colours)

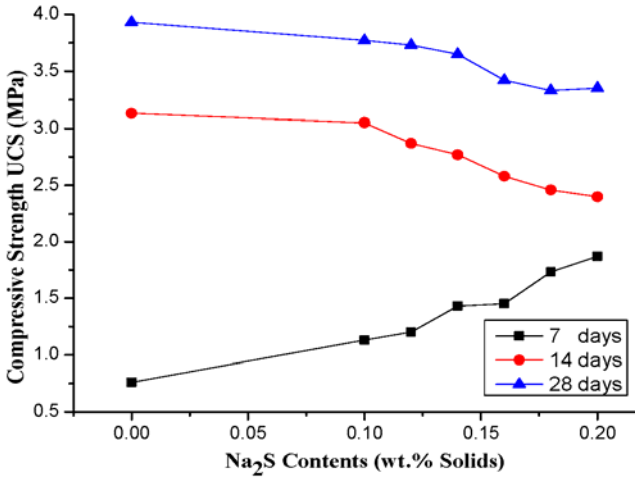

3.4 DSC-TG analysis of fill paste hydration products

To analyse the change of hydration products of fill paste before and after adding sodium sulphide by DSC-TG, the dehydration endothermic peak of CSH in cement paste slurry at about 105°C, AFt dehydration at 125°C–140°C, AFm dehydration at 175°C, hydrated calcium aluminate dehydration at 200°C–300°C, AH_3 dehydration at about 300°C, $Ca(OH)_2$ dehydration at 450°C and carbonate formed by hydration products appears decomposition peak at about 800°C. In the actual test, due to the influence of heating speed, the relative contents of material and the degree of crystallisation, and there will be some deviation with the peak value of the corresponding temperature.

Figure 9 is the DSC-TG map of 7d hydration products of fill paste without adding sodium sulphide. Compared with the cement paste, the peak on the curve in Figure 9 is very weak, this is mainly because less cement in fill paste. The endothermic peak appearing at 105°C is caused by dehydration of CSH, the peak appearing at 140°C caused by AFt, the peak appearing at 520°C caused by $Ca[Zn(OH)_3H_2O]_3$ and carbonate formed by hydration products appears decomposition peak at about 800°C. There is no $Ca(OH)_2$ dehydration peak in Figure 9, which means there is no $Ca(OH)_2$ generated in fill paste or only few generated and conversed to other substances under the condition of no sodium sulphide added.

Figure 9 The DSC-TG map of 7d hydration products of fill paste without adding Na_2S (see online version for colours)

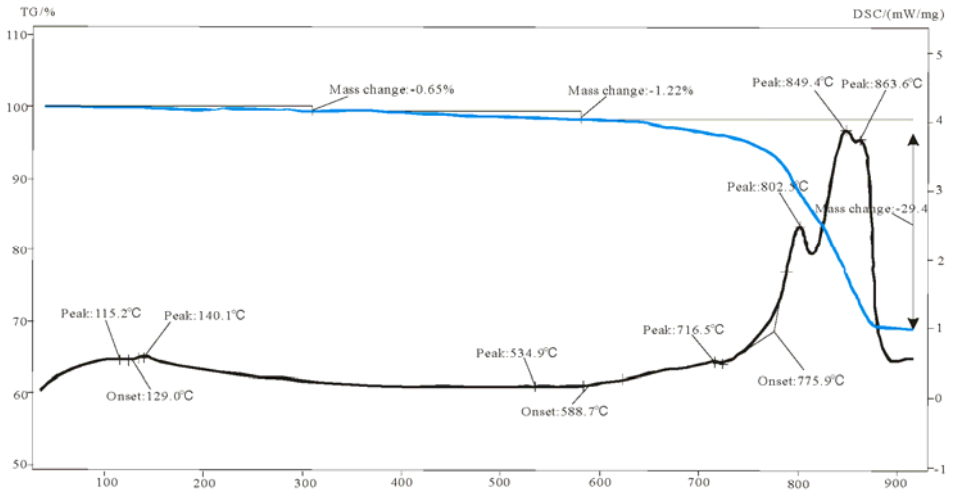

Figure 10 shows the DSC-TG map of 7d hydration products of fill paste with adding sodium sulphide. Figure 10 shows endothermic peak appears at about 105°C, 470°C and 800°C caused by CSH, $Ca(OH)_2$ and carbonate formed by hydration products. There is still no AFt endothermic peak appeared on the curve. Compared with hydration products of no sodium sulphide added, the content of hydrated calcium silicate and calcium hydroxide in fill paste increased significantly after adding sodium sulphide. This means zinc ions have significant inhibitory effect on fill paste hydration and adding sodium sulphide can eliminate the effect of zinc ions and promote the hydration.

Figure 10 The DSC-TG map of 7d hydration products of fill paste with adding Na_2S (see online version for colours)

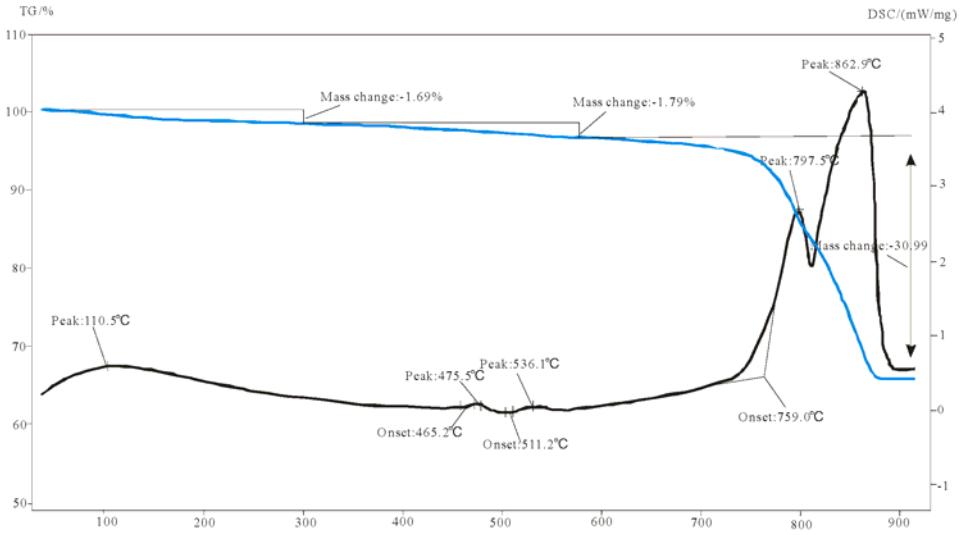

4 Feasibility analysis of adding sodium sulphide

Sulphide is often used to recycle or curing harmful heavy metals (Cd, Pb, Zn, Cr, etc.) in waste water and soil. Sodium sulphide is a kind of commonly used reagents in mineral processing, and widely used as depressant in flotation when processing non-ferrous metal minerals. Thus, the process of adding sodium sulphide to the paste can be learned from related fields of mature process route and safety measures to avoid the process of adding physical harm to workers.

Through the experiments in this paper, the method of adding sodium sulphide can reduce the setting time, increase the early strength and improve mining efficiency.

Therefore, as shown in Figure 11, the device was reformed. 1 # and 2 # grooves are used to alternately produce sodium sulphide. Flow meter and valve are used to control the quantity of the sodium sulphide. The sulphide solution automatically flow to the mixer too and stir the paste evenly transported to stope for filling. By calculation, after adding sodium sulphide filling, the costs will increase 0.5–0.7 USD/m^3, but the mining cycle can be reduced by 7 days to 4 days, the mining effectively improve the mining efficiency. Thus, adding sodium sulphide to the paste is feasible in terms of technic and economic.

After adding sodium sulphide to the fill paste, the solution contains S^{2-}, HS^-, OH^-, Na^+ and H_2S. On the one hand, S^{2-} reacts with Zn^{2+} and generates sulphide precipitate which can eliminate the effects of zinc ions to a certain extent. On the other hand, $HS^-$and S^{2-} can desorb these reagents on the surface of the tailings and form hydrophilic film on the surface of particles of the tailings and cement, and this can promote the hydration of fill paste. Therefore, adding the sodium sulphide will not affect the environment underground. It is because the quantity of sodium sulphide is less and the sodium sulphide is consumed in the process of chemical reactions which produces insoluble sulphides.

Figure 11 Schematic diagram of adding sodium sulphide (see online version for colours)

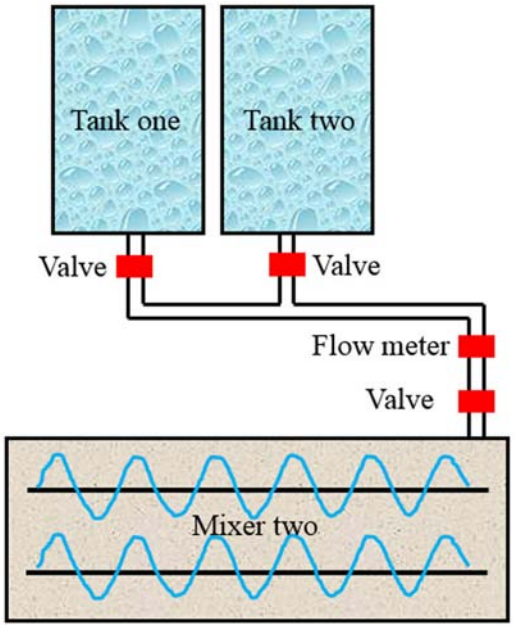

5 Conclusions

This paper takes the fill paste retarding phenomenon in Huize Lead-Zinc Mine as the research background, researches the influence law and mechanism of zinc ions on fill paste setting time and uses sodium sulphide as coagulant to eliminate the influence of zinc ions on fill paste setting time and early strength. The experiment has achieved ideal results and provides support for filling and mining successfully in Huize Lead-Zinc Mine.

- Zinc ions have significant effects on fill paste setting time and the setting time increased dramatically with the increase of zinc ions.
- Sodium sulphide has obvious coagulant function for fill paste and can shorten the setting time effectively. Setting time decreased from 128 h to 18 h with the content of sodium sulphide changed from 0% to 0.2% and it is sensitive to the content of sodium sulphide, and even small change can cause significant differences in setting time. Under the current filling ratio in Huize Lead-Zinc Mine (the mass concentration of fill paste is 80%, the ratio of tailings:water quenching slag:cement is 7 : 1 : 1), the reasonable addition amount of sodium sulphide is 0.11–0.13% of the tailings and the setting time controlled between 40 h and 50 h.
- Sodium sulphide has different influence on fill paste of different ages.
  The 7d UCS of fill paste increases with the increase of the amount of sodium sulphide, it increases from 0.76 MPa to 1.87 MPa with the content of sodium sulphide changes from 0% to 0.2%. The 14d and 28d UCS of fill paste all decreased with the increase of sodium sulphide content. As upward drift stoping and cemented filling is used in Huize Lead-Zinc Mine, a higher requirement (greater than 1.2 MPa) is needed to the early strength of fill paste especially the one before seven days. Therefore, the addition of sodium sulphide can greatly improve the compressive strength of fill paste before seven days and solve the problem of low early strength in Huize Lead-Zinc Mine.
- Analysed by DSC-TG, there is no $Ca(OH)_2$ dehydration peak in fill paste hydration products without adding sodium sulphide and CSH endothermic peak is also very weak. After adding sodium sulphide, $Ca(OH)_2$ dehydration peak appeared in fill paste hydration products, CSH endothermic peak and decomposition peak of carbonate formed by hydration products all stronger than that in no sodium sulphide added cases.

Acknowledgements

This work was financially supported by the National Natural Science Foundation of China (51374034, 51374035, 51304011), the Program for Chang Jiang Scholars and Innovative Research Team in University (IRT0950) the ‘12th Five-Year Plan’ national science and technology support program (2012BAB08B02, 2013BAB02B05).

References

Arliguie, G. and Grandet, J. (1985) 'Etude par Calorimétrie de L'Hydratation du Ciment Portland enprésence de Zinc', *CemConcr Res.*, Vol .15, pp.825–832.

Arliguie, G. and Grandet, J. (1990) 'Etude de l'hydratation du cimentenprésence de zinc.Influence de la teneurengypse', *CemConcr Res.*, Vol. 20, pp.346–354.

Arliguie, G. and Grandet, J. (1990) 'Influence de la composition d'un ciment Portland sur son hydratationenprésence de Zinc', *CemConcr Res.*, Vol. 20, pp.517–524.

Benkendorff, P.N. (2006) 'Potential of lead/zinc slag for use in cemented mine backfill', *Mineral Processing and Extractive Metallurgy (Trans. Inst. Min. Metall. C)*, Vol. 115, pp.171–173.

Chandra, A.P. and Gerson, A.R. (2009) 'A review of the fundamental studies of the copper activation mechanisms for selective flotation of the sulfide minerals', *Sphalerite and Pyrite*, Vol. 145, Nos. 1–2, pp.97–110.

Collivignarelli, C. and Sorlini, S. (2002) 'Reuse of municipal solid wastes incineration fly ashes in concrete mixtures', *Waste Management*, Vol. 22, pp.909–912.

De, J.G.M. and Stein, H.N. (1967) 'Hydration of tricalcium silicate', *Journal of Applied Chemistry*, Vol. 17, pp.246–250**.**

Delfini, M., Ferrini, M. and Mannib, A. (2003) 'Arsenic leaching by Na2S to decontaminate tailings coming from colemanite processing', *Minerals Engineering*, Vol. 16, pp.45–50.

Fernandez-Olmo, I., Chacon, E. and Irabien, A. (2001) 'Influence of lead, zinc, iron (III) and chromium (III) oxides on the setting time and strength development of Portland cement', *CemConcr Res.*, Vol. 31, pp.1213–1219.

Fukuta, T., Ito, T. and Sawada, K. (2004) 'Separation of nickel from plating solution by sulfuration treatment', *Asian J. Chem. Eng.*, Vol. 4, pp.24–31**.**

Gawlicki, M. and Czamarska, D. (1992) 'Effect of on the hydration of Portland cement', *Journal of Thermal Analysis*, Vol. 38, pp.2157–2161.

Gineys, N., Aouad, G. and Damidot, D. (2010) 'Managing trace elements in Portland cement – Part I: Interactions between cement paste and heavy metals added during mixing as soluble salts', *CemConcr Compos.*, Vol. 32, pp.563–570.

Gineys, N., Aouad, G. and Damidot, D. (2011) 'Managing trace elements in Portland cement – Part II: Comparison of two methods to incorporate Zn in a cement', *Cement & Concrete Composites*, Vol. 33, pp.629–636.

Hamilton, I.W. and Sammes, N.M. (1999) 'Encapsulation of steel foundry dusts in cement mortar', *Cem. Concr. Res.*, Vol. 29, pp.55–61.

Jawed, J. and Skalny, J. (1988) *Hydration of Portland Cement*, Pergamon Press, London.

Kuchar, D., Fukuta, T. and Onyango, M.S. (2006) 'Sulfidation of zinc plating sludge with Na_2S for zinc resource recovery', *Journal of Hazardous Materials*, Vol. B137, pp.185–191.

Li, J., Villaescusa, E. and Tyler, D. (2004) 'Factors affecting the quality underground mine back filling', *Mining Research and Development*, Vol. 24, pp.187–191.

Mellado, A., Borrachero, M.V. and Soriano, L. (2013) 'Immobilization of Zn(II) in Portland cement pastes Determination of microstructure and leaching performance', *J Therm. Anal. Calorim.*, Vol. 112, pp.1377–1389.

Ortego, J.D., Barroeta, Y., Cartledge, F.K. and Akhter, H. (1991) 'Leaching effects on silicate polymerization: An FTIR and 29Si NMR study of lead and zinc in Portland cement', *Environ. Sci. Technol.*, Vol. 25, pp.1171–1174.

Peyronnard, O. and Benzaazoua, M. (2012) 'Alternative by-product based binders for cemented mine backfill: Recipesoptimisation using Taguchi method', *Minerals Engineering*, Vol. 29, pp.28–38.

Peyronnard, O., Blanc, D., Benzaazoua, M. *et al*. (2009) 'Study of mineralogy and leaching behavior of stabilized/solidified sludge using differential acid neutralization analysis', *CemConc Res*., Vol. 39, pp.501–509.

Qiu, T.S., Ding, S.Q. and Zhang, B.H. (2012) 'Application situation of sodium sulfide in the flotation', *Nonferrous Metals Science and Engineering*, Vol. 6, pp.39–43.

Shi, H.S. and Shi, H.C. (2006) 'The effects of zinc and sulfides on cement-based material', *Cement*, Vol. 2, pp.15–18.

Tadros, M.E. and Kalyoncu, R.S. (1976) 'Early hydration of tricalcium silicate', *Journal of the American Ceramic Society*, Vol. 59, pp.344–347.

Thomas, N.L., Jameson, D.A. and Double, D.D. (1981) 'The effect of lead nitrate on the early hydration of Portland cement', *CemConcr Res.*, Vol. 11, pp.143–153.

Weeks, C., Hand, R.J. and Sharp, J.H. (2008) 'Retardation of cement hydration caused by heavy metals present in ISF slag used as aggregate', *CemConcr Compos.*, Vol. 30, pp.970–978.

Zhang, Q.L., Wang, X.M. and Tian, M.H. (2004) 'Influence of sulphide on cement back fill strength', *Mining Research and Development*, Vol. 24, pp.168–169.

Predicting shear strengths of mine waste rock dumps and rock fill dams using artificial neural networks

Rennie Kaunda

Mining Engineering Department,
Colorado School of Mines,
1500 Illinois Street,
Golden, CO 80401, USA
Email: rkaunda@mines.edu

Abstract: Three new back-propagation artificial neural networks (ANNs) for predicting the shear strength envelopes of mine waste rock dumps and rock fill dams are presented. Fourteen key material properties for rock fill characterisation are mustered for model development and evaluation. Using principal component analysis, the initial fourteen parameters are ultimately reduced to six through data compression. The neural net with the fewest parameters (ANNOPTC) is consistent over the widest range of confining stresses for shear strength prediction. The three artificial neural networks also perform better than multiple regression conducted on the same global database. Sensitivity analysis ranks input parameters as normal stress, minimum particle strength, dry unit weight, 10% passing sieve size, the coefficient of curvature of the particle size distribution, and the coefficient of uniformity of the particle size distribution in decreasing order of significance. Excellent agreement is observed between predicted and measured shear strengths for new cases.

Keywords: ANNs; artificial neural networks; mine waste rock; rock dump; rock fill; shear strength; large triaxial test; direct shear test.

Reference to this paper should be made as follows: Kaunda, R. (2015) 'Predicting shear strengths of mine waste rock dumps and rock fill dams using artificial neural networks', *Int. J. Mining and Mineral Engineering*, Vol. 6, No. 2, pp.139–171.

Biographical notes: Rennie Kaunda is an Assistant Professor at Colorado School of Mines, Mining Engineering Department. Prior he worked with consulting firms offering mining geotechnical engineering services for over seven years. He has been involved in more than 50 global projects in Africa, Asia, South America and North America. He has performed or coordinated geotechnical engineering services related to open pit and underground mines, dams, foundations and landslides. He is also a licensed Professional Engineer in the State of Colorado, USA.

1 Introduction

As the global population continues to expand, the demand for natural and energy resources has also increased. A consequence has been increased mining activity leading to, among other engineering marvels, progressively deeper open pits in excess of 400 m,

with accompanying large rock waste piles from stripping and other operational activities. Rock waste piles or dumps require careful design, siting and construction to remain stable during the life of the mine and its operations. A second consequence of increased energy/power demands has been a global rise in the aggressive construction of massive rock fill dams. The design of both rock fill dams and rock waste dumps/piles necessitate an understanding of the insitu properties of the rock material including deformation, permeability and shearing resistance or strength.

It is well recognised that the shear strengths of materials in mine waste rock dumps and rock fill embankment/dams are nonlinear (Leps, 1970; Indraratna et al., 1993; Linero et al., 2007; Barton, 2013). Although insitu and large scale laboratory tests at high confinement for these materials have proved to be invaluable, their undertaking is not trivial as these tests are very difficult and expensive. Characterisation of shear strength is further compounded by differences in the method of construction of mine waste rock dumps vs. rock fill embankments/dams (Linero et al., 2007). Whereas rock fill structures are typically placed in lifts and compacted systematically, waste dumps are generally built by simply overturning truck loads resulting in low initial densities. In this paper, the terms 'waste rock' and 'rock fill' are combinedly referred to as 'rockfill' from this point; unless when a clear distinction between the two is required.

The rock particle size distribution/gradation and degree of confinement significantly influence the shear strength and deformability of the particulate material. For instance, well-graded material displays higher inter-granular contact resulting in high densities and shear strength. Increased pressure and confinement induced by layering and height leads to greater particle breakage and thus declining angles of friction. In addition, the parent material (i.e., geologic origin) of the constituents of the rockfill is seldom uniform. Thus the relatively weaker particles tend to breakdown further during loading, transportation and placement changing the physics/characteristics of the particle size distribution and associated shear strengths (Linero et al., 2007). Several previous studies including Valstad and Strøm (1975), Soroush and Jannatiaghdam (2012) and Barton (2013) demonstrate that in addition to the foregoing factors, angularity/roundness, moisture, roughness, porosity, and degree of compaction also influence shear strengths in rockfill materials. These outlined issues clearly define a nonlinear problem, making it a suitable candidate for an artificial neural network-based approach for shear strength characterisation.

2 Artificial neural networks

The ability to learn complex relationships among datasets and extrapolating the acquired knowledge to a brand new dataset is a major advantageous feature of artificial neural networks (ANNs) over physically-based models in nonlinear problems. Given that specific interrelationships of the physical parameters of the modelled system are not required apriori, an ANN does not directly depend on the physical laws of the system to function. ANNs consist of meshes of computing nodes (i.e., processing elements) and connections or weights (Figure 1), which can be trained to map data in a non-linear fashion upon activation (Wasserman, 1989; Bishop, 1995; Nielsen, 1988; Haykin, 1999; Gurney, 2009). Each connection is assigned a numerical value (i.e., weight) which can be changed during ANN training using several learning algorithm options, such as the gradient descent technique via back propagation (Rumelhart et al., 1986) summarised as:

$$\Delta w_{ji} = \delta_{pj} x_{pi} \tag{1}$$

$$\Delta w_{kj} = \eta \delta_{pk} act_{pj} \tag{2}$$

where Δw_{ji} = changes in connection weights between hidden (i.e., *j*th layer) and input (i.e., *i*th layer) layers, δp_j = derivative of error output with respect to sum between input and hidden layers, x_{pi} = value received by each input node, Δw_{kj} = changes in connection weights between hidden and output layers (i.e., *k*th layer), η = proportion of change in weight to error, δ_{pk} = derivative of error output with respect to sum between hidden and output layers, act_{pj}= activation parameter of the nodes in the output layer.

Figure 1 Illustration of typical feed-forward artificial neural network architecture with three layers: input layer, hidden layer and output layer. Each layer consists of processing elements (or neurons), which are connected to neighbouring layer neurons via a network of connection weights

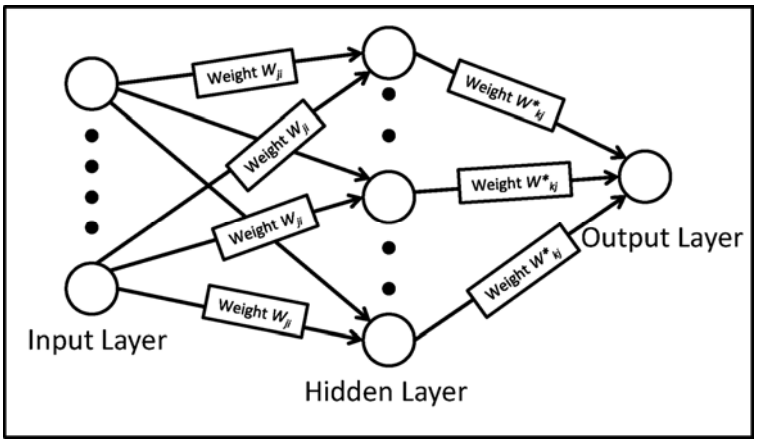

In general the procedure for developing a supervised ANN is to first select and prepare input and output parameters from raw data to create a training file. The ANN model architecture is then created, prior to inputting the training file into the ANN model. Next ANN training is initiated by implementing the gradient descent back propagation algorithm, using a training dataset and a validation dataset. If necessary, the ANN model is adjusted and refined based on training performance metrics. Upon completion of training, the ANN model weights are frozen and the ANN is ready to be tested on a fresh dataset.

During back propagation, a search for the global optimum combination of connection weights that yields minimum error is undertaken. During each iteration the accuracy of the ANN may be assessed using the mean squared difference between actual and predicted/output values (root mean squared error or RMSE):

$$\text{RMSE} = \sqrt{\frac{\sum_{i=1}^{T} (\text{error})^2}{T}} \tag{3}$$

where T is the total number of presented data.

During supervised ANN training, input/output data pairs are provided to the network. The provided inputs are used to predict outputs, which are in turn compared to the

provided target outputs. When selecting input/out pairs for ANN training, it is thus necessary to have some insight into the system dynamics of the problem to set constraints or boundaries for the problem. In addition the input/output suite prior to training should be developed such that the data patterns are statistically similar (i.e., mean, standard deviation and range) to the actual system being modelled (Masters, 1993).

Hammerstrom (1993) recommends using two-thirds of the overall dataset for model training and one-third for validation. In addition, ANN datasets should be pre-processed to ensure all variables receive equal attention during the training process (Masters, 1993; Maier and Dandy, 2000). The input data to the ANN model should match the limits of the transfer functions used in the network output layer (e.g., between –1.0 to 1.0 for the hyperbolic transfer function and 0.0 to 1.0 for the sigmoid transfer function) (Shahin et al., 2008). One hidden layer in an ANN is often sufficient to approximate any continuous function provided that sufficient connection weights/processing elements are given, and the appropriate activation function is used (Cybenko, 1989; Hornik et al., 1989; Bishop, 1995). A widely applicable activation function is the sigmoid (logistic) function: $y = 1/(1 + \exp^{-x})$ (Bishop, 1995). Caution should be taken not to overuse connections/weights as this may lead to ANNS that are more subjective to over-fitting the data and poor generalisation (Masters, 1993; Maren et al., 1990; Rojas, 1996). The number of hidden nodes should be kept to a minimum (Shahin et al., 2008), and perhaps the most efficient approach, is to begin with a small number of nodes and iteratively increase that number until no significant improvement in model performance is achieved (Nawari et al., 1999).

The performance of ANN models may be evaluated using the coefficient of correlation, R^2, root mean squared error, RMSE, and the mean absolute error, MAE, between the predicted and observed data (Shahin et al., 2008). Smith (1986) suggests the following guidelines for $|R|$ values between 0.0 and 1.0:

- $|R| \geq 0.8$ strong correlation exists between two sets of variables
- $0.2 < |R| < 0.8$ correlation exists between the two sets of variables
- $|R| \leq 0.2$ weak correlation exists between the two sets of variables.

The RMSE is the most popular measure of error and has the advantage that large errors receive much greater attention than small errors (Hecht-Nielsen, 1990). In contrast to RMSE, MAE eliminates the emphasis given to large errors. However, both RMSE and MAE may be desirable when the evaluated output data are smooth or continuous (Twomey and Smith, 1997). Being completely dependent on datasets is in one sense a handicap for ANNs because any errors present in the data are inherited by the ANN model, potentially leading to ANN models which are in contradiction to physical laws and reality. It is therefore imperative to understand the source and limits of available datasets, including the boundary condition of a particular ANN model.

3 Establishment of database

Prior to ANN model development, a selection of appropriate predictive input parameters controlling the shear strength of rockfill needs to be undertaken based on previous observations and experience. In this study, the input parameters were derived from the particle material size (or sieve) gradation, fineness modulus, gradation modulus,

material hardness, relative density, and confining (normal) stress, all discussed in Sections 3.1–3.6. The output variable was represented by large scale laboratory shear strengths upon conducting an extensive global literature review. The database compiled from the literature for the ANN development is summarised in Table 1. By collecting 189 datasets tested at more than 10 different sites around the world (Table 1), the ANN models were developed, trained and their overall performance evaluated. The data were then preprocessed using the guidelines discussed in Section 2, and further elaborated in Section 4. The rationale behind the selection of the particular set of input parameters used in this study is discussed as follows.

3.1 Material gradation

The effects of rockfill particle size gradation on shear strength have been confirmed by several researchers (e.g., Marachi et al., 1969; Douglas, 2002; Ghanbari et al., 2008). However, divergent views are presented in the literature with regards to the effects of specific particle size ranging from none (e.g., Charles and Watts, 1980), to reduced strengths when the particle size increases (Marachi et al., 1972; Marsal, 1973). Given that insitu particle sizes are often too large for large scale laboratory test apparatus, the standard procedure is often to scale down the distribution by either truncation or parallel scaling. In this work the percent passing sieve sizes corresponding to 10%, 30%, 60% and 90% (i.e., D10, D30, D60, and D90 respectively) were applied in reference to the scaled down gradation sizes. In addition, the traditional coefficients of uniformity (c_u) and curvature (c_c) were also used:

$$C_c = (D_{30})^2 / (D_{10})(D_{60}) \tag{4}$$

$$C_u = (D_{60}) / (D_{10}) \tag{5}$$

3.2 Fineness and gradation moduli

The fineness modulus (FM) is widely used in aggregate/concrete applications for characterisation purposes. The FM is defined as the sum of the percentages of a sample of aggregate retained on each of the specified series of standard sieves divided by 100 (Abrams, 1918). The sieve sizes used are typically #4 (4.75 mm), #8 (2.36 mm), #16 (1.18 mm), #30 (600 μm), #50 (300 μm), and #100 (150 μm). Popovics (1961) showed that the FM has an important theoretical basis tied to the specific surface area of an aggregate, and can be related to the logarithmical average of the particle size of grading. A larger numerical value of the FM implies coarser grading of a rockfill sample.

The gradation modulus (GM) has also been applied in characterisation studies by several researchers (e.g., Hudson and Waller, 1969; Richardson and Long, 1987; Indraratna et al., 1993; Lusher, 2004). Similar to the FM, the GM is calculated from the gradation results, except that it is the sum of the percent passing size of a series of standard sieves divided by 100. The sizes used are typically 1 ½ in. (37.5 mm), ¾ in. (19 mm), 3/8 in. (9.5 mm), #4 (4.75 mm), #8 (2.36 mm), #16 (1.18 mm), #30 (600 μm), #50 (300 μm), #100 (150 μm) and #200 (75 μm). The greater the numerical value of the GM, the higher the percentage of fines contained in the rockfill. Both the FM (designated as '*m*') and the GM (designated as '*alpha*') were used as separate input parameters to the ANN models.

Table 1 Global database used to develop the artificial neural networks

Case No.	*Location*	*D10* (mm)	*D30* (mm)	*D60* (mm)	*D90* (mm)	*cc*	*cu*	*alpha*	*m*	*R*	*min UCS* (MPa)	*max UCS* (MPa)	*dry unit wt* (kN/m^3)	*sig_n* (MPa)	*Shear stress* (MPa)	*Reference*
1	Canada	0.02	0.94	4	18	11.05	200.00	4.78	4.19	1	1	5	15.4	0.022	0.013	Azam et al. (2009)
2	Canada	0.02	0.94	4	18	11.05	200.00	4.78	4.19	1	1	5	15.4	0.044	0.025	Azam et al. (2009)
3	Canada	0.02	0.94	4	18	11.05	200.00	4.78	4.19	1	1	5	15.4	0.088	0.049	Azam et al. (2009)
4	Canada	0.03	2.1	6.6	18	22.27	220.00	4.22	4.73	1	1	5	38.9	0.022	0.013	Azam et al. (2009)
5	Canada	0.03	2.1	6.6	18	22.27	220.00	4.22	4.73	1	1	5	38.9	0.044	0.024	Azam et al. (2009)
6	Canada	0.03	2.1	6.6	18	22.27	220.00	4.22	4.73	1	1	5	38.9	0.088	0.048	Azam et al. (2009)
7	Canada	0.09	0.92	3.2	10	2.94	35.56	5.00	3.94	1	1	5	37.0	0.022	0.014	Azam et al. (2009)
8	Canada	0.09	0.92	3.2	10	2.94	35.56	5.00	3.94	1	1	5	37.0	0.044	0.027	Azam et al. (2009)
9	Canada	0.09	0.92	3.2	10	2.94	35.56	5.00	3.94	1	1	5	37.0	0.088	0.053	Azam et al. (2009)
10	UK	1	6	19	29	1.89	19.00	2.61	6.36	5	100	250	19.62	0.059	0.163	Gharavy (1996)
11	UK	1	6	19	29	1.89	19.00	2.61	6.36	5	100	250	19.62	0.098	0.218	Gharavy (1996)
12	UK	1	6	19	29	1.89	19.00	2.61	6.36	5	100	250	19.62	0.198	0.367	Gharavy (1996)
13	UK	1	6	19	29	1.89	19.00	2.61	6.36	5	100	250	19.62	0.299	0.513	Gharavy (1996)
14	UK	0.3	3.2	16	30	2.13	53.33	3.37	5.74	5	100	250	18.0504	0.058	0.150	Gharavy (1996)
15	UK	0.3	3.2	16	30	2.13	53.33	3.37	5.74	5	100	250	18.0504	0.097	0.204	Gharavy (1996)
16	UK	0.3	3.2	16	30	2.13	53.33	3.37	5.74	5	100	250	18.0504	0.195	0.330	Gharavy (1996)
17	UK	0.3	3.2	16	30	2.13	53.33	3.37	5.74	5	100	250	18.0504	0.297	0.456	Gharavy (1996)
18	UK	1	6	19	29	1.89	19.00	2.65	6.36	5	100	250	19.62	0.179	0.262	Gharavy (1996)
19	UK	1	6	19	29	1.89	19.00	2.65	6.36	5	100	250	19.62	0.538	0.697	Gharavy (1996)
20	UK	1	6	19	29	1.89	19.00	2.65	6.36	5	100	250	19.62	0.887	0.112	Gharavy (1996)
21	UK	0.3	3.2	16	30	2.13	53.33	3.37	5.74	5	100	250	18.0504	0.177	0.245	Gharavy (1996)

Table 1 Global database used to develop the artificial neural networks (continued)

Case No.	*Location*	*D10* (mm)	*D30* (mm)	*D60* (mm)	*D90* (mm)	*cc*	*cu*	*alpha*	*m*	*R*	*min UCS* (MPa)	*max UCS* (MPa)	*dry unit wt* (kN/m^3)	*sig_n* (MPa)	*Shear stress* (MPa)	*Reference*
22	UK	0.3	3.2	16	30	2.13	53.33	3.37	5.74	5	100	250	18.0504	0.529	0.666	Gharavy (1996)
23	UK	0.3	3.2	16	30	2.13	53.33	3.37	5.74	5	100	250	18.0504	0.876	0.102	Gharavy (1996)
24	Iran	0.1	1.2	7.5	17.3	1.92	75.00	4.32	7.42	4	50	100	9.3195	0.101	0.160	Rayhani (2000)
25	Iran	0.1	1.2	7.5	17.3	1.92	75.00	4.32	7.42	4	50	100	9.3195	0.301	0.340	Rayhani (2000)
26	Iran	0.1	1.2	7.5	17.3	1.92	75.00	4.32	7.42	4	50	100	9.3195	0.503	0.500	Rayhani (2000)
27	Iran	0.4	2.8	11	30	1.78	27.50	3.38	5.6	4	50	100	9.3195	0.172	0.207	Rayhani (2000)
28	Iran	0.4	2.8	11	30	1.78	27.50	3.38	5.6	4	50	100	9.3195	0.497	0.476	Rayhani (2000)
29	Iran	0.4	2.8	11	30	1.78	27.50	3.38	5.6	4	50	100	9.3195	0.830	0.751	Rayhani (2000)
30	Japan	1.3	4.6	15	32	1.09	11.54	2.68	6.28	5	100	250	17.81496	0.094	0.136	Yamaguchi et al. (2008)
31	Japan	1.3	4.6	15	32	1.09	11.54	2.68	6.28	5	100	250	17.81496	0.177	0.242	Yamaguchi et al. (2008)
32	Japan	1.3	4.6	15	32	1.09	11.54	2.68	6.28	5	100	250	17.81496	0.351	0.415	Yamaguchi et al. (2008)
33	Japan	1.3	4.6	15	32	1.09	11.54	2.68	6.28	5	100	250	17.81496	0.512	0.552	Yamaguchi et al. (2008)
34	Japan	0.6	2	16	30	0.42	26.67	3.24	5.86	4	50	100	21.8763	0.093	0.165	Yamaguchi et al. (2008)
35	Japan	0.6	2	16	30	0.42	26.67	3.24	5.86	4	50	100	21.8763	0.182	0.308	Yamaguchi et al. (2008)
36	Japan	0.6	2	16	30	0.42	26.67	3.24	5.86	4	50	100	21.8763	0.359	0.523	Yamaguchi et al. (2008)

Table 1 Global database used to develop the artificial neural networks (continued)

Case No.	*Location*	*D10* (mm)	*D30* (mm)	*D60* (mm)	*D90* (mm)	*cc*	*cu*	*alpha*	*m*	*R*	*min UCS* (MPa)	*max UCS* (MPa)	*dry unit wt* (kN/m^3)	*sig_n* (MPa)	*Shear stress* (MPa)	*Reference*
37	Japan	0.6	2	16	30	0.42	26.67	3.24	5.86	4	50	100	21.8763	0.535	0.744	Yamaguchi et al. (2008)
38	Iran	0.4	2.9	9.7	31	2.17	24.25	3.41	5.57	4	50	100	21	0.177	0.214	Araei et al. (2010)
39	Iran	0.4	2.9	9.7	31	2.17	24.25	3.41	5.57	4	50	100	21	0.514	0.525	Araei et al. (2010)
40	Iran	0.4	2.9	9.7	31	2.17	24.25	3.41	5.57	4	50	100	21	0.839	0.773	Araei et al. (2010)
41	Iran	0.4	2.9	9.7	31	2.17	24.25	3.41	5.57	4	50	100	21	1.172	1.070	Araei et al. (2010)
42	Iran	0.4	2.9	9.7	31	2.17	24.25	3.41	5.57	4	50	100	21	1.494	1.312	Araei et al. (2010)
43	Iran	0.4	2.9	9.7	31	2.17	24.25	3.41	5.57	4	50	100	21	1.970	1.648	Araei et al. (2010)
44	Iran	0.4	2.9	9.7	31	2.17	24.25	3.41	5.57	4	50	100	20.8	0.180	0.240	Araei et al. (2010)
45	Iran	0.4	2.9	9.7	31	2.17	24.25	3.41	5.57	4	50	100	20.8	0.500	0.447	Araei et al. (2010)
46	Iran	0.4	2.9	9.7	31	2.17	24.25	3.41	5.57	4	50	100	20.8	0.821	0.689	Araei et al. (2010)
47	Iran	0.4	2.9	9.7	31	2.17	24.25	3.41	5.57	4	50	100	20.8	1.142	0.930	Araei et al. (2010)
48	Iran	0.5	2.8	9.7	30	1.62	19.40	3.43	5.61	5	100	250	21.1	0.487	0.390	Araei et al. (2010)
49	Iran	0.5	2.8	9.7	30	1.62	19.40	3.43	5.61	5	100	250	21.1	0.972	0.766	Araei et al. (2010)
50	Iran	0.5	2.8	9.7	30	1.62	19.40	3.43	5.61	5	100	250	21.1	1.448	1.110	Araei et al. (2010)
51	Iran	0.2	2.5	19.4	42.2	1.61	97.00	3.19	5.77	5	100	250	21	0.168	0.157	Araei et al. (2010)
52	Iran	0.2	2.5	19.4	42.2	1.61	97.00	3.19	5.77	5	100	250	21	0.373	0.634	Araei et al. (2010)
53	Iran	0.2	2.5	19.4	42.2	1.61	97.00	3.19	5.77	5	100	250	21	0.731	1.088	Araei et al. (2010)
54	Iran	0.2	2.5	19.4	42.2	1.61	97.00	3.19	5.77	5	100	250	21	0.906	1.258	Araei et al. (2010)
55	Iran	0.2	2.5	19.4	42.2	1.61	97.00	3.19	5.77	5	100	250	21	1.262	1.699	Araei et al. (2010)
56	Iran	0.2	2.5	19.4	42.2	1.61	97.00	3.19	5.77	5	100	250	21	1.437	1.883	Araei et al. (2010)

Table 1 Global database used to develop the artificial neural networks (continued)

Case No.	*Location*	*D10* (mm)	*D30* (mm)	*D60* (mm)	*D90* (mm)	*cc*	*cu*	*alpha*	*m*	*R*	*min UCS* (MPa)	*max UCS* (MPa)	*dry unit wt* (kN/m^3)	*sig_n* (MPa)	*Shear stress* (MPa)	*Reference*
57	Iran	0.4	3.3	10.3	33.3	2.64	25.75	3.32	5.64	4	50	100	21.8	0.092	0.140	Araei et al. (2010)
58	Iran	0.4	3.3	10.3	33.3	2.64	25.75	3.32	5.64	4	50	100	21.8	0.179	0.230	Araei et al. (2010)
59	Iran	0.4	3.3	10.3	33.3	2.64	25.75	3.32	5.64	4	50	100	21.8	0.344	0.357	Araei et al. (2010)
60	Iran	0.4	3.3	10.3	33.3	2.64	25.75	3.32	5.64	4	50	100	21.8	0.514	0.520	Araei et al. (2010)
61	Iran	0.4	3.3	10.3	33.3	2.64	25.75	3.32	5.64	4	50	100	21.8	0.859	0.887	Araei et al. (2010)
62	Iran	0.4	3.3	10.3	33.3	2.64	25.75	3.32	5.64	4	50	100	21.8	1.186	1.149	Araei et al. (2010)
63	Iran	1.2	2.1	4.2	25.3	0.88	3.50	3.63	5.34	4	50	100	21.8	0.092	0.147	Araei et al. (2010)
64	Iran	1.2	2.1	4.2	25.3	0.88	3.50	3.63	5.34	4	50	100	21.8	0.178	0.220	Araei et al. (2010)
65	Iran	1.2	2.1	4.2	25.3	0.88	3.50	3.63	5.34	4	50	100	21.8	0.503	0.461	Araei et al. (2010)
66	Iran	1.2	2.1	4.2	25.3	0.88	3.50	3.63	5.34	4	50	100	21.8	1.148	0.959	Araei et al. (2010)
67	Iran	0.4	2.9	9.7	31	2.17	24.25	3.40	5.53	4	50	100	21	0.340	0.332	Araei et al. (2010)
68	Iran	0.4	2.9	9.7	31	2.17	24.25	3.40	5.53	4	50	100	21	0.990	0.843	Araei et al. (2010)
69	Iran	0.4	2.9	9.7	31	2.17	24.25	3.40	5.53	4	50	100	21	1.618	1.271	Araei et al. (2010)
70	Iran	0.4	2.9	9.7	31	2.17	24.25	3.40	5.53	4	50	100	21	2.399	1.799	Araei et al. (2010)
71	Iran	0.4	2.9	9.7	31	2.17	24.25	3.40	5.53	4	50	100	21.5	0.342	0.342	Araei et al. (2010)
72	Iran	0.4	2.9	9.7	31	2.17	24.25	3.40	5.53	4	50	100	21.5	0.994	0.865	Araei et al. (2010)
73	Iran	0.4	2.9	9.7	31	2.17	24.25	3.40	5.53	4	50	100	21.5	1.630	1.321	Araei et al. (2010)
74	Iran	0.4	2.9	9.7	31	2.17	24.25	3.40	5.53	4	50	100	21.5	2.422	1.891	Araei et al. (2010)
75	Australia	33.9	42.4	50	60.2	1.06	1.47	0.2	8.8	5	100	250	21.7	0.163	0.230	Indraratna et al. (1998)
76	Australia	33.9	42.4	50	60.2	1.06	1.47	0.2	8.8	5	100	250	21.7	0.215	0.275	Indraratna et al. (1998)

Table 1 Global database used to develop the artificial neural networks (continued)

Case No.	*Location*	*D10* (mm)	*D30* (mm)	*D60* (mm)	*D90* (mm)	*cc*	*cu*	*alpha*	*m*	*R*	*min UCS* (MPa)	*max UCS* (MPa)	*dry unit wt* (kN/m^3)	*sig_n* (MPa)	*Shear stress* (MPa)	*Reference*
77	Australia	33.9	42.4	50	60.2	1.06	1.47	0.2	8.8	5	100	250	21.7	0.412	0.424	Indraratna et al. (1998)
78	Australia	30	34	40.8	50	0.94	1.36	0.52	8.5	5	100	250	21.7	0.165	0.252	Indraratna et al. (1998)
79	Australia	30	34	40.8	50	0.94	1.36	0.52	8.5	5	100	250	21.7	0.215	0.280	Indraratna et al. (1998)
80	Australia	30	34	40.8	50	0.94	1.36	0.52	8.5	5	100	250	21.7	0.412	0.424	Indraratna et al. (1998)
81	Germany	4	11.7	36.2	98.2	0.95	9.05	1.47	7.55	4	50	100	24.2	1.039	1.114	Brauns (1993)
82	Germany	4	11.7	36.2	98.2	0.95	9.05	1.47	7.55	4	50	100	24.2	2.034	1.964	Brauns (1993)
83	Germany	4	11.7	36.2	98.2	0.95	9.05	1.47	7.55	4	50	100	24.2	3.004	2.705	Brauns (1993)
84	Germany	3	9.1	30.4	98.2	0.91	10.13	1.67	7.28	4	50	100	24.2	0.533	0.658	Brauns (1993)
85	Germany	3	9.1	30.4	98.2	0.91	10.13	1.67	7.28	4	50	100	24.2	1.039	1.114	Brauns (1993)
86	Germany	3	9.1	30.4	98.2	0.91	10.13	1.67	7.28	4	50	100	24.2	2.018	1.882	Brauns (1993)
87	Germany	4.2	12.8	41.2	99	0.95	9.81	1.37	7.62	4	50	100	24.2	0.512	0.512	Brauns (1993)
88	Germany	4.2	12.8	41.2	99	0.95	9.81	1.37	7.62	4	50	100	24.2	1.001	0.902	Brauns (1993)
89	Germany	4.2	12.8	41.2	99	0.95	9.81	1.37	7.62	4	50	100	24.2	1.987	1.728	Brauns (1993)
90	USA	0.9	3	18.8	99	0.53	20.89	2.64	6.35	5	100	250	21.7	0.861	0.898	Marsal (1972)
91	USA	0.9	3	18.8	99	0.53	20.89	2.64	6.35	5	100	250	21.7	1.670	1.509	Marsal (1972)
92	USA	0.9	3	18.8	99	0.53	20.89	2.64	6.35	5	100	250	21.7	4.049	3.198	Marsal (1972)
93	UK	0.44	1.5	6.99	27.5	0.73	15.89	3.82	5.16	4	50	100	18.7	0.159	0.189	Charles and Watts (1980)

Table 1 Global database used to develop the artificial neural networks (continued)

Case No.	*Location*	*D10* (mm)	*D30* (mm)	*D60* (mm)	*D90* (mm)	*cc*	*cu*	*alpha*	*m*	*R*	*min UCS* (MPa)	*max UCS* (MPa)	*dry unit wt* (kN/m^3)	*sig_n* (MPa)	*Shear stress* (MPa)	*Reference*
94	UK	0.44	1.5	6.99	27.5	0.73	15.89	3.82	5.16	4	50	100	18.7	0.471	0.424	Charles and Watts (1980)
95	UK	0.44	1.5	6.99	27.5	0.73	15.89	3.82	5.16	4	50	100	18.7	1.130	0.905	Charles and Watts (1980)
96	Iran	0.4	2.3	12.2	44.4	1.08	30.50	3.30	5.69	4	50	100	26.2	0.815	0.660	Rayhani (2000)
97	Iran	0.4	2.3	12.2	44.4	1.08	30.50	3.30	5.69	4	50	100	18.7	0.794	0.577	Rayhani (2000)
98	Iran	0.4	2.3	12.2	44.4	1.08	30.50	3.30	5.69	5	100	250	24.5	0.994	0.864	Rayhani (2000)
99	India	0.5	1.5	4.6	15.6	0.98	9.20	4.22	4.8	4	50	100	24.5	1.384	0.881	Varadarajan et al. (2003)
100	India	0.95	2.8	12.5	34.9	0.66	13.16	3.02	5.97	4	50	100	24.5	1.369	0.836	Varadarajan et al. (2003)
101	India	1.3	4.6	18.9	55.9	0.86	14.54	2.40	6.54	4	50	100	24.5	1.358	0.803	Varadarajan et al. (2003)
102	Iran (multiple)	0.5	3	10.4	31.2	1.73	20.80	3.36	5.63	4	50	100	26.2	1.056	0.625	BHRC (2006)
103	Iran (multiple)	0.4	2.8	9.2	30.1	2.13	23.00	3.42	5.53	4	50	100	24.5	0.501	0.451	BHRC (2006)
104	Iran (multiple)	0.4	2.8	9.2	30.1	2.13	23.00	3.42	5.53	4	50	100	24.5	0.986	0.827	BHRC (2006)
105	Iran (multiple)	0.4	2.8	9.2	30.1	2.13	23.00	3.42	5.53	4	50	100	24.5	1.479	1.241	BHRC (2006)
106	Iran (multiple)	0.5	3.3	10.2	31	2.14	20.40	3.28	5.7	5	100	250	24.5	0.485	0.379	BHRC (2006)

Table 1 Global database used to develop the artificial neural networks (continued)

Case No.	*Location*	*D10* (mm)	*D30* (mm)	*D60* (mm)	*D90* (mm)	*cc*	*cu*	*alpha*	*m*	*R*	*min UCS* (MPa)	*max UCS* (MPa)	*dry unit wt* (kN/m^3)	*sig_n* (MPa)	*Shear stress* (MPa)	*Reference*
107	Iran (multiple)	0.5	3.3	10.2	31	2.14	20.40	3.28	5.7	5	100	250	24.5	0.808	0.631	BHRC (2006)
108	Iran (multiple)	0.5	3.3	10.2	31	2.14	20.40	3.28	5.7	5	100	250	24.5	1.131	0.884	BHRC (2006)
109	Iran (multiple)	0.4	2.8	10.4	31.2	1.88	26.00	3.4	5.58	4	50	100	18.7	0.808	0.631	BHRC (2006)
110	Iran (multiple)	0.4	2.8	10.4	31.2	1.88	26.00	3.4	5.58	4	50	100	18.7	1.131	0.884	BHRC (2006)
111	USA	2.4	19.3	80.1	100	1.94	33.38	1.32	7.72	6	250	400	25.6	0.850	0.836	Marsal (1972)
112	USA	2.4	19.3	80.1	100	1.94	33.38	1.32	7.72	6	250	400	25.6	1.695	1.637	Marsal (1972)
113	USA	2.4	19.3	80.1	100	1.94	33.38	1.32	7.72	6	250	400	25.6	4.205	3.921	Marsal (1972)
114	Iran (multiple)	0.01	1	10.4	43.9	9.62	1040	4	4.93	4	50	100	24.2	0.241	0.183	MPEC (1996)
115	Iran (multiple)	0.01	1	10.4	43.9	9.62	1040	4	4.93	4	50	100	24.2	0.468	0.316	MPEC (1996)
116	Iran (multiple)	0.01	1	10.4	43.9	9.62	1040	4	4.93	4	50	100	24.2	0.921	0.582	MPEC (1996)
117	Iran (multiple)	0.01	1	10.4	43.9	9.62	1040	4	4.93	4	50	100	24.2	0.265	0.313	MPEC (1996)
118	Iran (multiple)	0.01	1	10.4	43.9	9.62	1040	4	4.93	4	50	100	24.2	0.511	0.506	MPEC (1996)
119	Iran (multiple)	0.01	1	10.4	43.9	9.62	1040	4	4.93	4	50	100	24.2	1.001	0.902	MPEC (1996)

Table 1 Global database used to develop the artificial neural networks (continued)

Case No.	*Location*	*D10* (mm)	*D30* (mm)	*D60* (mm)	*D90* (mm)	*cc*	*cu*	*alpha*	*m*	*R*	*min UCS* (MPa)	*max UCS* (MPa)	*dry unit wt* (kN/m^3)	*sig_n* (MPa)	*Shear stress* (MPa)	*Reference*
120	USA	0.2	0.56	1.2	2.6	0.10	6.00	6	3	4	50	100	16.1	0.021	0.029	Fakhimi and Housseinpour (2006)
121	USA	0.2	0.56	1.2	2.6	0.10	6.00	6	3	4	50	100	16.1	0.042	0.051	Fakhimi and Housseinpour (2006)
122	USA	0.2	0.56	1.2	2.6	0.10	6.00	6	3	4	50	100	16.1	0.068	0.071	Fakhimi and Housseinpour (2006)
123	India	0.1	1.3	6.5	15	2.60	65.00	4.42	4.55	5	100	250	19.9	0.054	0.005	Honkanadavar et al. (2011)
124	India	0.1	1.3	6.5	15	2.60	65.00	4.42	4.55	5	100	250	19.9	0.089	0.028	Honkanadavar et al. (2011)
125	India	0.1	1.3	6.5	15	2.60	65.00	4.42	4.55	5	100	250	19.9	0.110	0.049	Honkanadavar et al. (2011)
126	India	0.1	1.3	6.5	15	2.60	65.00	4.42	4.55	5	100	250	19.9	0.152	0.067	Honkanadavar et al. (2011)
127	India	0.1	1.3	6.5	15	2.60	65.00	4.42	4.55	5	100	250	19.9	0.191	0.081	Honkanadavar et al. (2011)
128	India	0.1	1.3	6.5	15	2.60	65.00	4.42	4.55	5	100	250	19.9	0.240	0.092	Honkanadavar et al. (2011)
129	India	0.1	1	6.2	17	1.61	62.00	4.5	4.44	5	100	250	22.3	0.706	0.940	Honkanadavar et al. (2012)
130	India	0.1	1	6.2	17	1.61	62.00	4.5	4.44	5	100	250	22.3	1.310	1.296	Honkanadavar et al. (2012)
131	India	0.1	1	6.2	17	1.61	62.00	4.5	4.44	5	100	250	22.3	1.868	1.536	Honkanadavar et al. (2012)

Table 1 Global database used to develop the artificial neural networks (continued)

Case No.	*Location*	*D10* (mm)	*D30* (mm)	*D60* (mm)	*D90* (mm)	*cc*	*cu*	*alpha*	*m*	*R*	*min UCS* (MPa)	*max UCS* (MPa)	*dry unit wt* (kN/m^3)	*sig_n* (MPa)	*Shear stress* (MPa)	*Reference*
132	India	0.2	2.9	12.3	32	3.42	61.50	3.46	5.53	5	100	250	22.3	0.702	0.903	Honkanadavar et al. (2012)
133	India	0.2	2.9	12.3	32	3.42	61.50	3.46	5.53	5	100	250	22.3	1.305	1.250	Honkanadavar et al. (2012)
134	India	0.2	2.9	12.3	32	3.42	61.50	3.46	5.53	5	100	250	22.3	1.862	1.486	Honkanadavar et al. (2012)
135	India	0.4	4.4	21.2	59.8	2.28	53.00	2.74	6.27	5	100	250	22.3	0.697	0.862	Honkanadavar et al. (2012)
136	India	0.4	4.4	21.2	59.8	2.28	53.00	2.74	6.27	5	100	250	22.3	1.283	1.167	Honkanadavar et al. (2012)
137	India	0.4	4.4	21.2	59.8	2.28	53.00	2.74	6.27	5	100	250	22.3	1.819	1.358	Honkanadavar et al. (2012)
138	Australia	27.1	32.6	41.3	53	0.95	1.52	0.57	8.5	5	100	250	15.3	0.002	0.007	Indraratna et al. (1998)
139	Australia	27.1	32.6	41.3	53	0.95	1.52	0.57	8.5	5	100	250	15.3	0.020	0.052	Indraratna et al. (1998)
140	Australia	27.1	32.6	41.3	53	0.95	1.52	0.57	8.5	5	100	250	15.3	0.032	0.072	Indraratna et al. (1998)
141	Australia	27.1	32.6	41.3	53	0.95	1.52	0.57	8.5	5	100	250	15.3	0.054	0.095	Indraratna et al. (1998)
142	Australia	27.1	32.6	41.3	53	0.95	1.52	0.57	8.5	5	100	250	15.3	0.111	0.168	Indraratna et al. (1998)
143	Australia	27.1	32.6	41.3	53	0.95	1.52	0.57	8.5	5	100	250	15.3	0.162	0.217	Indraratna et al. (1998)

Table 1 Global database used to develop the artificial neural networks (continued)

Case No.	*Location*	*D10* (mm)	*D30* (mm)	*D60* (mm)	*D90* (mm)	*cc*	*cu*	*alpha*	*m*	*R*	*min UCS* (MPa)	*max UCS* (MPa)	*dry unit wt* (kN/m^3)	*sig_n* (MPa)	*Shear stress* (MPa)	*Reference*
144	Australia	27.1	32.6	41.3	53	0.95	1.52	0.57	8.5	5	100	250	15.3	0.209	0.259	Indraratna et al. (1998)
145	Australia	27.1	32.6	41.3	53	0.95	1.52	0.57	8.5	5	100	250	15.3	0.401	0.409	Indraratna et al. (1998)
146	Australia	20.7	26.7	32.8	53	1.05	1.58	0.89	8.2	5	100	250	15.3	0.003	0.008	Indraratna et al. (1998)
147	Australia	20.7	26.7	32.8	53	1.05	1.58	0.89	8.2	5	100	250	15.3	0.021	0.062	Indraratna et al. (1998)
148	Australia	20.7	26.7	32.8	53	1.05	1.58	0.89	8.2	5	100	250	15.3	0.035	0.089	Indraratna et al. (1998)
149	Australia	20.7	26.7	32.8	53	1.05	1.58	0.89	8.2	5	100	250	15.3	0.058	0.116	Indraratna et al. (1998)
150	Australia	20.7	26.7	32.8	53	1.05	1.58	0.89	8.2	5	100	250	15.3	0.115	0.191	Indraratna et al. (1998)
151	Australia	20.7	26.7	32.8	53	1.05	1.58	0.89	8.2	5	100	250	15.3	0.155	0.206	Indraratna et al. (1998)
152	Australia	20.7	26.7	32.8	53	1.05	1.58	0.89	8.2	5	100	250	15.3	0.209	0.259	Indraratna et al. (1998)
153	Australia	20.7	26.7	32.8	53	1.05	1.58	0.89	8.2	5	100	250	15.3	0.394	0.401	Indraratna et al. (1998)
154	Thailand	3.1	7.8	22	46.4	0.89	7.10	1.98	7.01	4	50	100	21	0.833	0.745	Pramthawee et al., 2011
155	Thailand	3.1	7.8	22	46.4	0.89	7.10	1.98	7.01	4	50	100	21	1.649	1.407	Pramthawee et al. (2011)

Table 1 Global database used to develop the artificial neural networks (continued)

Case No.	*Location*	*D10* (mm)	*D30* (mm)	*D60* (mm)	*D90* (mm)	*cc*	*cu*	*alpha*	*m*	*R*	*min UCS* (MPa)	*max UCS* (MPa)	*dry unit wt* (kN/m^3)	*sig_n* (MPa)	*Shear stress* (MPa)	*Reference*
156	Thailand	3.1	7.8	22	46.4	0.89	7.10	1.98	7.01	4	50	100	21	2.451	2.010	Pramthawee et al. (2011)
157	Thailand	3.1	7.8	22	46.4	0.89	7.10	1.98	7.01	4	50	100	21	3.223	2.492	Pramthawee et al. (2011)
158	Thailand	3.5	7.1	19.8	45.7	0.73	5.66	2.03	6.98	4	50	100	21	0.808	0.631	Pramthawee et al. (2011)
159	Thailand	3.5	7.1	19.8	45.7	0.73	5.66	2.03	6.98	4	50	100	21	1.592	1.169	Pramthawee et al. (2011)
160	Thailand	3.5	7.1	19.8	45.7	0.73	5.66	2.03	6.98	4	50	100	21	2.338	1.576	Pramthawee et al. (2011)
161	Thailand	3.5	7.1	19.8	45.7	0.73	5.66	2.03	6.98	4	50	100	21	3.140	2.178	Pramthawee et al. (2011)
162	Netherlands	11	15	23	32	0.89	2.09	1.48	7.48	5	100	250	16.8	0.014	0.028	Emha (2011)
163	Netherlands	11	15	23	32	0.89	2.09	1.48	7.48	5	100	250	16.8	0.028	0.048	Emha (2011)
164	Netherlands	11	15	23	32	0.89	2.09	1.48	7.48	5	100	250	16.8	0.055	0.082	Emha (2011)
165	Netherlands	11	15	23	32	0.89	2.09	1.48	7.48	5	100	250	16.8	0.108	0.143	Emha (2011)

D10, D30, D60, and D90 = 10%, 30%, 60% and 90% percent passing sieve sizes respectively; cu = coefficients of uniformity; cc = curvature; 'alpha' = gradation modulus; m = fineness modulus; R = ISRM hardness rating; 'min UCS' = minimum uniaxial compression strength of group; 'max UCS' = maximum uniaxial compression strength of group; 'dry unit wt' = dry unit weight at corresponding normal stress; and 'sig_n' = normal stress.

3.3 Material hardness

At high confinement of rockfill, particle crushing may be induced depending on the hardness of the material leading to varied size gradation from that of the original material. Also the material hardness can play a significant role given the influence of the individual rock particles on the dilatancy of rockfill at relatively higher confinement, as discussed further in Section 3.5. To characterise the material hardness, index hardness test values of the parent rock (where available) were used in conjunction with the International Society of Rock Mechanics (ISRM) strength ratings (Brown, 1981) summarised in Table 2. In addition, the lower bound and upper bound uniaxial compressive strength value (in MPa) for each category rated were both used as independent inputs.

Table 2 International Society of Rock Mechanics (ISRM) rock strength ratings

Point load index (MPa)	*UCS* (MPa)	*R-Rating*	*Example*
>10	>250	6	Fresh basalt, chert, diabase, gneiss, granite, quartzite
4–10	100–250	5	Amphibolite, sandstone, basalt, gabbro, gneiss, granodiorite, limestone, marble, rhyolite, tuff
2–4	50–100	4	Limestone, marble, phyllite, sandstone, schist, shale
1–2	25–50	3	Claystone, coal, concrete, schist, shale
–	5–25	2	Chalk, rocksalt, potash
–	1–5	1	Highly weathered or altered rock
–	0.25–1	0	Stiff fault gouge

Source: Brown (1981)

3.4 Relative density

In general the shear strength of rockfill increases with increasing relative density (Leps, 1970; Marsal, 1973; Douglas, 2002). The higher the density, the greater the inter-particle interlock leading to large values of friction angles and hence shear strength. In large triaxial tests of rockfill, relative density is typically controlled throughout the testing procedure. Thus relative density was an important input parameter considered the development of the ANN models discussed herein.

3.5 Confining pressure/normal stress

The effects of confinement on the shear strength of rockfill have been well documented by several researchers (Marachi et al., 1969; Leps, 1970; Indraratna et al., 1993; Emha, 2011). The strength envelope of rockfill has generally been observed to be curved especially at low confinement, implying that friction angles decrease with increasing normal stress. It is believed that at very low confinement, the particles are relatively free to move with respect to each other allowing for dilatancy and increased friction angles. However as the normal stress increases, dilatancy effects gradually dissipate as a result of particle crushing leading to significantly reduced friction angles, and consequentially shear strengths. The normal stresses were critical inputs to the ANN models developed in this work.

3.6 Shear strength

Rockfill has a peculiar style of shear strength. Typically rockfill behaves as a Mohr/ Coulomb material, but with no cohesion and with relatively high angles of internal friction. Loosely layered crushed rockfill may behave as a coarse sand. Compaction increases the angle of internal friction significantly by dilation effects due to interacting asperities of contacting rock particle surfaces. Such behaviour makes it even more challenging to design representative/realistic large scale strength tests, in addition to limiting effects of large particle sizes on test apparatus. The objective parameter selected to represent shear strength for the ANN models developed in this work was the shear stress value at failure of test samples, and was the single output variable.

4 Principal component analysis

Upon compilation of the database, principal component analysis (PCA) was used to identify the key parameters for ANN prediction. PCA is a data compression technique commonly used in statistics to reduce the dimensionality of datasets (Bishop, 2006; Rencher and William, 2012), and has been applied in rock mechanics by researchers such as Majdi and Beiki (2010) and Tiryaki (2008). PCA transforms the original set of several variables via an orthogonal transformation to a new set of uncorrelated variables (or principal components). In essence the technique conducts a rotation from the original axes to the new ones deriving components in decreasing order of importance. The first few components can then be said to account for most of the variation in the original data. Given that PCA has been extensively described elsewhere (e.g., Kramer, 1991; Oja, 1992; Singh et al., 1998; Bishop, 2006; Ilin and Tapani, 2010; Rencher and William, 2012), only a summary is presented below.

In the simplest matrix form, each data variable or observation $\boldsymbol{X}$, can be considered quantitatively as a function of a score $\boldsymbol{T}$, a loading or weight, $\boldsymbol{P}$ and a residue, $\boldsymbol{E}$ as:

$$\boldsymbol{X} = \boldsymbol{TP} + \boldsymbol{E} \tag{6}$$

Prior to conducting PCA, the data are standardised by centering and scaling. Centering is implemented for each variable in the database as:

$$x_{new} = x_{obs} - \left(\frac{\sum_{i=1}^{n} (x_{obs})}{n} \right). \tag{7}$$

Scaling is then conducted by dividing each variable by the standard deviation for each parameter in the database, known as unit variance scaling.

Suppose an $m \times n$ matrix $\boldsymbol{X}$ of initial observed data is linearly transformed into another $m \times n$ matrix $\boldsymbol{Y}$ by a $\boldsymbol{P}$ matrix of $m \times m$ dimensions as follows:

$$\boldsymbol{PX} = \begin{pmatrix} p_1.x_1 & p_1.x_2 & \cdots & p_1.x_n \\ \vdots & p_2.x_2 & \ddots & \vdots \\ p_m.x_1 & p_m.x_2 & \cdots & p_m x_m \end{pmatrix} = \boldsymbol{Y} \tag{8}$$

For the variables in the transformed matrix $\boldsymbol{Y}$ to be as uncorrelated as possible, the covariances of different variables in the covariance matrix $\boldsymbol{C_Y}$ should be as close to zero as possible. The covariance of $\boldsymbol{Y}$ can then be expressed as:

$$\boldsymbol{C_Y} = \frac{1}{n-1}\boldsymbol{YY}^T = \frac{1}{n-1}(\boldsymbol{PX})(\boldsymbol{PX})^T = \frac{1}{n-1}(\boldsymbol{PX})(\boldsymbol{X}^T\boldsymbol{P}^T) \tag{9}$$

$$\Rightarrow \boldsymbol{C_Y} = \frac{1}{n-1}\boldsymbol{P}(\boldsymbol{XX}^T)\boldsymbol{P}^T \tag{10}$$

By choosing the rows of the transformation matrix $\boldsymbol{P}$ to be the eigen vectors $\boldsymbol{XX}^T$, $\boldsymbol{P}$ can be equated to the matrix $\boldsymbol{E}^T$ where $\boldsymbol{E}$ is an $m \times m$ orthogonal matrix whose columns are the orthogonal vectors of $\boldsymbol{XX}^T$. The eigen values and eigen vectors of $\boldsymbol{XX}^T$ are then the principal components which can be sorted in descending order corresponding to the relative importance of the principal components. The largest variance then corresponds to the first principal component, and so on.

PCA was applied to all the variables from Table 1, and the results are summarised in Tables 3 and 4. Table 3 shows the variance and the percent of variance attributed to each principal component. As shown, the first seven components account for about 97% of the total variance and therefore contain most of the information. In addition, the first four principle components alone explain approximately 86% of the variance in the dataset. Table 4 shows the loadings (weights or coefficients) for the 14 principal components representing the linear combinations of the original variables that generate the new variables. The largest coefficients in the first column (first principal component) are the elements corresponding to the variables of D10, D30, D60, alpha and m. Considering the dominant, largest coefficients in the first seven principal components (97% of total variance), it was decided to select the D10, cc, cu, min UCS, unit weight and normal stress variables as the predictors in the first stage of ANN model development for shear strength prediction. Next the first four principal components (86% of total variance) were considered to establish the variables with the largest coefficients which corresponded to D10, D60, D90, cc, cu, m a, alpha, R, min UCS, max UCS and normal stress as inputs for the second ANN model. Finally all 13 parameters were used as predictors in the third ANN model developed.

5 ANN architecture and training

Three ANN models were constructed to predict rockfill shear strength: ANNOPTA, ANNOPTB, and ANNOPTC (Figure 2) using the database discussed in Section 3 (Table 1). The criteria for selection of inputs (predictors) for each ANN model were based on the PCA conducted and described in Section 4. For ANNOPT A, all the parameters shown in Table 1 were used as inputs. The parameters D10, D60, D90, cc, cu, m, alpha, R, min UCS, max UCS and normal stress were used as inputs in ANNOPTB. Finally D10, cc, cu, unit weight, min UCS and normal stress were used as inputs for ANNOPTC. For each model, a multilayer feed-forward network architecture with the back propagation algorithm was used. One hidden layer of sigmoid neurons followed by an output layer of linear neurons was used. Given that the tangent sigmoid nonlinear transfer function was implemented, and based on explanations given in Section 2, all data had to be mapped to the boundary condition [0 : 1] via the transfer function:

$$y^T = \frac{y - y_{\min}}{y_{\max} - y_{\min}} \tag{11}$$

The number of hidden layers to use and the proper number of neurons to include in each hidden layer were determined via optimisation resulting in three hidden neurons for ANNOPTA, eight hidden neurons for ANNOPTB, and seven hidden neurons for ANNOPTC. Prior to implementation of the network training, the dataset was divided into training and validation sets in a 3 : 1 ratio respectively, based on the rationale provided in Section 2.

The ANN models were built, trained, and implemented by using back propagation with the Levenberg–Marquardt algorithm. The initial range of the weights for the neurons was [–1 : 1], which were modified during training. Plots of the training and validation process are presented in Figure 3, used to check the progress of the ANN learning up to 1000 cycles. The ANN activations and biases for the weights as observed at the end of network training are summarised in Table 5. The validation results appear reasonable and do not seem to indicate that over fitting has occurred. However, good validation results are not necessarily an indication of high performance of the networks, given that those data have been used in the training phase. It is important to test the ANNs' independence from memorisation (i.e., over fitting) of the data. Therefore, the trained ANNs must be evaluated on completely new output and target test sets. The results of this evaluation are discussed in Section 6.

Figure 2 Schematic illustrating input and output parameters for the three ANN models created: (A) ANNOPTA; (B) ANNOPTB and (C) ANNOPTC. The number of hidden neurons is shown at the centre of each figure

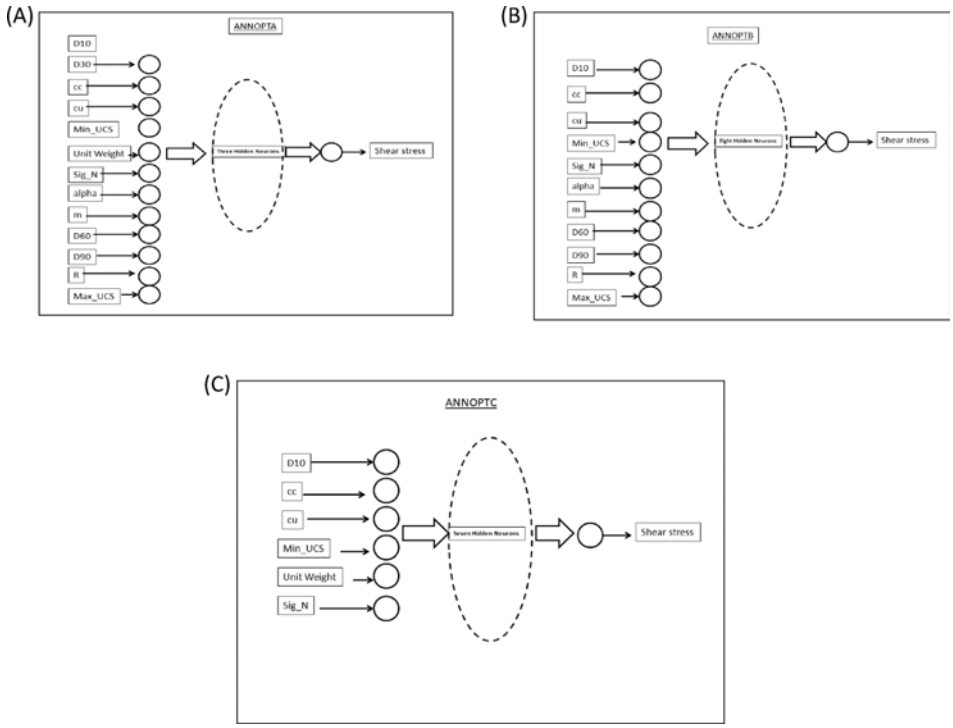

Table 3 Principal components showing the degree of variance and the cumulative variance

Principal component	*PC(1)*	*PC(2)*	*PC(3)*	*PC(4)*	*PC(5)*	*PC(6)*	*PC(7)*	*PC(8)*	*PC(9)*	*PC(10)*	*PC(11)*	*PC(12)*	*PC(13)*	*PC(14)*
Variance	6.09	2.45	2.07	1.40	0.76	0.47	0.34	0.18	0.12	0.05	0.04	0.03	0.01	0.01
Proportion	43.5%	17.5%	14.8%	10.0%	5.4%	3.4%	2.4%	1.3%	0.9%	0.4%	0.3%	0.2%	0.1%	0.0%
Cum. proportion	43.5%	61.0%	75.7%	85.8%	91.1%	94.5%	96.9%	98.2%	99.1%	99.4%	99.7%	99.9%	100.0%	100.0%

Table 4 The loadings (weights) for the principal components

	Principal component loadings (Coefficients/Weights)													
Parameters	*PC(1)*	*PC(2)*	*PC(3)*	*PC(4)*	*PC(5)*	*PC(6)*	*PC(7)*	*PC(8)*	*PC(9)*	*PC(10)*	*PC(11)*	*PC(12)*	*PC(13)*	*PC(14)*
D10 (mm)	0.305	0.280	0.207	–0.041	0.014	0.460	–0.295	0.151	–0.348	–0.065	–0.119	–0.103	0.270	–0.489
D30 (mm)	0.344	0.205	0.237	–0.020	–0.031	0.284	–0.115	0.236	–0.082	0.177	0.082	–0.003	–0.232	0.730
D60 (mm)	0.359	–0.063	0.207	0.116	–0.091	–0.162	0.199	0.476	0.417	0.234	0.000	0.077	–0.343	–0.397
D90 (mm)	0.264	–0.282	0.274	0.063	0.104	–0.588	0.081	0.104	–0.603	–0.076	0.022	–0.135	0.080	0.053
cc	–0.200	0.086	0.344	0.474	–0.035	0.277	0.601	–0.255	–0.188	0.258	0.006	–0.040	0.005	–0.043
cu	–0.130	0.017	0.172	0.592	0.613	–0.050	–0.388	0.065	0.201	–0.158	0.005	0.050	–0.006	0.039
alpha	–0.366	–0.019	–0.238	0.091	–0.028	0.061	0.014	0.435	–0.169	0.019	–0.476	–0.533	–0.258	0.039
m	0.362	0.042	0.212	–0.123	0.115	–0.052	0.111	–0.461	0.331	–0.231	–0.476	–0.411	–0.049	0.066
R	0.284	–0.055	–0.428	0.180	0.115	–0.058	–0.246	–0.337	–0.127	0.677	–0.049	–0.107	–0.118	–0.088
min UCS (MPa)	0.287	–0.076	–0.334	0.372	–0.193	0.017	0.177	0.230	0.209	–0.069	0.010	–0.157	0.656	0.191
max UCS (MPa)	0.284	0.014	–0.365	0.350	–0.187	0.124	0.076	–0.131	–0.212	–0.536	0.058	0.167	–0.472	–0.061
Dry unit weight (kN/m^3)	–0.141	–0.216	0.321	0.276	–0.690	–0.074	–0.480	–0.160	0.082	0.027	–0.074	–0.059	–0.012	0.013
sig_n (MPa)	0.037	–0.600	0.042	–0.096	0.127	0.371	–0.012	–0.023	0.069	–0.065	0.498	–0.450	–0.096	–0.063
Shear stress (MPa)	0.060	–0.608	0.018	–0.053	0.107	0.296	0.033	0.050	–0.061	0.045	–0.516	0.488	0.067	0.076

Figure 3 Progress of neural network training for 1000 cycle for the three models: (A) ANNOPTA; (B) ANNOPTB and (C) ANNOPTC (see online version for colours)

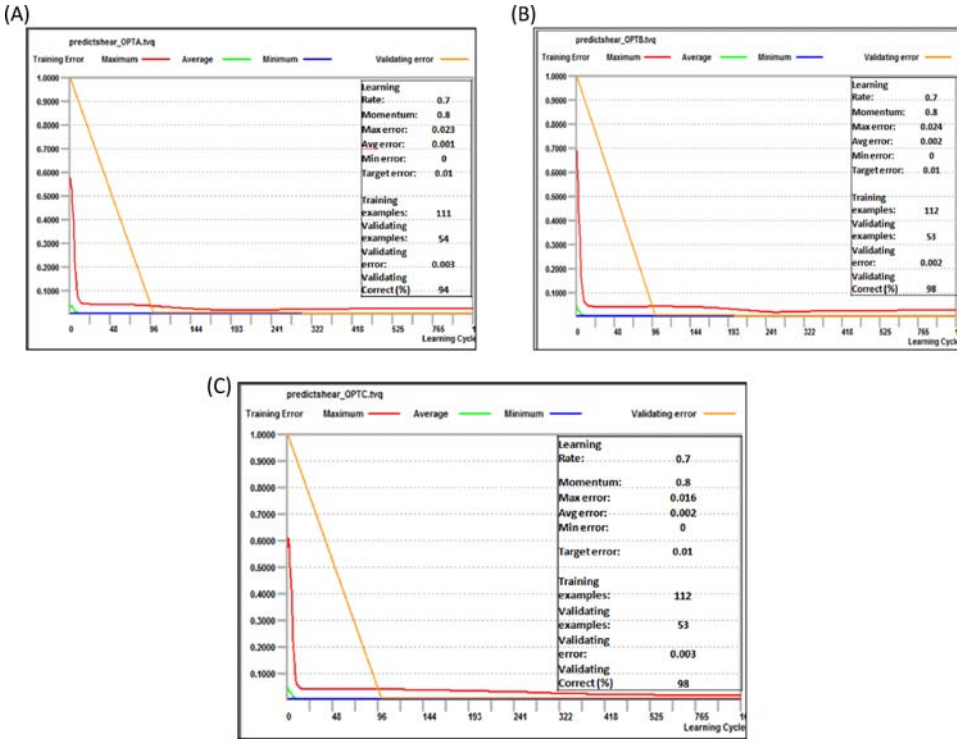

Table 5 ANN activations and biases after training

Activation/Bias	*ANNOPTA*	*ANNOPTB*	*ANNOPTC*
w_1^1	0.2549	0.0847	0.4163
w_2^1	0.3022	0.1037	0.5327
w_3^1	0.9974	0.4344	0.4746
w_4^1	–	0.9786	0.5363
w_5^1	–	0.1302	0.4432
w_6^1	–	0.1503	0.4203
w_7^1	–	0.1211	0.6462
w_8^1	–	0.1611	–
w_1^2	0.0424	0.0453	0.0452
b_1^1	0.1419	–0.2049	–0.0025

Table 5 ANN activations and biases after training (continued)

Activation/Bias	*ANNOPTA*	*ANNOPTB*	*ANNOPTC*
b_2^1	0.7808	–0.2342	0.5992
b_3^1	3.5141	–1.174	–1.2739
b_4^1	–	3.3352	0.6149
b_5^1	–	–0.2891	0.1996
b_6^1	–	–0.3464	0.095
b_7^1	–	–0.2683	0.6462
b_8^1	–	–0.3924	–
b_1^2	4.0973	3.8606	3.3416

wij is the activation of the *j*th neuron of the *i*th layer and, *bij* is the bias of the *j*th neuron of *i*th layer.

6 Test prediction results of ANN models

After ANN training and validation is complete, changing of the final weights and parameters of ANN models is not permitted. To assess the field applicability of the three newly proposed ANN models, five new case histories (i.e., not used in the training database) were selected. These test cases correspond to a wide range of insitu conditions at very large (1000 metric tons of material up to 900 m high) waste rock dumps at an open-pit mine located in Chile, South America discussed in great detail by Linero et al. (2007). This particular case study was selected for testing because the complexity of the site data would provide a rigorous test for the ANN models. In addition, the statistical distributions of the training data, validation data, and testing data need to be similar in ANN modelling. Figure 4 shows the relationship between target rockfill strength envelopes and those predicted by ANNs at various confinement (normal) stresses. Figure 5 shows the relation between corresponding target angles of internal friction and those predicted by ANNs at the same range of confinement. The observed declining trend of friction angles with increasing confinement agrees with several previous studies. At low normal stresses (<1 MPa), ANNOPTC predicts friction angles closest to measured values. At mid range normal stresses (approximately 1–2.5 MPa), ANNOPTA and ANNOPTC predict the most accurate friction angles. For normal stresses greater than about 2.5 MPa, ANNOPTB and ANNOPTC predict friction angles closest to measured values. It should be noted, as shown on Figure 2, that the input parameters present in ANNOPTB and absent from ANNOPTC (and vice-versa) appear to influence the performance at lower bound confining stresses and at upper bound confining stresses. The results suggest that the inputs used to build the ANNOPTC provide an optimum combination of variables suitable for making predictions over a broad range of confining stresses, while those variables used in ANNOPTB are more useful at higher confinement.

As can be seen from plots on Figure 6 and statistical summaries in Table 6, the ANN-predicted shear strength values are reasonably close to the measured ones for all three models. Combined data points display a linear trend, and are symmetrically scattered about the line of best fit. The highest degree of scatter for ANNOPTA and ANNOPTB is related to increasing normal stresses as expected, given that high confinement represents a wide range of rockfill behaviour including particle crushing, altered particle size distribution, and dilation. The results from ANNOPTC, however, closely match the line of best fit and appear to be unaffected by progressively higher confinement effects. Table 6 presents the performance of ANNs in terms of RMSE and the linear correlation coefficient (R^2) between experimental data and ANN outputs. These results in conjunction with the plots on Figures 4–6 indicate that the ANN models predict the rockfill shear stress with reasonable correlations and relatively low errors. Therefore the predictions based on the ANN models are reasonably consistent with site observations, confirming the applicability of the proposed approach.

Figure 4 Comparisons of target rockfill strength envelopes and those predicted by ANNs at a range of confinement (normal) stresses. Power curve fits to the ANN predictions are also shown (see online version for colours)

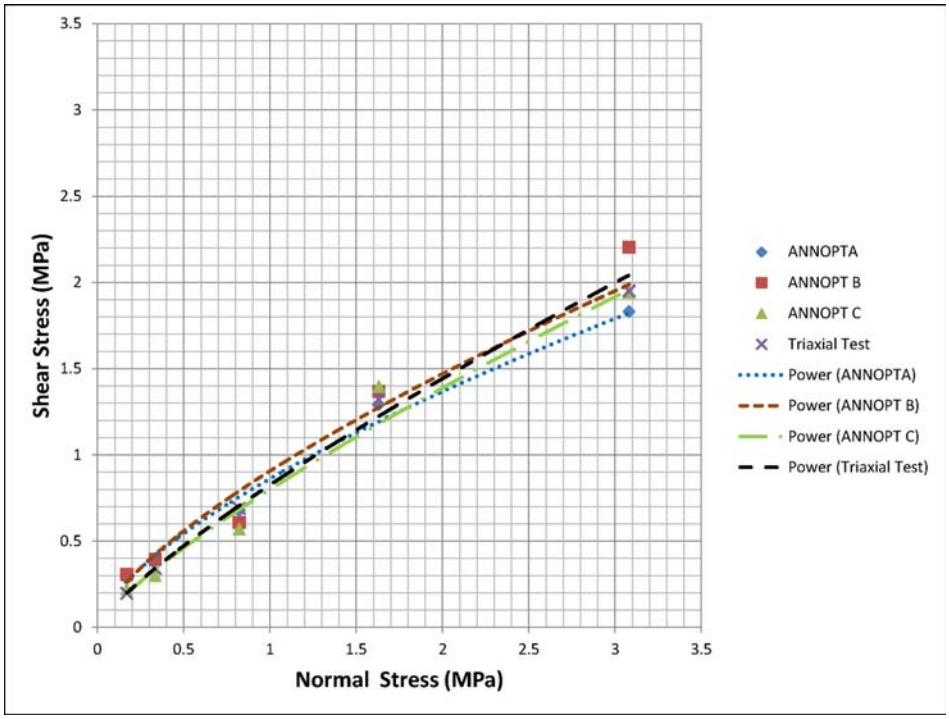

Table 6 Prediction error and correlation coefficient results of ANNs

Prediction index	*ANNOPTA*	*ANNOPTB*	*ANNOPTC*
RMSE	0.072	0.133	0.067
R^2	0.99	0.98	0.99

Figure 5 Angles of internal friction based on predictions made by the three ANN models over a range of confining stresses. Note that the rockfill strength characteristic of decreasing trends at higher confining stresses is captured by the ANNs (see online version for colours)

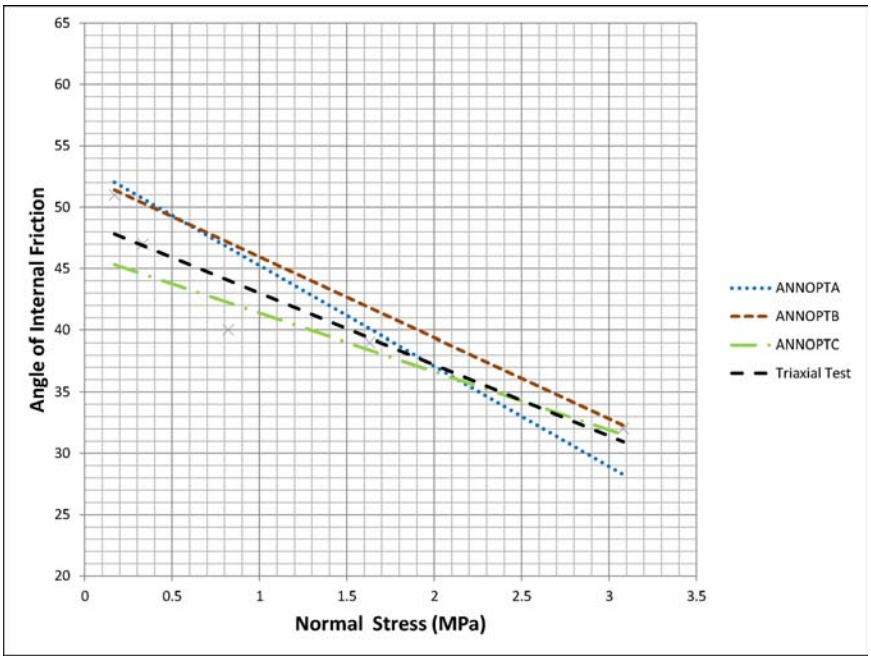

Figure 6 Comparisons of predicted vs. measured rockfill shear stress values. The line of ideal fit is also shown (see online version for colours)

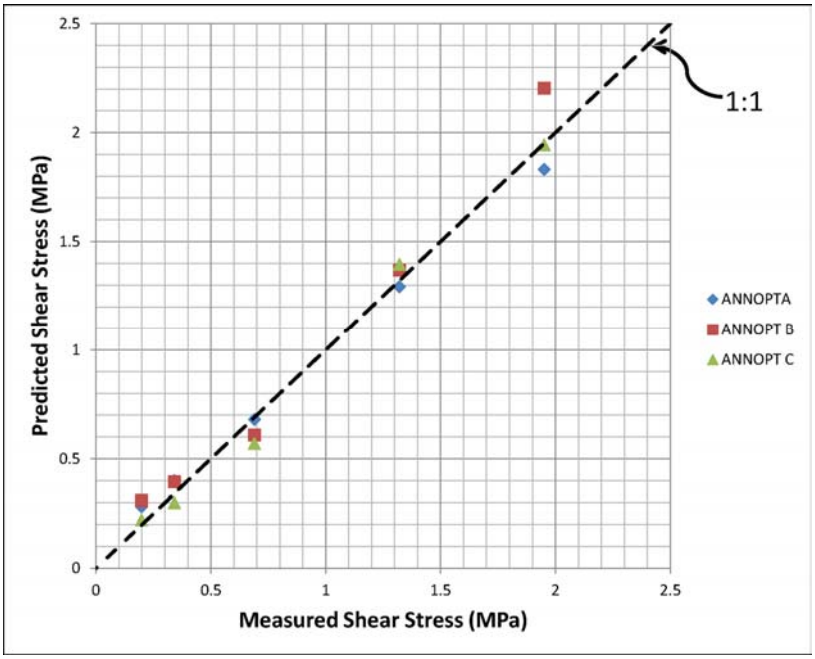

7 Sensitivity analysis

Sensitivity analyses were conducted to assess the interrelationships between the input predictor variables and the output variable, rockfill shear strength, based on an approach discussed by Coppola et al. (2005). The sensitivity analyses quantify and rank the importance of each input variable by computing the variation in RMSE ratios, if a particular input variable is not used as:

$$\text{Ratio} = \frac{\text{RMSE of ANN model prediction with specific input parameter excluded}}{\text{RMSE of initial ANN model prediction}} \quad (12)$$

The sensitivity analysis results obtained from the test data are presented in Table 7 for each of the three ANN models. For example, for the model ANNOPTA eliminating the hardness rating, *R*, input variable increases the RMSE for the validation dataset by a factor of 1.8 (i.e., RMSE ratio), which ranks this predictor variable as the least important (i.e., rank 13) for this particular model. Conversely, eliminating the normal stress parameter, sig_n, from the input variables of ANNOPTA increases the RMSE by a factor of 19.3, ranking this variable as the most important predictor (i.e., rank 1). The coefficient of curvature, cc, had the lowest rank (11) for ANNOPTB, while the coefficient of uniformity, cu, had the lowest rank (6) for ANNOPTC. As would be expected, the normal stress had the highest rank in all three cases because this variable exerts the largest influence on rockfill strength as discussed in Section 3.5.

8 Multiple regression analysis

Multiple regression analysis was conducted between the ANN inputs and the corresponding targets for each of the three networks to generate three equations of the form:

$$y = \beta_0 + \beta_1 x_1 + \beta_2 x_2 + \cdots + \beta_n x_n \quad (13)$$

where y = shear stress, β = regression coefficients and x = predictive input parameter.

The coefficients for each of the regression equations corresponding to the three ANNs are shown in Table 8. Regression Equations A, B and C are based on the input parameters used in ANNOPTA, ANOPTB, and ANNOPTC respectively. Analysis of variance (ANOVA) statistics for the multiple regression are also summarised in Table 9. For a 95% confidence interval, parameters D30, D60, minimum UCS, and normal stress are statistically significant (i.e., p-value < 0.05) in Equation A. Parameters D10, D60, alpha, minimum UCs, maximum UCS and normal stress are statistically significant in Equation B at 95% confidence interval. For regression Equation C, the minimum UCS and the normal stress variables are statistically significant.

The performance of the three regression equations on fresh test data (Section 6) was compared to the respective ANNs, and the results are summarised in Table 10. RMSE values for all ANN models are lower than those from multiple regression, even though correlation coefficient (R^2) values are comparable. This contrast is especially considerable for ANNOPTA where the ANN model gives RMSE values of about 14 times less than that of the regression equation.

The relatively lower prediction error values for the ANNs compared to those for multiple regression models indicate that the models that were developed by ANN technology in this study are superior to those developed by multiple regression.

Table 7 Sensitivity analysis results and input parameter rankings

Parameter	*D10*	*D30*	*D60*	*D90*	*cc*	*cu*	*alpha*	*m*	*R*	*min_UCS*	*max_UCS*	*dry_unit_weight*	*sig_n*
OPTA RMSE Ratio	4.22	5.30	6.24	6.36	2.36	4.77	4.41	4.43	1.78	4.34	4.86	4.27	19.29
(Rank)	**(11)**	**(4)**	**(3)**	**(2)**	**(12)**	**(6)**	**(8)**	**(7)**	**(13)**	**(9)**	**(5)**	**(10)**	**(1)**
OPTB RMSE Ratio	2.07	–	1.38	1.66	1.04	2.11	1.80	2.11	1.65	1.57	1.72	–	8.00
(Rank)	**(4)**		**(10)**	**(7)**	**(11)**	**(2)**	**(5)**	**(3)**	**(8)**	**(9)**	**(6)**		**(1)**
OPTC RMSE Ratio	1.24	–	–	–	0.79	0.7	–	–	–	6.53	–	1.92	16.61
(Rank)	**(4)**				**(5)**	**(6)**				**(2)**		**(3)**	**(1)**

Table 8 Multiple regression coefficients

ID	*Parameter, x*	*Equation A Coefficients, ß*	*Equation B Coefficients, ß*	*Equation C Coefficients, ß*
0	*Intercept*	–0.0792	–0.1059	–0.0074
1	*D10*	0.2051	–0.0641	–0.0145
2	*D30*	–0.3717	–	–
3	*D60*	0.3570	0.2261	–
4	*D90*	0.0284	0.0372	–
5	*cc*	0.0208	0.0034	–0.0203
6	*cu*	–0.0363	–0.0192	0.0015
7	*alpha*	0.0774	0.1133	–
8	*m*	–0.0036	0.0081	–
9	*R*	0.0665	0.0642	–
10	*min_UCS*	–0.2392	–0.2888	0.0835
11	*max_UCS*	0.1137	0.1490	–
12	*dry_unit_weight*	–0.0019	–	0.0198
13	*sig_n*	0.8157	0.8180	0.8438

Table 9 Multiple regression analysis of variance statistics at 95% confidence interval

	Equation A; R-Square = 0.95		*Equation B; R-Square = 0.95*		*Equation C; R-Square = 0.94*	
	t-Stat	*P-value*	*t-Stat*	*P-value*	*t-Stat*	*P-value*
Intercept	–1.082	0.281	–1.653	0.100	–0.614	0.540
D10	1.467	0.145	–2.134	0.034	–1.039	0.300
D30	–1.971	0.051	–	–	–	–
D60	3.296	0.001	2.632	0.009	–	–
D90	0.884	0.378	1.167	0.245	–	–
cc	0.520	0.604	0.087	0.931	–0.663	0.508
cu	–1.371	0.172	–0.764	0.446	0.068	0.946
alpha	1.146	0.253	1.804	0.073	–	–
m	–0.066	0.947	0.161	0.873	–	–
R	1.149	0.252	1.128	0.261	–	–
min_UCS	–1.693	0.093	–2.065	0.041	3.500	0.001
max_UCS	1.500	0.136	2.016	0.046	0.826	–
dry_unit_weight	–0.073	0.942	–	–	–	0.410
sig_n	38.281	1.26E-79	38.663	7.34E-81	43.544	6.54E-90

Table 10 Comparison of prediction results from ANN modelling vs. multiple regression

Model	*RMSE*	R^2
ANNOPTA	0.072	0.99
Regression equation (A)	1.020	0.99
ANNOPTB	0.133	0.98
Regression equation (B)	0.380	0.99
ANNOPTC	0.067	0.99
Regression equation (C)	0.132	0.99

9 Conclusions

ANN technology was used to accurately predict rockfill shear strength values based on specified material properties and test conditions in response to small scale and large scale loading. By considering the results from PCA and network training trials, the ANN structure consisting of six input neurons, one hidden layer with seven neurons, and one output neuron was found to be most practical. The final weights and threshold values were obtained for a training cycle of 1000. Test prediction values ranged from 0.2 MPa to 1.9 MPa under confining stresses ranging from 0.1 MPa to 3 MPa. When the ANN test results were compared against multiple regression, the ANN approach proved advantageous over the regression modelling method. It is possible that as rockfill nonlinear behaviour becomes more pronounced at progressively increased loading the ANN model performance does not deteriorate, unlike multiple regression, due to ANNs inherent nonlinear modelling capabilities. However this detail requires future investigations.

It cannot be overemphasised that the rockfill parameters and behaviour used to develop the ANN models herein are not meant to be exhaustive. There is need to further research the exact roles on strength of additional critical factors such as rock particle dilation, degree of saturation/unsaturation, material deformation/strain, and particle crushing during loading, from a modelling perspective. Hence, the ANN models developed herein can be said to be limited, in this sense. A significant contribution of this work to the subject of rockfill shear strength, however, is the narrowing down of a few key material properties for strength prediction with high accuracy via PCA and ANNs. More importantly, this study demonstrates that ANN technology can contribute to, or provide insights into important cause and effect relationships of the dynamics of such a complex physical system as rockfill shear strength characterisation, leading to better designs of mine waste rock dumps/piles and rock fill dams. From a practical standpoint, ANNOPTC can be used as a preliminary tool to estimate the shear strength of in-place rockfill under the stipulated guidelines prior to detailed engineering design.

References

Abrams, D.A. (1918) *Design of Concrete Mixtures*, Structural Materials Research Laboratory, Lewis Institute Bulletin, Vol. 1, Chicago.

Araei, A.A., Soroush A. and Rayhani, M. (2010) 'Large scale triaxial testing and numerical modeling of rounded and angular rockfill materials', *Scientia Iranica Transaction A Civil Engineering,* Vol. 17, No. 3, pp.169–183.

Azam, S., Wilson, G.W., Fredlund, D.G. and Van Zyl, D. (2009) 'Geotechnical characterization of mine waste rock', *Proceedings of the 17th International Conference on Soil Mechanics & Geotechnical Engineering*, 5–9 October, Alexandria, Egypt.

Barton, N. (2013) 'Shear strength criteria for rock, rock joints, rockfill and rock masses: problems and some solutions', *Journal of Rock Mechanics Geotechnical Engineering*, Vol. 5, No. 4, pp.249–261.

Bishop, C. (1995) *Neural Networks for Pattern Recognition*, Oxford Press, New York.

Bishop, C.M. (2006) *Pattern Recognition and Machince Learning*, Springer, Cambridge.

Brauns, J. (1993) *Laboratory Tests Report on Materials of Masjed Soleyman Dam*, Division of Earth Dam and Landfill Technology, University of Karlsruhe, Karlsruhe, Germany.

Brown, E.T. (1981) *Rock Characterization, Testing and Monitoring, ISRM Suggested Methods*, Pergamon Press, Oxford.

Building Housing Roads Research Center (BHRC) (2006) *Testing of Rockfill Materials with Largescale Triaxial Equipment*, Technical Report, Geotechnical Department, Tehran, Iran.

Charles, J.A. and Watts, K.S. (1980) 'The influence of confining pressure on the shear strength of compacted rockfill', *Geotechnique,* Vol. 30, No. 4, pp.353–367.

Coppola, E.A., Rana, A.J., Poulton, M.M., Szidarovsky, F. and Uhl, V.W. (2005) 'A neural network model for predicting aquifer water level elevations', *Ground Water*, Vol. 43, No. 2,pp.231–241.

Cybenko, G. (1989) 'Approximation by superpositions of a sigmoidal function', *Mathematics of Control, Signals and Systems*, Vol. 2, No. 4, pp.303–314.

Douglas, K.J. (2002) *The Shear Strength of Rock Mass*, PhD thesis, University of New South Wales, New South Wales, Australia.

Emha, F.Y. (2011) *Shear Strength of Bremanger Sandstone*, PhD thesis, Delft University of Technology, Delft, Netherlands.

Fakhimi, A. and Hosseinpour, H. (2008) 'The role of oversize particles on the shear strength and deformational behavior of rock pile material', *42nd US Rock Mechanics Symposium (USRMS)*, 29 June–2 July, San Francisco, CA.

Ghanbari, A., Sadeghpour, A.H., Mohamadzadeh, H. and Mohamadzadeh, M. (2008) 'An experimental study on the behavior of rockfill materials using large scale tests', *Electronic Journal of Geotechnical Engineering*, Vol. 13, pp.1–16.

Gharavy, M. (1996) *Experimental and Numerical Investigations into the Mechanical Characteristics of Rockfill Materials*, PhD thesis, University of Newcastle Upon Tyne, UK.

Gurney, K. (2009) *An Introduction to Neural Networks*, UCL Press, New York.

Hammerstrom, D. (1993) 'Working with neural networks', *Spectrum IEEE*, Vol. 30, No. 7, pp.46–53.

Haykin, S. (1999) *Neural Networks: A Comprehensive Foundation*, 2nd ed., Prentice Hall, New Jersey.

Hecht-Nielsen, R. (1990) *Neurocomputing*, Addison-Wesely Publishing Company, Reading.

Honkanadavar, N., Gupta, S. and Ratnam, M. (2012) 'Effect of particle size and confining pressure on shear strength parameter of rockfill materials', *International Journal of Advances in Civil Engineering and Architecture*, Vol. 1, No. 1, pp.49–63.

Honkanadavar, N.P., Gupta, S.L. and Bajaj, S. (2011) 'Deformability characteristics of quarried rockfill material', *International Journal of Earth Sciences and Engineering,* Vol. 4, No. 6, pp.128–131.

Hornik, K., Stinchcombe, M. and White, H. (1989) 'Multilayer feed-forward networks are universal approximators', *Neural Networks*, Vol. 2, No. 5, pp.359–366.

Hudson, S.B. and Waller, H.F. (1969) *Evaluation of Construction Control Procedures: Aggregate Gradation Variations and Effects*, Highway Research Board, Washington DC, pp.1–58.

Ilin, A. and Tapani, R. (2010) 'Practical approaches to principal component analysis in the presence of missing values', *The Journal of Machine Learning Research*, Vol. 99, pp.1957–2000.

Indraratna, B., Ionescu, D. and Christie, H.D. (1998) 'Shear behavior of railway ballast based on large-scale triaxial tests', *Journal of Geotechnical and Geoenvironmental Engineering*, Vol. 124, No. 5, pp.439–449.

Indraratna, I., Wijewardena, L.S.S. and Balasubramaniam, A.S. (1993) 'Large-scale triaxial testing of Greywacke rockfill', *Geotechnique*, Vol. 43, No. 1, pp.37–51.

Kramer, M.A. (1991) 'Nonlinear principal component analysis using autoassociative neural networks', *AIChE Journal*, Vol. 37, No. 2, pp.233–243.

Leps, T. (1970) 'Review of shearing strength of rockfill', *Journal of Soil Mechanics and Foundation Div.*, Vol. 96, pp.1159–1170.

Linero, S., Palma, C. and Apablaza, R. (2007) 'Geotechnical characterization of waste material in very high dumps with large scale triaxial testing', in Potvin, Y. (Ed.): *Proceedings of International Symposium on Rock Slope Stability in Open Pit Mining and Civil Engineering*, Australian Center for Geomechanics, Perth, Australia, pp.12–14.

Lusher, S.M. (2004) *Prediction of the Resilient Modulus of Unbound Granular Base and Subbase Materials based on the California Bearing Ratio and other Test Data*, MS Thesis, University of Missouri-Rolla, Rolla, USA.

Maier, H.R. and Dandy, G.C. (2000) 'Neural networks for the prediction and forecasting of water resources variables: a review of modeling issues and applications', *Environmental Modelling and Software,* Vol. 15, No. 1, pp.101–124.

Majdi, A. and Beiki, M. (2010) 'Evolving neural network using a genetic algorithm for predicting the deformation modulus of rockmasses', *International Journal of Rock Mechanics and Mining Sciences*, Vol. 47, No. 2, pp.246–253.

Marachi, D.N, Chan, C.K. and Seed, H.B. (1972) 'Evaluation of properties of rockfill materials', *Journal of the Soil Mechanics and Foundations Division*, Vol. 98, pp.195–114.

Marachi, D.N., Chan, K.C., Seed, B.H. and Duncan, B.H. (1969) *Strength and Deformation Characteristics of Rockfill Materials*, University of California Report, TE-69-5, Berkeley, CA.

Maren, A., Harston, C. and Pap, R. (1990) *Handbook of Neural Computing Applications*, Academic Press, San Diego.

Marsal, R.J. (1972) *Mechanical Properties of Rockfill in Embankment Dam Engineering*, *Casagrande Volume*, Wiley and Sons, New York.

Marsal, R.J. (1973) 'Mechanical properties of rockfill', in Hirschfeld, R.C. and Poulos, S.J. (Eds.): *Embankment-Dam Engineering*, Wiley-Interscience, New York, pp.110–200.

Masters, T. (1993) *Practical Neural Network Recipes in C++*, Academic Press, San Diego.

Moshanir Power Engineering Consultants (MPEC) (1996) *Review on Additional Laboratory Tests on Materials of Masjed Soleyman Dam*, Technical Report, Tehran, Iran.

Nawari, N.O., Liang, R. and Nusairat, J. (1999) 'Artificial intelligence techniques for the design and analysis of deep foundations', *Electronic Journal of Geotechnical Engineering*, Vol. 4, pp.1–21.

Nielsen, R.H. (1988) 'Neurocomputing, picking the human brain', *Spectrum IEEE*, Vol. 25, No. 3, pp.36–41.

Oja, E. (1992) 'Principal components, minor components, and linear neural networks', *Neural Networks*, Vol. 5, No. 6, pp.927–935.

Popovics, S. (1961) *A Method of Evaluating Grading on Concrete Aggregates*, Joint Highway Research Project, Indiana Department of Transportation and Purdue University, Publication FHWA/IN/JHRP-61/07, West Lafayette, Indiana.

Pramthawee, P., Jongpradist, P. and Kongkitkul, W. (2011) 'Evaluation of hardening soil model on numerical simulation of behaviors of high rockfill dams', *Sonklanakarin Journal of Science and Technology*, Vol. 33, No. 3, pp.325–334.

Rayhani, M.H.T. (2000) *Investigation of the Behavior of Earth and Rockfill Dam Shell Materials based on Triaxial and Direct Shear Tests*, MS thesis, Tarbiat Moallem University, Iran.

Rencher, A.C. and William, F.C. (2012) *Methods of Multivariate Analysis*, Vol. 709, John Wiley & Sons, New York.

Richardson, D.N. and Long, J. (1987) 'The sieved slake durability test', *Bulletin of the Association of Engineering Geologists*, Vol. 24, No. 2, pp.247–258.

Rojas, R. (1996) *Neural Networks: A Systematic Introduction*, Springer-Verlag, Berlin.

Rumelhart, D.E., Hinton, G.E. and Williams, R.J. (1986) 'Learning internal representation by error propogation', in Rumelhart, D.E. and McClelland, J.L. (Eds.): *Parallel Distributed Processing*, MIT Press, Massachusetts, Vol. 1, pp.318–362.

Shahin, A., Jaksa, B. and Maier, R. (2008) 'State of the art of artificial neural networks in geotechnical engineering', *Electronic Journal of Geotechnical Engineering*, Vol. 8, pp.1–26.

Singh, H.P., Ravi, K.G. and Ranjan, G. (1998) 'Stellar spectral classification using principal component analysis and artificial neural networks', *Monthly Notices of the Royal Astronomical Society*, Vol. 295, No. 2, pp.312–318.

Smith, G.N. (1986) *Probability and Statistics in Civil Engineering: An Introduction*, Collins, London.

Soroush, A. and Jannatiaghdam, R. (2012) 'Behavior of rockfill materials in triaxial compression testing', *International Journal of Civil Engineering*, Vol.10, No. 2, pp.153–161.

Tiryaki, B. (2008) 'Predicting intact rock strength for mechanical excavation using multivariate statistics, artificial neural networks, and regression trees', *Engineering Geology*, Vol. 99, No. 1, pp.51–60.

Twomey, J.M. and Smith, A.E. (1997) 'Validation and verification', in Kartam, N., Flood, I. and Garrett, J.H. (Eds.): *Artificial Neural Networks for Civil Engineers: Fundamentals and Applications*, ASCE, New York, pp.44–64.

Valstad, T. and Strøm, E. (1975) 'Investigation of the mechanical properties of rockfill for the Svartevann Dam, using triaxial, oedometer and plate bearing tests', *Norwegian Geotechnical Institute Publication*, Vol. 110, pp.3–8.

Varadarajan, A., Sharma, K.G., Venkatachalam, K. and Gupata, A.K. (2003) 'Testing and modeling two rockfill materials', *Journal of Geotechnical and Geoenvironmental Engineering*, Vol. 129, No. 3, pp.206–218.

Wasserman, P.D. (1989) *Neural Computing: Theory and Practice*, Van Nostrand Reinhold, New York.

Yamaguchi, Y., Satoh, H., Hayashi, N. and Yoshinaga, H. (2008) 'Strength evaluation of rockfill materials considering confining pressure dependency', *Journal of Japan Society of Dam Engineers*, Vol. 18, No. 3, pp.166–181.

A review on utilisation of coal mine overburden dump waste as underground mine filling material: a sustainable approach of mining

Anup Kumar Gupta* and Biswajit Paul

Department of Environmental Science and Engineering,
Indian School of Mines,
Dhanbad 826004, India
Email: guptaanup007@gmail.com
Email: dr_bpaul@yahoo.com
*Corresponding author

Abstract: This paper reviews the application of coal mine overburden (OB) dump material for backfilling in underground mine voids created due to coal mining in deeper seams/horizons. Backfilling, which is commonly known as stowing, provides stability of ground by preventing land subsidence, reducing mine fire and improving the coal production by increasing extraction of coal pillars. Different materials have been used for backfilling in underground mine voids such as river sand, fly ash, mine tailing and waste foundry sand (WFS). From last few decades, coal mining industry in India is facing scarcity of river sand owing to some new mining legislations and its heavy demand in infrastructure development. The existing coal mine overburden dumps might be a good alternative for sand and provide a sustainable mining practice. Geotechnical and physicochemical characterisation is required to evaluate the suitability of OB dump material to be used as an alternative of river sand.

Keywords: backfill; land subsidence; mine fire; overburden dump; OB; sustainable mining.

Reference to this paper should be made as follows: Gupta, A.K. and Paul, B. (2015) 'A review on utilisation of coal mine overburden dump waste as underground mine filling material: a sustainable approach of mining', *Int. J. Mining and Mineral Engineering*, Vol. 6, No. 2, pp.172–186.

Biographical notes: Anup Kumar Gupta is a Research Scholar (JRF) at the Department of Environmental Science and Engineering (ESE), Indian School of Mines, Dhanbad. He has completed his Master's Degree in Environmental Science and Bachelor's Degree in Science from VBS Purvanchal University (UP), India. He has also qualified the national eligibility test (NET) conducted by UGC in 2011 and 2012. As a researcher, he is working on sustainable waste management (waste rock or overburden dump material). He has a key interest in sustainable development aspects of mining, water pollution and their conservation.

Biswajit Paul is an Associate Professor, having teaching experience of about nine years at the Department of Environmental Science and Engineering, Indian School of Mines, Dhanbad, India. He received his BTech (Mining Engineering) and PhD (Mining Environment) from Indian School of Mines, Dhanbad, India. He has lot of work experience as mining manager in mine backfilling, sustainable mining and mine reclamation. He has key research interest in the field of mining environment (mine fill surface and underground),

land reclamation, soil mechanics, mine fire and environmental planning for mines. He has a number of patents in the field of mining and presented a number of research papers in various seminars, symposium and conferences.

1 Introduction

Coal is a key energy resource of power production in India as most of the other countries like USA, China and Australia. The power sector in India is dominated by coal, which accounts for more than 70% of total electricity generation (Chikkatur, 2005). As we are the second most populated country of the world, there is a need to produce coal in a large scale to fulfil the energy demand of the country. Coal seams are found lying beneath the surface of sedimentary rock mass or lying very near to the surface. Opencast mines (blasting and digging) are used to extract the less deep coal seams whereas the coal seams that are found deeper are mined out with underground mining practice.

Opencast mining is a dominated mining process that generates huge amount of rock waste along with valuable minerals (Table 1). Waste rock material generated along with mining is called mine overburden (Prashant et al., 2010). Generally, the amount of waste rock is more in case of open pit mining rather than underground mining (Lu et al., 2012). The US coal mines produce more than 150 million tons of coal refuse annually (Karafakis et al., 1996). Dumping or management of this mine refuse is a big environmental problem for the mining industry. Most of this waste is disposed of at the surface, which inevitably requires extensive planning and control to minimise the environmental impact of the mining.

Table 1 Global production of land won minerals including waste and overburden

Year	*Production net weight, 1.000 tons*	*% Increase since 1975*	*Materials moved gross weight 1000 tons*	*% Increase since 1975*
2000	20,933070	47.7	62,265038	48.2
1998	20,610531	45.4	60,015452	42.9
1995	19,735291	39.3	57,548678	36.8
1988	18,607294	31.1	56,864321	35.4
1985	16,942603	19.5	52028252	23.9
1980	16,196957	11.4	47407590	12.8
1975	14,172463		4200725	

Source: Sustainable mining practices a global perspective, Rajaram et al. (2005)

Opencast mining is a developmental activity, which is bound to damage the natural ecosystem by several mining activities. During opencast mining, the overlying soil is removed and the fragmented rock is heaped in the form of overburden dumps (Ghosh, 2002). OB dump is considered as a major contributor to the ecological and environmental degradation as soil erosion and environmental pollution (Yaseen et al., 2012). Presently, most of this OB material is disposed temporarily over valuable land mass, which inevitably requires extensive planning and control to reduce their negative impacts over

environment (Barapanda, 2001). It also results in non-productive use of land and atmospheric pollution.

OB generated along with valuable mineral shows a specific ratio (mineral/OB) called stripping ratio. It may vary from place to place with the change in topography. The average stripping ratio in Indian coal mines is found to be about 1.97 m^3/t in the last few decades (Chaulya et al., 2000).

Underground mining that accounts for about 15–20% of total coal production in India produces huge mine voids simultaneously (Sivakugan et al., 2004).

Mine voids created during the underground mining should be filled otherwise it may cause land subsidence owing to collapse of the upper strata (Figure 1). Thus, to provide ground supports to minimise the land subsidence problems and mine safety aspects, backfilling is the valuable part of mining (Kesimal et al., 2002; Barret et al., 1978). River sand is widely used, as it is easily available and economically feasible and the most important is its geotechnical properties.

Figure 1 Cross section of subsidence trough, a zone of shattered roof beds over mine excavation (see online version for colours)

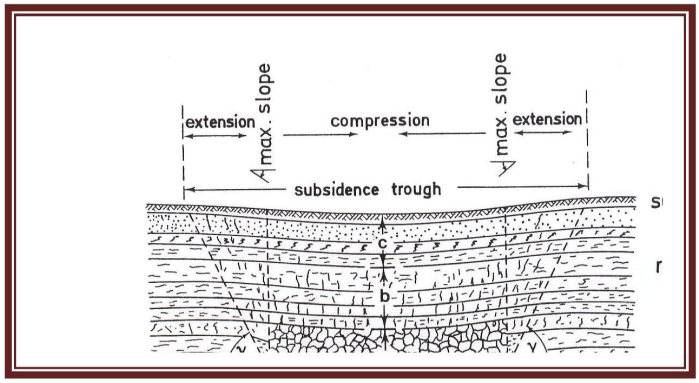

Source: Kratzsch (1983)

On the other hand, its overexploitation may negatively affect the riverine ecosystem as well as the productivity of nearby land mass. Some legislations are there going to be implemented in India (Kumar et al., 2003) to overcome these implications owing to overexploitation of river sand. In this way, this is a challenge for mining industries to find other materials as alternative of river sand for backfilling.

Fly ash, WFS, mine tailings, etc., have been used as the alternative of the sand (Mishra and Rao, 2006) but they do not at least provide the economic value of the production. It is often observed that sand or mill tailings as backfilling material remain loose and merely serve as temporary working platform rather than offering any lateral stress on the opening walls to improve the stability situation. Another drawback with the sand backfilling is its cost and is estimated that it tends to be 10–20% of the total operating cost of the mine and the additive cement represents up to 75% of that cost (Grice, 1998).

Backfilling with mine overburden or waste rock material may provide an alternative for river sand. Utilisation of these nearby mine overburden dumps as backfilling material in underground mine voids might be a good alternative of river sand (Prashant et al.,

2010). Backfill underground mine voids with OB material are not only significant to the environmental restoration and mining condition, but also beneficial for disposal of OB or waste rock generated during mining (Lu et al., 2012). Backfilling with mine refuse and waste rock also includes the elimination of the environmental, health, safety and social problems associated with surface disposal (National Academy of Sciences, 1975).

2 Selection of an alternative material for backfilling

Selection of an alternative material to be used for backfilling in underground mine void is based on its physical and geotechnical properties. Different backfilling techniques such as paste backfilling, rock backfilling and hydraulic backfilling have been developed (Grice, 1998).

A sharp difference between mine cycle time period with slurry backfill and paste backfill has been reported (Mark et al., 1990). They performed a hypothetical mining practice, i.e., vertical retreat mining (VRM) where stops were backfilled first with a paste (Figure 2).

Figure 2 Comparative study of mining cycle between using paste backfill and slurry backfill in a VRM stope (see online version for colours)

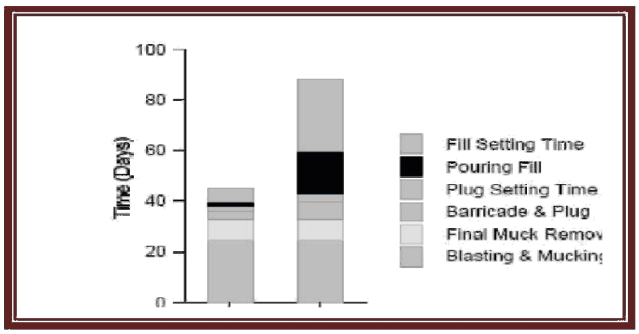

Source: Mark et al. (1990)

2.1 Backfilling suitability assessment (BSA)

Selection of any alternative material to be used for backfilling should be examined for its short- and long-term mechanical properties and expected behaviour following placement. Kortnik (2003) postulated a brief description about suitability assessment for the waste materials to be used for backfilling in mine voids. This includes the following partial approaches.

- assessment of the suitability of waste material composite (WMC) as backfilling materials
- assessment of the rock as a geological/technical barrier after backfill installation
- assessment of the geotechnical properties of backfill.

3 Techniques in mine filling

Different techniques have been successfully implemented in mine filling worldwide. Some of the important techniques are as follows.

3.1 Mechanical backfill

Mechanical backfilling technique involves introduction of conveyors into underground mining operations and has been used for backfilling of the waste rock and for the construction of pack walls with less effort and permits fast placement of material in underground.

3.2 Pneumatic backfill

Pneumatic backfill technique involves transportation of a material through pipeline in the presence of air pressure and finally dumping the material in mine voids. Material used for pneumatic backfill must be dry and free flowing**.** Pneumatic backfill techniques strictly require air pressure to pump the material at destination.

3.3 Paste backfill

Paste backfilling is a technique of backfilling, which involves high solids content; this is usually conducted with a density of 75–88% solids by weight (Amaratunga and Yaschyshyn, 1997). The best part of this technique is placing about 100% mine tailing in mine voids.

Significant reduction of tailing waste and reduction in rehabilitation costs is some other important advantages of the paste backfill (Kesimal et al., 2002). Mine tailings contain different types of minerals such as sulphide and pyrite that are unstable in the presence of air and water posing the environmental problems. Aref et al. (1992) proposed a conceptual model for designing a high-density paste backfill system (Figure 3), which shows main aspects of backfilling material for determining their sources, transportation and placement requirements and should be reconciled so as to satisfy backfill quality and schedule requirements.

Underground cemented paste backfill (CPB) is an important component of paste backfill (Figure 4) used for underground stope extraction (Landriault et al., 1997; Naylor et al., 1997). It not only provides ground support to the pillars and walls but also helps to prevent caving and roof falls and enhances pillar recovery therefore ultimately improves productivity (Belem et al., 2004). Self-support stresses govern backfill design and the conventional design has been that of a free standing wall that demands a uniaxial compressive strength (UCS) equal to the overburden stress at the bottom of the filled stope (Belem et al., 2004). However, in many cases, the adjacent rock walls can actually support the fill through boundary shear and arching effects that mutually supports the backfill and rock wall (Mitchell, 1989). In backfilled stopes, when arching occurs, the vertical pressure at the bottom of filled stope, an analogy similar to a trap door, is less than the weight of overlying fill (OB weight) owing to horizontal pressure transfer (Martson, 1930). Sulphur content of mine tailing may cause acid mine drainage (AMD) thus utilisation of mine tailing as backfilling material reduces the problem.

Figure 3 Flow chart for conceptual design of mine back fills system (see online version for colours)

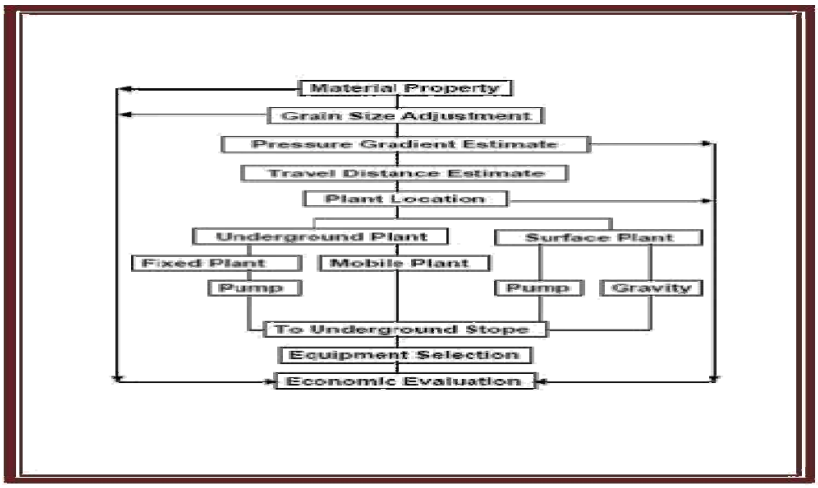

Source: Aref et al. (1992)

Figure 4 Underground paste backfilling mechanism (see online version for colours)

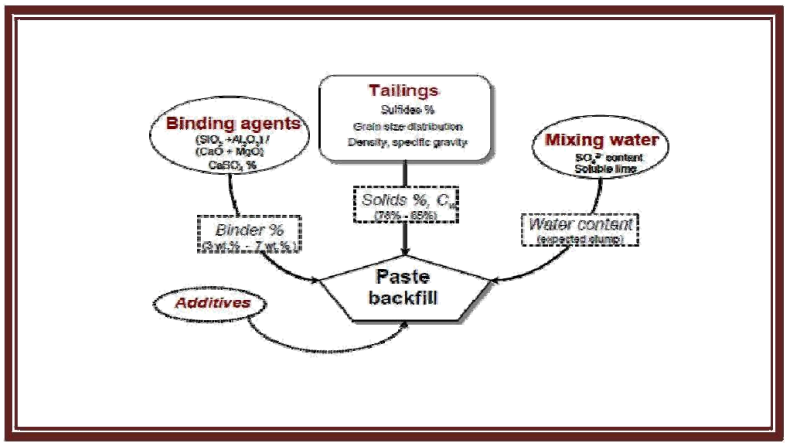

Source: Landriault et al. (1997)

Advantage and disadvantages of Paste backfill

Advantages:

- shorter mine cycle owing to earlier development of higher compressive strength
- reduced binder need for equivalent or better slurry backfill strength. High tailings usage thereby reducing surface disposal needs.

Disadvantages:

- requires superior dewatering facilities and greater technical precision. Presence of increased pipeline pressure.

3.4 Hydraulic backfill (hydraulic stowing)

Hydraulic stowing or backfilling involves filling of mine voids with slurry or fluid density in the range of 55–75% solids for weight, as much as 30% of the total initial fills volume is lost by dewatering (Amaratunga and Yaschyshyn, 1997). Hydraulic sand stowing (HSS) is one of the most popular mine fill techniques used for backfilling in underground mine voids (Grice, 1998; Prakash et al., 2009). Transportation of sand slurry from surface to underground mine voids is one of the important stages of hydraulic stowing. Successful slurry transportation is based on the number of physical and geotechnical properties of the slurry (Table 2). Hydraulic stowing is mainly performed with pump-based transportation and gravity transportation. Gravity transportation is the widely used technique for the same, which is based on gravity system to move material down through vertical or inclined chutes, boreholes or pipes. These techniques are currently used to move material to depths of up to 600 m, e.g., in the Doubrava Mine of Czechoslovakia.

Table 2 Physical and mechanical parameters of backfill slurry

Factor	*Value*
Density of cement/(gcm^{-3})	3.00
Unit weight of cement/(gcm^{-3})	1.30
Density of gangue/(gcm^{-3})	2.65
Unit weight of gangue/(gcm^{-3})	1.41
Density of fly ash/(gcm^{-3})	2.44
Unit weight of fly ash/(gcm^{-3})	1.02
Density of mixture/(gcm^{-3})	2.62
Unit weight of mixture/(gcm^{-3})	1.42
Mediate size of mixture/mm	0.32
Average size of mixture/mm	0.83
Density of backfill slurry/(gcm^{-3})	1.77
Mass fraction of backfill slurry (%)	72.0
Volume fraction of slurry (%)	49.5
Mass ratio of solid-liquid of slurry	2.57
Volumetric solid liquid ratio of slurry	0.98
Volume liquid solid ratio of slurry	1.02

Particles whose diameters are less than the mediate size make up half of total backfill mixture Zheng et al. (2008).

Pipe diameter, particle size, slurry density, etc., are some of the parameters that influence the slurry transportation through this technique. The most effective pipe diameter is 300 mm when the material is up to 80 mm diameter with some clay content. The best part of the gravity transport systems is its ability to be installed in ventilation shafts, thus easing congestion in roadways, etc. All methods of gravity transport generally require the lowering of backfill via the vertical or declined pipe, which is accompanied by continuous unloading at the bottom via some discharge/feeder mechanism.

4 Backfill materials

Different materials have been implemented as mine fill or backfill material in underground mine voids. This mainly includes fly ash, bottom ash, WFS, river sand, mine tailing, etc. Backfilling materials must have some specific geotechnical and physical properties to fulfil the filling requirements and should be economically beneficial.

4.1 Waste Foundry Sand (WFS) as backfilling material

WFS is another good alternative of river sand used for mine filling (Deng et al., 2007). WFS has been practised in different sectors earlier as related to infrastructure engineering and rehabilitation works such as highway embankment construction (Ham et al., 1990; Javed et al., 1994) and ground improvement (Vipulanadan and Sunder, 2000); all of these alternative and beneficial uses of waste are economically as well as environmental friendly.

4.2 Fly ash as backfilling material

Huge amount of fly ash is generated from thermal power plants. This is dumped in ash ponds, nearby land mass or in river stream that imposes negative impacts over water quality and damages the nearby land fertility. Typically, it has been used for soil stabilisation (Chu et al., 1955), as an embankment material (Raymond, 1961), structural fill (Digioia and Nuzzo, 1972) and as injection grouting (Joshi et al., 1981). Utilisation of fly ash in underground mine fill may provide land subsidence control (Maser et al., 1975), as effective stabilisation to the coal pillars and minimise the risk of subsidence (Fawconnier and Korsten, 1982), to improve the strata control (Galvin and Wagner, 1982). With paste backfilling technology, 60–70% of coal combustion by products (CCBs) and coal processing waste is possible to inject into underground mines (Chugh et al., 2001). A combination of fly ash with additive such as lime and gypsum at 15%–20% and 0%–5% by weight, respectively, may be used as good alternative material for backfilling in mine voids (Mishra and Rao, 2006).

4.2.1 Advantages and disadvantages with fly ash utilisation

Fly ash, which is used for backfilling in underground mine voids, has a number of positive and negative points. Mass utilisation of fly ash in mine backfilling provides a suitable waste management option. It will reduce some of the environmental problems related with its transportation and dump, and provides an alternative of river sand, etc.

On the other hand, negative part of fly ash utilisation in mine backfilling is related with ground water contamination; leaching and cost is another factor.

4.3 OB, mine refuse or waste rock as backfilling material

A number of researches have been performed based on the possible utilisation of coal mine overburden dump as a material to be used in mine backfilling. Prashant et al. (2010) and Karafakis et al. (1996) have performed their work based on characterisation of coal mine refuse or waste rock utilisation in underground mine backfilling. Waste crushed

rock and OB material are found to be useful in backfilling in underground mine voids as an alternative of river sand. Prashant et al. (2010) concluded that most of the physical and geotechnical parameters like bulk density and specific gravity are comparable with river sand while porosity will achieve the same with washing efforts (Table 3). Grain size distribution results show that finer particles present in OB sample hinder some properties such as percolation but by washing it can also be achieved near to river sand at 150 micron cut-off size.

Table 3 Physical properties of OB dump material

S. no.	*Parameters*	*OCP I*	*OCPII*	*OCP III*	*River sand*
1	Specific gravity	2.51	2.57	2.51	2.56
2	Bulk density (g/cc)/ Porosity (%)	1.51/40	1.54/40	1.51/40	1.54/40
3	Percolation rate (cm/h)	236.6	195.9	310.19	276.8

Source: Prashant *et al*. (2010)

4.3.1 Importance of physicochemical analysis

Physicochemical properties of OB material have their own importance in different manners such as reaction takes place owing to the presence of different elements in the OB and simultaneous combustion of OB. Presence of nitrogen (N), phosphorus (P), sulphur (S), etc., causes different chemical reactions to the environment. Presence of various elements in OB material may lead to different types of chemical changes with available water sources and result to AMD or may cause some of the atmospheric pollution by simultaneous combustion.

4.3.2 Physical and geotechnical properties of OB

A number of geotechnical and physical properties are there to be tested to check the suitability of any material for backfilling in underground mine voids. Karafakis et al. (1996) found that slake durability, plasticity, particle size analysis and triaxial compression test are some of the key tests that must be performed for backfilling material (Table 4). Some of them are as follows.

Table 4 Desired properties of coal refuse as backfill material

Test	*Desired properties*
Slake durability test	I_{d1} greater than 95, I_{d2} greater than 85
Plasticity	Refuse should not be plastic
Grain size analysis	Minus 0.075 mm material should not exceed 10% for hydraulic stowing systems, the minus 3 mm material should not exceed 20% for pneumatic stowing systems, C_u greater than 4, C_c between 1 and 3
Permeability	Coefficient of permeability should be at least 2.78×10^{-5} m/s
Triaxial compression	Residual angle of internal friction should be at least 30º confined modulus of deformation comparable to modulus of deformation of a failing coal pillar

Source: Karafakis et al.(1996)

- *Grain size analysis*

There is a significant importance of grain size over geotechnical assessment of filling material. Backfilling material, which contains well-graded particles, should offer more resistance to displacement and settlement than one with uniformly graded particles. Kesimal (2004) found that particle size distribution analysis is one of the most important parameters for backfilling materials. Maximum grain size of a grain used in filling should be less than 1/5th of the pipe bore to limit the critical velocity of flow in pipe (Prashant et al., 2010). Sieve analysis result (Table 5) of OB samples from Jharia coal field shows that there is significant amount of sand, i.e., about 60–74% (Arvind et al., 2011). Because of the presence of higher amount of sand particles in the OB samples, there will be fast removal of water passing through the dump material that is one of the characteristic features of stowing material (Ghosh, 2002). The amount of water flow through coal mine refuse can be empirically related to its gradation and void ratio (Senyur, 1989). Permeability decreases with a decrease in the effective size of the material. An indication of the gradation of the refuse can be computed from a grain-size distribution curve for grain sizes larger than the 0.075 mm sieve using the coefficient of uniformity (Cu) and coefficient of curvature (Cu). Both values can be calculated provided that not more than 10% of the grain sizes are less than 0.075 mm (Bowles, 1979).

Table 5 Grain size distribution of overburden samples

S. no.	*Sampling sites*	*Gravel* (%)	*Sand* (%)	*Silt + Clay* (%)
1	Nudkhurkee	31	68	0.8
2	Muriadih	25.6	73.6	0.8
3	Akashkinaree	28.9	69.7	0.6
4	Mudidih	24.9	71.3	0.8
5	Nichitpur	26.2	70	2.4

Source: Arvind et al. (2011)

- *Atterberg limit testing*

This is required to check the consistency of the material to be utilised as backfilling in mine voids. Consistency of the material is measured with Cassagrand apparatus (IS: 2720, Part 5, 1995). An unconsolidated material with lattice or no clay such as gravel and clean sands will not exhibit plasticity and is considered as non-cohesive (Sowers, 1979). Such type of non-cohesive material should be used as backfilling. Dunn et al. (1980) and Morgenstern and Eigenbrod (1974) reported that there is a relationship between liquid limit and amount of slaking of argillaceous rocks. Liquid limit has also correlation with compressibility of soils.

- *Slake durability test*

There is possibility with the backfilling material that it may experience a cyclic change of wetting and drying during flowing placement, which can degrade the particles and subsequently alter the fill mechanical properties. Thus, this is important to examine the slake durability of the material to be used as backfilling material. It provides a qualitative assessment of the resistance offered by weak rocks, as shales, mudstone, silt stone and clay-bearing rocks, to weakening and disintegration during the cycle of drying

and wetting. This is an index test and can be used to compare the slake properties of two different materials (ASTM D 4644-87). Gamble (1971) proposed that there is a direct relationship between slake durability and the Atterberg limits. Rocks with low slake durability index should be subjected to the plasticity test to characterise better their potential behaviour with water. He proposed a classification based on the results of slake durability as well as Atterberg limits test, whereby analysing the durability index for first and second cycles (I_{d1} and I_{d2}). We can give each sample with a general durability ranking on Gamble's slake durability ranking (Figure 5).

Figure 5 Gamble's (1971) classification for the test of slake durability of coal mine refuse (see online version for colours)

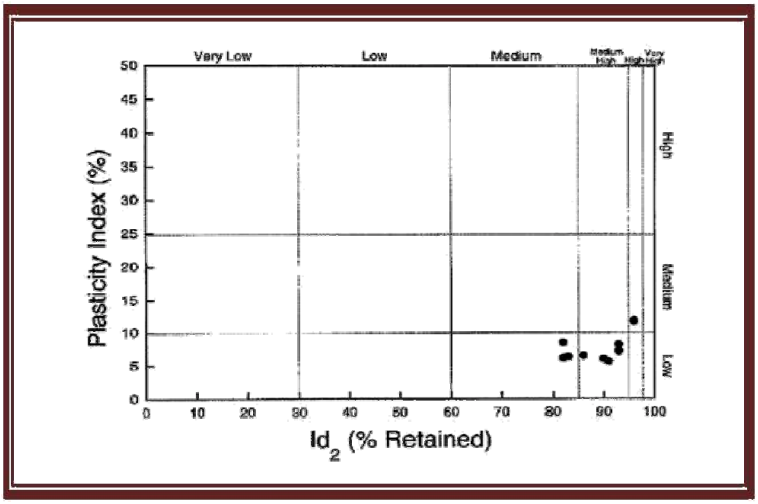

- *Standard proctor compaction test*

Compaction analysis is important to determine the moisture content of the refuse material, which will achieve the maximum dry density for a material that has been compacted with a given compactive effort. It can analyse the potential of the stowing materials. For two different soil samples, it can provide an indication that which material may achieve higher densities following compaction by whatever means, including by failing mine roof and pillars.

- *Falling head permeability test*

Permeability is the ability of a porous material to allow a liquid to pass through its pores. Since the pores are connected with each other, the flow of a liquid takes place through the pores if there is difference in head at the two ends of the sample. Permeability is an important parameter to check the suitability of a material to allow fluid flow through it. For backfilling material, it is important to analyse the nature of water flow through an unconsolidated material, as it has a great effect on its physical properties and its flow behaviour. Higher permeability value ensures fast water seepage from slurry thereby easy and quick consolidation of the slurry. It also provides fast out flow of water from barricading. Falling head permeability test is performed with IS: 2720 (Part: XVII). This test is important for the calculation of seepage through earth dams or under sheet pile

walls, seepage rate from waste storage facilities (landfills, ponds, etc.) and for the calculation of the rate of settlement of clayey soil deposits.

5 Conclusions and future prospects

This paper provides a brief overview on the importance of backfilling in underground mine voids. It briefly discussed the advantages, disadvantages of different materials and possible alternative materials. A number of materials have been used for backfilling in underground mine voids to reduce the mining problems such as subsidence, roof fall, mine fire etc. River sand is the widely used material in mine filling but the resource is reducing due to its high demand in construction sectors. Thus there is a scope for finding a suitable material that may be used as an alternative of river sand, which should be eco-friendly and cost effective. The OB waste generated during mining activities is temporarily dumped on valuable land for long period due to lack of any proper management and causes various environmental problems. This OB dump material might be a good alternative of river sand.

However evaluation of heavy metal contents of the OB material is required before its utilisation in backfilling to reduce leaching impacts in ground water.

Thus utilisation of OB waste as backfilling material will replace river sand, reduce negative impacts of sand mining in river ecosystem and ensure a sustainable method of mining.

Acknowledgement

Authors are highly grateful to the Head of Department, Department of Environmental Science and Engineering, Indian School of Mines, Dhanbad, India. We also like to acknowledge lab mates and friends, S.K. Mritunjay, Jitin Rahul, A Chowdhury (ISM JRF) for their help.

References

Amaratunga L.M. and Yaschyshyn, D.N. (1997) 'Utilization of gold mill tailings as secondary resources in the production of a high strength total tailings paste fill', *CIM Bull.*, Vol. 90, No. 1012.

Aref, K., Brummer, R. and Alan, M. (1992) 'Paste: The fill of the future? (Part 2)', *Canadian Mining Journal*, pp.40–43.

Arvind, R., Paul, B. and Singh, G. (2011) 'A study on physicochemical properties of overburden dump materials from selected coal mining areas of Jharia coalfields, Jharkhand, India', *Journal of Environmental Science*, Vol. 1, No. 6, pp.1350–1360.

Barapanda, P. (2001) 'Utilization of coal mining wastes', *An Overview, National Seminar on Environmental Issues and Waste Management in Mining and Allied Industries,* Regional Engg. College, Rourkela, Orissa, India, pp.177–182.

Barret, J.R., Coulthard, M.A. and Dight, P.M. (1978) 'Determination of fill stability in mining with backfill', *12th Canadian Rock Mechanics Symposium, Canadian Institute of Mining and Metallurgy*, Quebec. Special, Vol. 19, pp.85–91.

Belem, T., Harvey, A., Simson, R. and Aubertin, M. (2004) 'Measurement and prediction of internal stresses in an underground opening during its filling with cemented fill',

in Villaescusa, E. and Potvin, Y. (Eds.): P*roceedings of the Fifth International Symposium on Ground Support in Mining and Underground Construction*, September, Perth, pp.28–30.

Bowles, J.E. (1979) *Physical and Geotechnical Properties of Soils*, McGraw-Hill, New York, p.478.

Chaulya, S.K., Singh R.S., Chakraborty M.K. and Tewary, B.K. (2000) 'Bioreclamation of coal mine overburden dumps In India'*, Land Contamination & Reclamation*, Vol. 8, No. 3, pp.1–7.

Chikkatur, A. (2005) 'Making the best use of india's coal resources', *Economic and Political Weekly*, Vol. 40, pp.5457–5461.

Chu, T.Y., Davdson, D.T., Goecker, W.L. and Moh, Z.C. (1955) 'Soil stabilization with lime-fly ash mixtures: preliminary studies with silty and clayey soils', *Highway Research Board Bulletin*, Vol. 108, pp.102–112.

Chugh, Y.P., Deb, D. and Biswas, D. (2001) 'Underground placement of coal processing waste and coal combustion byproducts based paste backfill for enhanced mining economics', *Mining in 21st Century, Proceedings of 19th World Mining Congress*, New Delhi, pp.1327–1341.

Deng, A., Paul, J. and Tikalsky, P.J. (2007) 'Geotechnical and leaching properties of flowable fill incorporating waste foundry sand', *Waste Management*, Vol. 28, No. 11, pp.2161–2170.

Digioia, A.M. and Nuzzo, A.M. (1972) 'Fly ash as structural fill', *Journal of Power Div, ASCE*, Vol. 98, No. 1, pp.77–92.

Dunn, I.S., Anderson, L.R and Kiefer, F.W. (1980) 'Characterization of coal mine refuse as backfilling material', *Geotechnical and Geological Engineering*, Vol. 14, pp.129–150.

Fawconnier, C.J. and Korsten, R.W.O. (1982) 'Ash fill in pillar design- increased underground extraction of coal', *The SAIMM Monograph Series 4*, pp.277–361.

Galvin, J.M. and Wagner, H. (1982) 'Use of ash to improve strata control in bord and pillar working'. *Proceeding Symposium on Strata Mechanics*, University of New castle upon Tyne, pp.264–269.

Gamble, J.C. (1971) *Durability, Plasticity, Classifications of Shales and Other Argillaceous Rocks*, Ph.D. Thesis. Univ. of Illinois, USA.

Ghosh, R. (2002) *Land Use in Mining Areas of India*, Envis Monograph No. 9 by CME, ISSN: 0972-4656.

Grice, T. (1998) 'The 2nd annual summit – mine tailings disposal system', *Brisbane*, 24–25 November, pp.1–13.

Ham, R.K., Boyle, W.C. and Blaha, F.J. (1990) 'Comparison of leachate quality in foundry waste land- fills to leaching test abstracts', *Journal of Hazardous and Industrial Solid Waste Testing and Disposal*, Vol. 6, pp.29–44.

Javed, S., Lovell, C. W., and Wood, L. E. (1994) *Waste Foundry Sand in Asphalt Concrete*, Transportation Research Board (TRB), Record No. 1437, National Research Council, Washington DC, pp.27–34.

Joshi, R.C., Natt, G.S. and Wright, P.J. (1981) 'Soil improvement by lime-fly ash slurry injection', *Proc. 10th Int. Conference on Soil Mechanics & Foundation Engg.*, Stockholm, Vol. 3, pp.707–712.

Karafakis, M.G., Bowman, C.H. and Gamble, T.E. (1996) 'Characterization of coal mine refuse as backfilling material'. *Journal of Geotechnical and Geological Engineering*, Vol. 14, pp.29–150.

Kesimal, A., Yilmaz, E. and Ercikdi, B. (2002) 'Evaluation of paste backfill mixtures consisting of sulfide-rich mill tailings and varying cement contents, Evaluation of paste backfill mixtures consisting of sulfide-rich mill tailings and varying cement contents', *Cement and Concrete Research*, Vol. 34, pp.1817–1822.

Kortnik, J. (2003) 'Backfilling waste material composites environmental impact assessment', *Journal of South African Institute of Mining and Metallurgy*, pp.391–396.

Kratzsch, H. (1983) *Mining Subsidence Engineering*, Springer-Verlag New York, pp.543.

Kumar, V., Ahuja, B.P., Dattatryulu, J.V., Bhaskar Rao, B., Ghosh, C.N. and Sharma, A.K. (2003) 'Hydraulic stowing of pond ash in underground mines of Manuguru, India', *Proceed. 3rd Int. Conf. on Fly ash utilization and Disposal*, 19–21 February, New Delhi, India, pp.VI-1-7.

Landriault, D.A., Verburg, R., Cincilla, W. and Welch, D. (1997) *Paste Technology for Underground Backfill and Surface Tailings Disposal Applications*, Short Course Notes, Canadian Institute of Mining and Metallurgy, Technical Workshop, Vancouver, British Columbia, Canada, pp.120.

Lu, Z., Cai, M. and Caib, M. (2012) 'Disposal methods on solid wastes from mines in transition from open-pit to underground mining', *7th International Conference on Waste Management and Technology, Procedia Environmental Sciences*, Vol. 16, pp.715–721.

Mark, R., Corrigan, R. and Cochrane, L. (1990) *Internal Report INCO Ltd., Ontario Division*, Third Report to Lucky Friday Mine regarding High Density Backfill, pp.7.

Marston, A. (1930) *The Theory of External Loads on Closed Conduits in the Light of Latest Experiments*.

Maser, K.R., Wallhagen, R.E and Dieckman, J. (1975) *Development of Fly Ash Cement Mine Sealing System*, USBM, Open File Report, NTIS–PB-250611, pp.26–76.

Mishra, M.K. and Rao, U.M. (2006) 'Geotechnical characterization of fly ash composites for backfilling mine voids, world coal ash conference', *Journal of Geotechnical and Geological Engineering*, Vol. 24, No. 6, pp.1749–1765.

Mitchell, R.J. (1989) 'Stability of cemented tailings backfill', *Computer and Physical Modelling in Geotechnical Engineering*, Balkema, Rotterdam, pp.501–550.

Morgenstern, N.R. and Eigenbrod, K.D. (1974) 'Classification of argillaceous soils and rocks', *Journal of Geotechnical Engineering Division*, Vol. 100, pp.1137–1157.

National Academy of Sciences (1975) *Underground Disposal of Coal Mine Wastes*, National Academy of Engineering, Washington DC, p.172.

Naylor, J., Famermery, R.A. and Tenbergen, R.A. (1997) 'Paste backfill at the macassa mine with flash paste production and storage mechanism', *Proceedings of the 29th annual meeting of the Canadian Mineral Processors (Division of the CIM)*, 21–23 January, Ottawa, Ontario, pp.408–420.

Prakash, A., Lokhande, R.D. and Singh, K.B. (2009) 'Surface ground deformation in Jharia and Raniganj coalfields over old mine workings', *International Journal of Environment Protection*, Vol. 29, No. 4, pp.289–293.

Prashant, Ghosh, C.N. and Mandal, P.K. (2010) 'Use of crushed and washed overburden for stowing in underground mines, a case study', *Journal of Mines, Metals & Fuels*, Vol. 58, Nos. 1–2, pp.7–12.

Rai, A.k., Paul, B. and Singh, G. (2011) 'A study on physicochemical properties of overburden dump materials from selected coal mining areas of Jharia coalfields, Jharkhand, India', *Journal of Environmental Science*, Vol. 1, No. 6, pp.1350–1360.

Rajaram, V., Rajaram, R. and Rajaram, R. (2005) 'Sustainable mining practices: a global perspective', *British Library Cataloging in Publication Data*, pp.60–80.

Raymond, S. (1961) 'Pulverized fuel ash as embankment material', *Proc.-Inst. Civ. Eng*., Paper No. 6538, pp.515–536.

Senyur, S. (1989) 'The flow characteristics through hydraulic filling materials produced from coal washery rejects', *Proceedings of the 4th International Symposium on Mining with Backfill*, Innovation in Mining Backfill Technology, Montreal, October, A.A. Balkema, Amsterdam, pp.307–314.

Sivakugan, N., Rankine, R.M., Rankine K.J. and Rankine, K.S. (2004) 'Geotechnical consideration in mine backfilling in Australia', *Journal of Cleaner Production*, Vol. 14, pp.1168–1175.

Sowers, G.F. (1979) *Introductory Soil Mechanics and Foundations*, Macmillan, New York, p.621.

Vipulanadan, C. and Sunder, S. (2000) 'Effects of meta-kaolin clay on the working and strength properties of cement Gouts', *Grounting and Deep Mixing*, pp.1739–1747.

Yaseen, S., Pal, A., Singh, S. and Yousuf, I. (2012) *A Study of Physico-Chemical Characteristics of OB Dump Materials from Selected Coal Mining Areas of Raniganj Coal Fields, Jharkhand, India*, Global Journals Inc., USA.

Zheng, J.J., Zhang, Q.L., Wang, X.M. *et al*. (2008) 'The prediction of backfilling drill-hole's life based on BP neutral networks', *Journal of Xiangtan Normal University (Natural Science Edition)*, Vol. 30, No. 4, pp.40–44.

Bibliography

ASTM D4644-87 (1987) 'Slake durability of shales and similar weak rocks, Annual Book of ASTM Standards', *American Society for Testing and Materials*, Philadelphia, Vol. 4.08, pp.848–850.

Benzaazoua, M. and Bussière, B. (1999) 'Desulphurization of tailings with low neutralization potential: kinetic study and flotation modeling', in Goldsack, P., Belzile, N., Yearwood, P. and Hall, G. (Eds.): *Proceedings of Sudburry Mining and the Environment II*, Vol. 1, pp.29–38.

Brackebusch, F.W. (1994) 'Basics of paste backfill systems', *Mineral Engineering*, Vol. 46, No. 10, pp.1175–1178.

Kuganathan, K. and Sheppard, I.A. (2001) 'A non-segregating "Rocky Pastefill" (RPF) produced by co-disposal of cemented de-slimed tailings slurry and graded rockfill', in Stone, D. (Ed.): *Minefill: Proceedings of the 7th International Symposium on Mining with Backfill*, *Society for Mining, Metallurgy and Exploration (SME)*, pp.27–41.

Lokhnde, R.D., Singh, K.B. and Singh, K.K.K. (2005) 'Subsidence control measure in coal mines', *Journal of Scientific & Industrial Research*, Vol. 64, pp.323–332.

Mishra, D. and Das, S. (2010) 'A study of physicochemical and mineralogical properties of Talcher coal fly ash for stowing in underground coal mines', *Material Characterization*, pp.1252–1259.

Moreno, N. and Querol, X. (2005) 'Physico-chemical characteristics of European pulverized coal combustion fly ashes', *Fuel*, Vol. 84, pp.1351–1363.

Nantel, J. (1998) 'Recent developments and trends in backfill practices in Canada', *Proceedings of the Sixth International Symposium on Mining with Backfill, Mine fill AIMM*, Brisbane, pp.11–14.

Petrolito, J., Anderson, R.M. and Pigdon, S.P. (2005) 'A review of binder materials used in stabilized backfills', *CIM Bull.*, Vol. 98, No. 1085, p.85.

Planning Commission (2002) *Tenth Five-Year Plan*, Planning Commission, Government of India.

Svarovsky, L. (1987) *Powder Testing Guide*, Elsevier Applied Science Powder Testing Guide, BMHB, p.146.

Yilmaz, E., Kesimal, A. and Ercidki, B. (2004) 'Evaluation of acid producing sulphidic mine tailings as a paste backfill', *Mining with Backfilling*, pp.341–348.

Zhang, Q. and Wang, X. (2007) 'Performance of cemented coal gangue backfill', *Journal of Central South University of Technology*, Vol. 14, No. 2, pp.216–219.

Kinetic studies on the reoxidation of beneficiated ilmenite by non-isothermal thermogravimetric analysis

K. Harikrishna Bhat*

Material Sciences and Technology Division,
CSIR-National Institute for Interdisciplinary
Science and Technology (NIIST),
Thiruvananthapuram 695 019, Kerala, India
Email: karvalbhat@gmail.com
*Corresponding author

Mahesh R. Patil and B.P. Ravi

Department of Studies and Research in Mineral Processing,
Vijayanagara Sri Krishnadevaraya University – PG Centre,
Nandihalli, Sandur 583 119,
Bellary, Karnataka, India
Email: krutica.mrp@gmail.com
Email: ravibelavadi@gmail.com

Abstract: Synthetic rutile is an important titanium feedstock for the production of titanium dioxide pigment and titanium metal. More attention is focussed in recent years on the development of environment friendly processes for the production of synthetic rutile with minimum acidic effluents. CSIR-NIIST, Trivandrum, India, had successfully developed a more environment friendly process for the production of high grade synthetic rutile containing more than 94% TiO_2. The process is comprised of metallisation of ilmenite followed by aeration rusting for the production of beneficiated ilmenite and the reoxdiation of beneficiated ilmenite followed by acid leaching. Reoxidation of beneficiated ilmenite plays a major role in rendering the product amenable to acid attack and removal of residual iron. This paper describes in detail the kinetic studies carried out on the reoxidation of beneficiated ilmenite by thermogravimetric technique under non-isothermal conditions. Assuming the oxidation mechanism to be in the form $(1 - \alpha)^n$ and considering a contracting spherical model with $n = 2/3$, the basic equation of non-isothermal reaction was analysed and solved by integral approach. The kinetic parameters such as activation energy, pre-exponential factor and the order of the oxidation reaction were computed from the weight gain data under linear rise in temperature. The paper also discusses the optimisation of reoxidation temperature and residence time for the maximum removal of iron during acid leaching, which in turn results in synthetic rutile of maximum TiO_2 content.

Keywords: synthetic rutile; reoxidation; thermogravimetry; beneficiated ilmenite; non-isothermal thermogravimetric analysis.

Reference to this paper should be made as follows: Bhat, K.H., Patil, M.R. and Ravi, B.P. (2015) 'Kinetic studies on the reoxidation of beneficiated ilmenite by non-isothermal thermogravimetric analysis', *Int. J. Mining and Mineral Engineering*, Vol. 6, No. 2, pp.187–198.

Biographical notes: K. Harikrishna Bhat has obtained his Postgraduate Degree in Metallurgical Engineering in Process Metallurgy from the National Institute of Technology, Surathkal, Karnataka, India (NITK), in 1985. Since joining CSIR-NIIST, Trivandrum in 1986, he has served in various capacities and currently he is heading minerals and metallic materials activities. His research areas include chemical beneficiation of beach sand minerals, plasma processing, rotary kiln reduction of mineral sands, pyrometallurgical extraction of rare earth metals and their purification. He has significant contributions in the successful development of two major technologies for the production of synthetic rutile from ilmenite. He has about 30 publications in reputed journals and nine national and international patents to his credit.

M.R. Patil obtained his Master's and Doctorate Degrees in Mineral Processing from Gulbarga University in the year 1982 and 2002, respectively. He is currently working as an Associate Professor in the Department of Mineral Processing VSK University Bellary with 24 years academic and research experience. His areas of interest are mineral processing and environmental management.

B.P. Ravi obtained his Master's Degree in Mineral Processing from Karnataka University in the year 1980 and Doctorate Degree in Mineral Processing from Gulbarga University in 1986. After working in various capacities in public-sector gold and copper mills, and headed ore dressing laboratories of Indian Bureau of Mines, he is currently working as a Professor and Chairman in the Department of Mineral Processing VSK University Bellary. He has 35 years of experience in industrial research mineral processing. His areas of interest are process evolution, characterisation, process auditing and waste processing – reuse.

This paper is a revised and expanded version of a paper entitled 'Kinetic studies on the reoxidation of beneficiated ilmenite by non isothermal thermal analysis' presented at *IXth International Heavy Minerals Conference – 2013*, Vishakapatnam, India, 27–29 November, 2013.

1 Introduction

Synthetic rutile prepared from abundantly available ilmenite mineral is one of the important titanium feedstocks for the production of titanium dioxide pigment and titanium metal. Although a large number of technologies have been developed for the beneficiation of ilmenite for the production of synthetic rutile, only a few are significant in terms of commercial exploitation by the industries. In addition to the quality of the synthetic rutile in terms of TiO_2 content, the beneficiation processes must also take into account the safe disposal of acidic iron effluents generated in large quantities. Hence, continued efforts are focused on the development of technologies that are environment friendly and recover majority of the iron values from the waste generated in addition to high-grade synthetic rutile.

Becher et al. (1965) invented a process for the production of synthetic rutile from ilmenite. The process essentially composed of the reduction of iron component of ilmenite to metallic form followed by the removal of same as iron oxide by aeration rusting. The residual iron from the beneficiated ilmenite (product after rusting) was further removed by mild acid leaching for the production of synthetic rutile. Mohan Das et al. (2006) developed a more environmentally friendly process involving the above-mentioned unit operations with additional step of reoxidation of beneficiated ilmenite prior to leaching for the preparation of high-grade synthetic rutile with more than 94% TiO_2. Reoxidation of beneficiated ilmenite is an important unit operation in the overall process flowsheet as it renders the beneficiated ilmenite more susceptible to acid leaching and hence resulting in synthetic rutile of higher TiO_2 content. However, there exists a lacuna in the detailed understanding of kinetics and mechanism of reoxidation of beneficiated ilmenite. This paper describes the details of the kinetic studies carried out on the reoxidation of beneficiated ilmenite, an intermediate product generated in the process by thermogravimetric technique. In view of inadequacy of isothermal kinetic studies by virtue of very small size of the ilmenite particles, efforts were made to elucidate valid kinetic parameters of reoxidation of beneficiated ilmenite by thermogravimetry under non-isothermal conditions.

1.1 Non-isothermal analysis

No reaction takes place isothermally because all the reactions are accompanied by a heat change. Most of the industrial processes involve gradual heating up of the reactants and the reaction proceeds under rising and fluctuating temperature conditions. Reactions such as exothermic oxidation cause significant changes in the sample temperature. Hence, the kinetic data must be analysed in terms of possible heat transfer effects owing to deviations of the temperature of the sample from that of isothermal conditions. In addition, there may be some pre-reaction during the heating of the reaction system to the predetermined temperature and a part of the sample may change before the beginning of the kinetic run. Isothermal technique is often inadequate for the complex reactions involving several series of parallel or independent overlapping reactions. As most of the reactions take place by heating the reactants gradually, any kinetic parameters derived under isothermal conditions are not applicable to processes taking place non-isothermally.

In view of the above, there have been several attempts in recent years in the development of mathematics of non-isothermal kinetics and its application in solid-state reactions and only the kinetic parameters determined under non-isothermal conditions are viewed as valid.

Thermogravimetry, a technique where the sample is heated to linear rise in temperature, has been used by Haque et al. (1992) for non-isothermal kinetic studies. The theoretical treatment of the kinetic data under rising temperature conditions depends largely on three basic equations.

The first being the kinetic law in the differential form

$$\mathrm{d}\propto/\mathrm{d}t = k(T)\cdot f(\propto)\cdot\phi(\propto,T) \tag{1}$$

where $\propto$ is the fraction reacted, k is the temperature-dependent rate constant, ϕ and f denote functions, t is the time and T is the temperature. With $\phi(\alpha, t)$ being assumed as unity, one can write

$$\mathrm{d}a / \mathrm{d}t = k\left(T\right) \cdot f(\alpha). \tag{2}$$

The second equation required is the temperature coefficient of rate constant

$$K = A \cdot T^{m} \cdot \mathrm{e}^{-E/RT} = A\mathrm{e}^{-E/RT} \tag{3}$$

where E is the activation energy, A is the pre-exponential factor, R is the gas constant and m is a constant generally assumed to be zero.

The third important data required for the analysis of the non-isothermal equation is the variation of temperature with time. For a constant linear heating rate, one can write

$$T = T_o + Bt \tag{4}$$

where T_o is the initial temperature and B is the heating rate.

By incorporating equations (3) and (4) in equation (2), we get

$$\mathrm{d}\alpha / f(\alpha) = A / B \cdot \mathrm{e}^{-E/RT} \cdot \mathrm{d}T. \tag{5}$$

Equation (5) is the basic equation for non-isothermal kinetic analysis. There are two distinct approaches available for the analysis of the non-isothermal kinetic data.

In an integral method, integrated form of equation (5) is employed for the evaluation of kinetic constants wherein the weight-temperature plots are just sufficient with known program of time-temperature.

Alternatively, the data in a differential form is obtained and the values of dα/dt, α and T were suitably incorporated in the derived form of equations. However, this approach requires a special derivative thermogravimetric analysis (DTG) apparatus or involves lengthy procedures of graphical differentiation of TG curves.

A straightforward approach for the analysis of the basic non-isothermal equation (5) employed by Ray (1993) as detailed here is devoid of complex mathematical approaches and based on well-defined mathematical procedures and approximations.

In an integral approach, the integrated form of kinetic law is given by

$$g(\alpha) = kt \tag{6}$$

which on differentiation becomes

$$\mathrm{d}\alpha / \mathrm{d}t = k / g(\alpha) = k \cdot f(\alpha) \tag{7}$$

then,

$$\int \mathrm{d}\alpha / f(\alpha) = \int g'(\alpha) \cdot \mathrm{d}\alpha = g(\alpha) \tag{8}$$

and hence on integrating equation (5), we get

$$g(\alpha) = A / B \int \exp\left(-E / RT\right) \cdot \mathrm{d}T. \tag{9}$$

In the above-mentioned equation, it is to be noted that $g(\alpha)$ is obtained only when integrated form of equation (6) is known or analytical form of $f(\alpha)$ is known. Furthermore, right-hand side of equation (9) cannot be integrated in finite form.

Coats and Redfern (1964) have suggested a graphical procedure, which is considered as one of the best solutions to the problem of integration. For a reaction with a mechanism in the form $(1 - \alpha)^n$ and considering a contracting sphere model with $n = 2/3$, we have

$$\int \mathrm{d}\alpha / (1-\alpha)^n = A / B \int \mathrm{e}^{-(E/RT)} \mathrm{d}T \tag{10}$$

$$\cong \mathrm{ART}^2 / \mathrm{BE} \cdot \mathrm{e} - \left(E / RT\right)\left[1 - 2RT / E\right] \tag{11}$$

when $n = 1$,

$$\log 10 \left[-\ln (1-\alpha) / T^2\right] = \log 10\, AR / BE \left[1 - 2RT / E\right] - E / 2.3RT. \tag{12}$$

A plot of LHS against 1/T gives a straight line with slope of –(E/2.3R)

If $n \neq 1$, then $\int (1-\alpha)^{-n} \mathrm{d}\alpha = -(1-\alpha)^{1-n} / (1-n)$

$$1 - (1-\alpha)^{1-n} / \left(1-n\right)T^2 = AR / BE \left\{1 - 2RT / E\right\} \mathrm{e}^{-(E/RT)}. \tag{13}$$

Considering the pre-exponential term in RHS of the above-mentioned equation almost constant, a plot of log10 (LHS) against 1/T gives a straight line with slope –(E/2.3R).

2 Materials and methods

2.1 Non-isothermal gravimetric analysis

The beneficiated ilmenite employed in the present investigation was prepared by the reduction of ilmenite followed by rusting of metallised ilmenite. Commercial-grade ilmenite from Quilon deposits supplied by Indian Rare earths Ltd., Chavara, Kerala, India, having the composition as given in Table 1 was reduced using coal as the reductant. The details of the reduction of ilmenite were discussed elsewhere by Mohan Das et al. (1990).

Table 1 Chemical composition of Quilon grade Kerala ilmenite

Constituents	*TiO_2*	*Fe_2O_3*	*FeO*	*Al_2O_3*	*MnO*	*Cr_2O_3*	*V_2O_5*	*MgO*	*P_2O_5*	*ZrO_2*	*SiO_2*	*Rare earths*
% Wt.	58.0	25.5	9.70	1.1	0.4	0.13	0.15	0.60	0.20	0.40	0.90	Trace

Rusting of metallised ilmenite in the presence of ammonium chloride catalyst was carried out in a stirred tank reactor and the beneficiated ilmenite was separated from hydrated iron oxide by decantation and several washings. The experimental details and the rusting parameters are discussed by Jeya Kumari et al. (2001). The chemical composition of beneficiated ilmenite is given in Table 2.

Table 2 Chemical composition of beneficiated ilmenite

Constituents	TiO_2	Fe_2O_3	Al_2O_3	MnO	Cr_2O_3	V_2O_5	MgO	ZrO_2	SiO_2	*Rare earths*
% Wt.	84.85	13.575	0.643	0.555	0.147	0.220	0.479	0.062	1.227	Trace

A SHIMADZU, Model TGA-50 thermogravimetric analyser supported by TA-50WSI thermal analysis system was used for carrying out thermogravimetric experiments. TA-50WSI system is composed of a single personal computer of IBM PC/AT compatible types of 286PS/2 model 30 series. About 10 mg of beneficiated ilmenite was taken in a platinum sample cell and the same was loaded into hanging balance inside the furnace.

High purity oxygen gas was purged continuously into the reaction tube at a flow rate of 10 mL/min for the oxidation of beneficiated ilmenite to take place. The furnace was heated at a rate of 20ºC/min continuously up to a temperature 1000ºC. All the outputs in terms of weight-temperature and weight-time mode were recorded. Experiments were carried out on samples of particle sizes (−0.355 + 0.25), (−0.25 + 0.18), (−0.18 + 0.125) and (−0.125 + 0.09) mm, respectively. Effect of heating rate on the reoxidation was also studied by carrying out the oxidation at varying heating rates of 5, 10 and 20ºC/min, respectively. The data obtained in weight-time-temperature mode were used for the elucidation of kinetic parameters such as activation energy, pre-exponential factor and order of the oxidation reaction. Weight-time-temperature data at temperatures lower than 500ºC and at temperatures above 800ºC were not considered for the analysis as the weight gain owing to oxidation at these temperature ranges were not appreciable. Only data in the temperature range 500–800ºC were employed in the analysis of the kinetic parameters. From the data, the function α is calculated as

$$\alpha = m(T) - m(T_s) / m(T_f) - m(T_s) \tag{14}$$

where $m(T)$ is the weight of the sample at temperature T, $m(T_s)$ is the weight of the sample at initial temperature (T_s) and $m(T_f)$ is the weight of the sample at final temperature T_f.

Equation (13) was solved using the standard technique of error minimisation. Incorporating the assumed initial values for n, E and A/B, α was calculated using equation (13) at a given temperature (T). The values of calculated α were then compared with the experimental value of α computed from the thermogravimetric data using equation (14). By iteration, the values of n, E and A/B were arrived at such that the difference between the calculated α and the experimental α is minimum.

2.2 Optimisation of reoxidation temperature and residence time

Reoxidation of beneficiated ilmenite of different size fractions was carried out in an inconel tubular reactor provided with opening at both the ends. About 10 g of the material was spread uniformly into a thin layer in an alumina boat and a continuous flow of dry air was maintained over the sample at predetermined temperature and residence time.

2.2.1 Optimisation of reoxidation temperature

Beneficiated ilmenite of size range (−0.18 + 0.125) mm, having the highest percentage by weight in the bulk sample, was used for the optimisation of oxidation conditions. Reoxidation was carried out at varying temperatures of 500, 700, 800 and 1000ºC, respectively, while the residence time in all the experiments was maintained constant at 30 min. Oxidised products from all the experiments were subsequently leached with hydrochloric acid to assess the leachability. The leach residues were analysed for the residual iron.

2.2.2 Optimisation of residence time of reoxidation

To optimise the residence time of reoxidation, oxidation experiments were carried out at a constant temperature of 500ºC for varying durations of 30, 60 and 120 min, respectively. The leachability of the oxidised samples was analysed by the estimation of residual iron in the leach residue.

2.3 Acid leaching of reoxidised sample

Leaching experiments were carried out in a 3-necked flat bottom flask. One of the necks was used for introducing thermometer while the other was used for drawing liquid/solid samples at regular intervals. A water-cooled condenser was fitted into the third neck. Required quantity of the acid (100 mL) was taken in the flask and heated to 90ºC in an oil bath, which in turn was heated electrically through a dimmerstat. Hydrochloric acid of 20% concentration was used for the leaching of iron from oxidised products prepared under varying conditions of oxidation temperature and residence time. On reaching a preset temperature, weighed quantity of oxidised sample was introduced into the acid and continuously stirred at regulated and constant speed through a magnetic stirrer. After leaching, the leach residue was analysed for the residual iron and percentage removal of iron was calculated.

2.4 X-ray diffraction analysis

Finely ground samples were used for X-ray diffraction studies by powder diffraction technique using Philips X-Ray Diffractometer. A monochromatic radiation CuK_α ($\lambda = 1.5418$ A°) was used for the investigation. Scanning was carried out in the angle 2θ range 20–60° and at a scan rate of 2°/min. The '*d*' values of the major peaks in the diffractogram were measured from the corresponding 2θ values and the phases were identified by comparing the experimental '*d*' values with that of standards.

2.5 Scanning electron microscopy

A Jeol JSM 5600 make scanning electron microscope was used for the investigation of surface morphology of beneficiated ilmenite. Samples of beneficiated ilmenite after reoxidation were also subjected to scanning electron microscope (SEM) studies for the analysis of grain surface morphology. A few grains of the sample were fixed onto a brass stud using an adhesive and subsequently coated with gold for a better conduction of electron beam. All the investigations were carried out using 15 kV electron beam.

3 Results and discussion

3.1 Isothermal studies

Initial run of thermogram with beneficiated ilmenite sample when heated continuously from ambient temperature to 1000ºC showed the onset of weight gain owing to oxidation at 500°C. To explore the possibility of using isothermal conditions for the analysis, a few experiments were carried out at isothermal temperatures of 500, 550, 600, 700 and 800°C, respectively. About 10 mg of the sample was taken in the platinum sample holder and heated from ambient temperature to the required set temperature at heating rate of 20ºC/min during which N_2 gas was purged into the reaction chamber to avoid the oxidation. As soon as the sample reached the set temperature, oxygen gas was purged into the chamber and the oxidation is allowed to continue at the set isothermal temperature for about 60 min.

It was observed that at all the isothermal set temperature, the onset of oxidation and hence the weight gain in the sample started before the sample reaching the set isothermal temperature. As the particle size of the sample was very small, the oxidation of the sample before reaching to isothermal set temperature could not be avoided. Hence, non-isothermal approach was resorted to for the elucidation of oxidation kinetic parameters.

3.2 Non-isothermal studies

3.2.1 Effect of heating rate

When beneficiated ilmenite of particle size in the range –0.25 + 0.18 mm was oxidised at three different heating rates of 5, 10 and 15ºC/min, respectively, it was observed that the variation of heating rate during non-isothermal oxidation had resulted in variation in the value of A/B in the kinetic equation and no change was observed in the value of activation energy.

3.2.2 Effect of particle size

Keeping the heating rate of 10ºC/min constant, non-isothermal thermograms were run for beneficiated ilmenite of size fractions (−0.5 + 0.355), (−0.355 + 0.25), (−0.25 + 0.18) and (−0.18 + 0.125) mm, respectively. Analysis of the thermograms showed a gradual shift of onset of oxidation towards higher temperatures as the particles became more and more coarser. However, there was no appreciable change in the value of activation energy. Beyond 800ºC, finer size fractions showed a decreased rate of oxidation probably owing to the faster kinetics of oxidation and sintering of grains at elevated temperatures.

3.2.3 Kinetic parameters

Assuming different values for n, E and A/B in equation (13), the value of α was calculated using a computer program and by a method of minimisation of error. Values of calculated α and the measured value of α as in equation (14) were then compared. The assumed values of n, E and A/B for which the difference between the measured values of α and its calculated value is minimum are considered the best-suited values of the above-mentioned kinetic parameters. The following set of values was obtained.

Parameters	*Unit*	*Range*
n	Dimensionless	6.07
E	KJ/mol	171
A	$M^{-2}.min^{-1}$	20.13×10^{11}

The above-mentioned values are in close agreement with the values reported in the literature for the oxidation of natural ilmenite pellets by Sun et al. (1992).

3.3 Characterisation of oxidised samples

3.3.1 X-ray diffraction analysis

X-ray diffraction pattern of the reoxidised samples of beneficiated ilmenite as in Table 3 revealed characteristic peaks corresponding to rutile, anatase, pseudorutile and haematite. The presence of predominant peaks corresponding to haematite and pseudorutile ($3TiO_2$. Fe_2O_3) in the reoxidised samples indicates the oxidation of the metallic iron and ferrous iron present in the beneficiated ilmenite.

Table 3 XRD analysis of beneficiated ilmenite after reoxidation at 800ºC

2Theta	*d*(A^0)	*Description*	*Assignment*
25.40	3.528	Weak	Anatase
27.60	3.2589	Strong	Rutile
33.30	2.710	Weak	Hamatite
36.00	2.4927	Medium	Psuedorutile
41.40	2.1909	Weak	Psuedorutile
51.60	1.6892	Medium	Psuedorutile

Ilmenite is an extraordinary inactive material from which the selective removal of iron is extremely difficult. By resorting to a pre-oxidation, this inactive material was converted to highly reactive for further processing wherein iron associated with the titanium is selectively removed. It has been reported by various researchers that the pre-oxidation of ilmenite has the following advantages (Becher et al., 1965; Hussein and El-Tawil, 1967; Sinha, 1973):

- Introducing defects (grain-boundaries, micro-cracks, etc.) in the ilmenite grain.
- Brings about homogenisation in the composition of ilmenite. Converting all the ferrous iron into ferric state, which overcomes the problem of different ferrous to ferric ratios in ilmenite from different deposits and thereby making the process capable of treating all ilmenites irrespective of their origin.
- Improvement in the reducibility of ilmenite owing to the alteration of equilibrium conditions.

The effect of reoxidation temperature of beneficiated ilmenite on the degree of iron removal during subsequent hydrochloric acid leaching is given in Figure 1. The percentage removal of iron from the oxidised samples of beneficiated ilmenite decreased

with the increase in reoxidation temperature. Though reoxidation of beneficiated ilmenite brings about lattice expansion due to the oxidation of residual iron, reoxidation at elevated temperature beyond 500°C leads to sintering of the grains. Closure of pores owing to sintering at high temperature renders the product not amenable to acid attack during leaching. A similar phenomenon was also observed when the residence time of reoxidation was increased from 30 min to 120 min as shown in Figure 2. The loss of porous morphology of the grains at prolonged duration of reoxidation resulted in the poor leachability of the product.

Figure 1 Effect of reoxidation temperature on the degree of iron removal during hydrochloric acid leaching (see online version for colours)

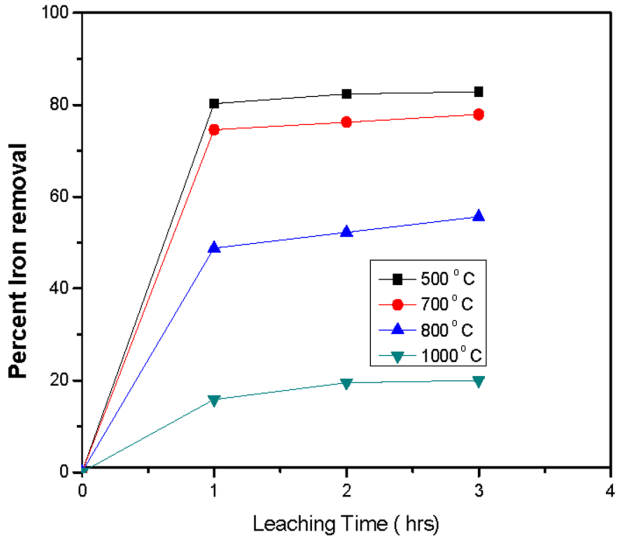

Figure 2 Effect of reoxidation time on the removal of iron from beneficiated ilmenite with hydrochloric acid (see online version for colours)

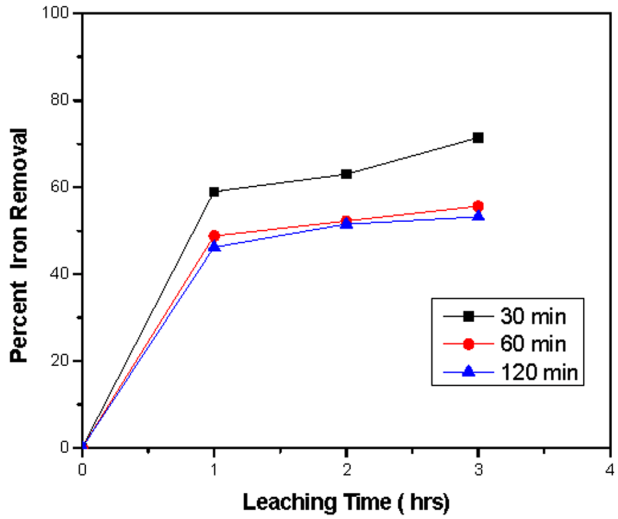

It has further been reported (Sinha, 1973) that that the reoxidation temperature had a significant effect on the subsequent reduction and acid leaching of ilmenite. Pre-treatment (oxidation and reduction) of ilmenite has been found advantageous in the leaching of iron owing to breaking up of the grain structure resulting in a large number of grain boundaries.

3.3.2 Scanning electron microscopy

Scanning electron microscope examination of beneficiated ilmenite before (Figure 3(a)) and after reoxidation (Figures 3(b) and (c)) demonstrates the formation of significant cracks and voids on the surface of oxidised products, which were essentially due to the lattice expansion of the grains during the rutilation and oxidation of metallic iron. These voids and cracks in the oxidised samples had facilitated easier iron removal and faster kinetics in acid leaching.

Figure 3 Scanning electron micrographs of beneficiated ilmenite before and after reoxidation

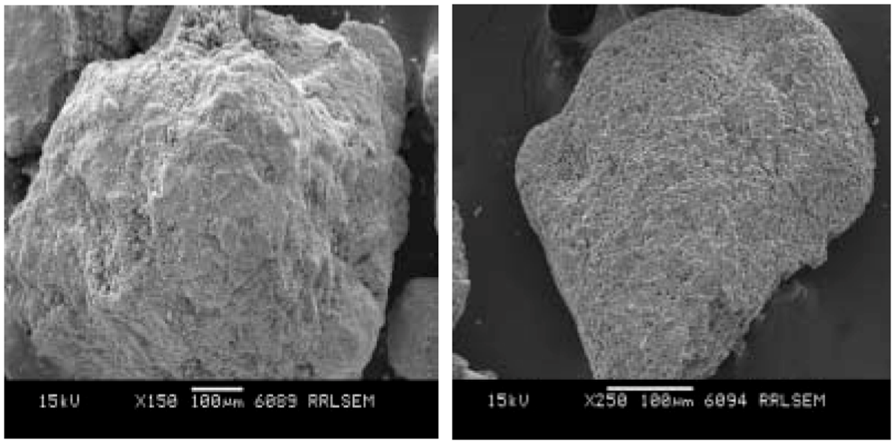

(a) (b)

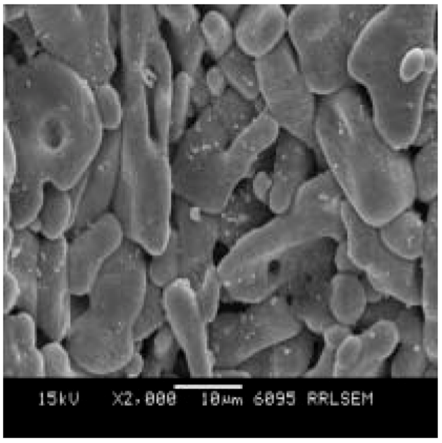

(c)

4 Conclusions

Oxidation reaction of beneficiated ilmenite with particle size range 0.125–0.355 mm could not be studied by isothermal analysis as considerable oxidation took place prior to the sample reaching the isothermal temperature. Hence, non-isothermal technique was employed to study the oxidation reaction and elucidating kinetic parameters such as activation energy by solving the kinetic equation by integral method. The technique appeared reasonably correct as the activation energy computed was in close agreement with the literature values reported for similar systems. Reoxidation of beneficiated ilmenite prior to acid leaching has proved advantageous as the oxidation of residual iron in the lattice brings about lattice expansion, development of voids and cracks on the surface. Porous surface morphology in turn facilitates the acid attack and greater iron removal during acid leaching. Sintering of the grain surface and closure of pores resulted during reoxidation at elevated temperature (>500ºC) and residence time (30 min) as evidenced from the scanning electron micrographs is attributed to the inferior leachability of beneficiated ilmenite.

References

Becher, R.G., Canning, R.G., Goodheart, B.A. and Uusna, S. (1965) 'A new process for upgrading ilmenite mineral Sands', *Proc. Australian Institute of Minerals and Metals*, Vol. 21, pp.21–31.

Coats, A.W. and Redfern, J.P. (1964) 'Kinetic parameters from thermogravimetric data', *Nature*, London, Vol. 201, p.68.

Haque, R., Ray, H.S. and Mukherjee, A. (1992) 'Reduction of iron ore fines by coal char fines – development of a mathematical model', *Scandinavian Journal of Metallurgy*, Vol. 21, pp.78–85.

Hussein, M.K. and El-Tawil S.Z. (1967) 'Solid state reduction of egyptian black sand ilmenite with hydrogen', *Indin Journal of Technology*, Vol. 5, pp.97–100.

Jeya Kumari, E., Bhat, K.H., Sasibhooshanan, S. and Mohan Das, P.N. (2001) 'Catalytic removal of iron from reduced ilmenite', *Minerals Engineering*, Vol. 14, pp.365–368.

Mohan Das, P.N., Damodaran, A.D., Bhat, K.H., Velusamy, S. and Sasibhushanan, S. (2006) *Indian Patent No. 196947* dated 11 August, 2006.

Mohan Das, P.N., Velusamy, S., Sathyanarayana, K.G. and Damodaran, A.D. (1990) 'Reduction of ilmenite and its application as welding electrode flux material', *Transaction of Indian Institute of Metals*, Vol. 43, No. 3, pp.47–50.

Ray, H.S. (1993) *Kinetics of Metallurgical Reactions*, Oxford & IBH Publishing Co. Pvt. Ltd., New Delhi.

Sinha, H.N. (1973) 'Murso process for producing rutile substitute', in Jaffe, R.I. and Burte, H.M. (Eds.): *Titanium Science & Technology, Proc. International Conference*, Plenum Press, New york, pp.233–245.

Sun, K., Ishii, M., Takahashi, R. and Yagi, J. (1992) 'Oxidation kinetics of cement – bonded natural ilmenite pellets', *ISIJ International*, Vol. 32, No. 4, pp.489–495.